1991

Analysis of cutting tool and conditions of milling operation.

Jason. Yien
University of Windsor

ANALYSIS OF CUTTING TOOL AND CONDITIONS OF MILLING OPERATION

by

Jason Yien

A Thesis Submitted to the
Faculty of Graduate Studies and Research
through the Department of Industrial Engineering
in Partial Fulfilment of the requirements
for the degree of
MASTER OF APPLIED SCIENCE
At
the University of Windsor

Windsor, Ontario, Canada
1991

ISBN 0-315-69866-7

I hereby declare that I am the sole author of this thesis. I authorize the University of Windsor to lend this thesis to other institutions or individuals for the purpose of scholarly research.

Jason Yien

I further authorize the University of Windsor to reproduce this thesis by photocopying or by other means, in total or in part, at the request of other institutions or individuals for the purpose of scholarly research.

Jason Yien

The University of Windsor requires the signature of all persons using or photocopying this thesis. Please sign below, and give address and date.

To my parents

Abstract

The focus of this research was on the effects of the operating conditions on the cutting forces and the tool life in the milling operations. Experiments were conducted to measure the on-line cutting forces, and the tool life under a dry condition. Based on the experimental results, mathematical models of cutting force and tool life were developed. They were functions of the operating conditions, i.e., the cutting speed, the feed rate, and the depth of cut. Further analyses were performed on the cutting force patterns. The process optimization that was based on the minimum part production cost was applied by using mathematical models. A practical problem with numerical values was also presented in this thesis.

ACKNOWLEDGEMENTS

I wish to express my grateful appreciation to Dr. G. Abdou, who is my major advisor, for his guidance, support, and encouragement throughout the research. I would also like to thank Dr. S. P. Dutta, who is my co-advisor, for his support, and Dr. W. North and Dr. Z. F. Rief for their precious suggestions. Much thanks are extended to Mr. Tom Williams, Ms. Jacquie Mummery, and Mr. Dieter Liebsch for their assistance. Thanks also to Ms. Amy Chiu for her help in the final preparation of the thesis.

Finally, I would like to give thanks to my friends and particularly to Ms. May Tang for their support, prayers and concern.

Table of Contents

List of Figures

List of Tables

NOMENCLATURE

a = permanent component

a_1, b_1 = constants

b = linear trend component

C_w = cost of workpiece ($)

C_s = set-up cost ($)

C_m = machining cost ($)

C_o = overhead cost of the whole cutting process ($)

C_r = tool replacement cost ($)

C_t = tool cost ($)

D = diameter of the cutter (inch)

d = depth of cut per pass (inch)

d_0 = required depth of removed material (inch)

eff = the efficiency of the machine tool

e_t = random error at t-th sample

F = cutting force (N)

f = feed rate (ipm)

k = constant

L = length of workpiece (inch)

N = spindle speed (rpm)

n = number of teeth

P = power of the motor (hp)

R = surface roughness (μm)

Re = real part of a complex function

SN_t = seasonal component

T = tool life (min)

t = sample number

t_m = machining time (sec)

t_0 = overhead time (sec)

t_r = tool replacement time (sec)

t_s = set-up time (sec)

U_i = unit cost of item i ($/unit)

v = cutting speed (ipm)

Chapter 1

Introduction

The development of Computer Integrated Manufacturing (CIM) systems has been fairly rapid in recent years due to the development of computer technology, and the demand for higher productivity. CIM systems call for the coordinated integration of computers into all phases of a manufacturing company. These phases include the design of a product, the planning of production, the unattended manufacturing of parts, automatic assembly and inspection, computer-control of the flow of materials and parts throughout the plant, and the communication of information within the whole company. They have to be integrated into one computer network, supervised by the CIM central computer which monitors the interrelated tasks and controls each of these based on an overall management strategy. Figure 1 shows the hierarchy of such a CIM system [1].

Among the aforementioned phases, unattended production in the CIM system is known as a flexible manufacturing system (FMS), it consists of automated machining cells and an automated material handling system. A control system, known as the Direct Numerical Control (DNC) system is interfaced with the computers and process controllers of the robot and the CNC (Computer Numerical Control) machines. It receives

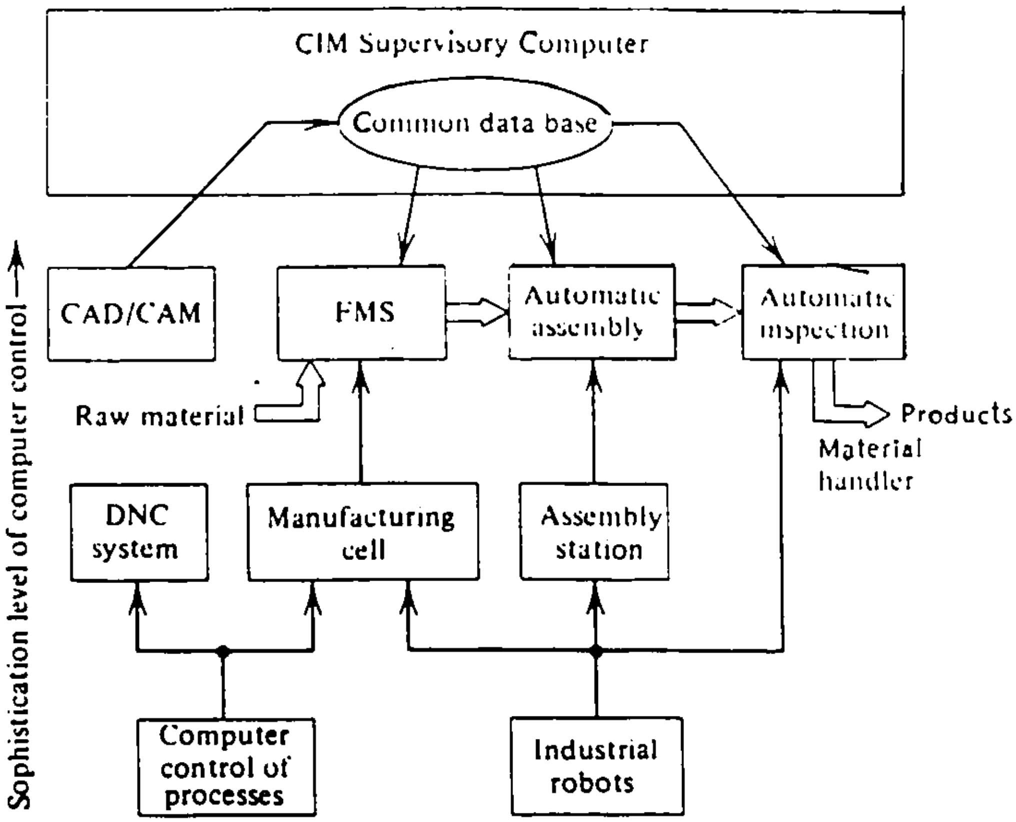

Fig.1 The hierarchy of a typical CIM system

signals from CNC machines and issues instructions to the robot to load and unload the machines and change their tools. The CNC machine is a machine tool that is controlled by a microprocessor which executes the NC part program that incorporates the control variables, i.e., spindle speed, feed rate and depth of cut. Therefore, such variables can be optimized and executed more accurately.

Although stand-alone CNC machine tools and computer network schemes are now well established in FMS, such networks have to be improved in two ways [2] so as to extend automation effectively and efficiently. First, they should communicate more effectively with the computer networks of both a local manufacturing cell and the entire CIM system. Second, the machine tool must be equipped with sensors so that it can monitor the state of the cutting tool and the cutting process while effecting adaptive control of the operating parameters.

In a conventional system, a machine tool operator is employed to oversee the machine tool, the cutting tool, and the process. Furthermore, the machinist may perform some adaptive control. In case of a tool breakage or a tool replacement, he or she may then take some actions. On the contrary, the CNC machine tools in FMS cannot sense any unpredicted situation nor take any remedial action.

Therefore, a major problem in running an unattended machining is the possibility of system malfunction that can result in catastrophic failures and damage to the system. Tooling-related malfunction is of particular concern since tooling is, by nature, a wear component. In fact, any undesirable tooling condition can cause the following: loss of the dimensional part accuracy, loss of the required surface finish, tool breakage or chipping, and excessive torque. For instance, in the case of a tool breakage, the whole production has to be stopped, thus leading to a loss in terms of productivity. Apart from the tooling problem, there is also a possibility that the machine tool may execute the pre-determined codes inaccurately.

In order to ensure system reliability and enhance productivity in an unattended manufacturing environment, it is necessary to implement sensing and corrective devices that can detect and correct system malfunctions. Over the last decade, researchers have put their effort into on-line monitoring of the machining process, especially the recognition of tool breakage, because of the rapid development of computer integrated manufacturing systems and sensor-based machining processes.

Recently, the application of on-line monitoring has just extended to those processes in which multi-point cutting tool is used such as milling. This is due to its complicated nature, i.e., the stochastic nature of the process, and the different degree of wear along different cutting edges. Actually, the milling process is a very common process that can generate a wide range of shapes and obtain the desired surface finish. It also gives a very high material removal rate. In fact, the problems mentioned above are the main difficulties in studying the behaviour of the milling operation. There are also many other factors that affect the cutting process. Hence, the tool life, the tool wear, and the cutting forces are stochastic so that they are not easy to be accurately predicted. Therefore, the output of such a cutting process varies from period to period and machine to machine, even though it is ostensibly the same cutting condition.

Of the research being done, two applications have received most of the attention. The first one is the recognition of a tool breakage while the second one is the adaptive control of the operating parameters. However, there is no effective tool wear sensing system to predict a tool breakage, particularly for a process in which multi-point cutting tools are used. Moreover, very limited applications of on-line monitoring have been developed. Besides, the available relationships among different cutting parameters, production cost and production rate are no longer valid for unattended manufacturing ever since CNC machines have been introduced. Moreover, in determining the optimal machining parameters, the depth of cut is always ignored. In reality, it affects the cutting time because the number of passes needed depends on the depth of cut per pass. It also affects the power required and the cutting forces generated.

Therefore, this investigation has been conducted to find out the stochastic nature of the cutting process, and to probe the details of the behaviour of the cutting parameters and their effects.

Chapter 2

Literature Survey

During the last decade, the trend towards unattended manufacturing emphasised the need for sensing the variables in-process that could affect the state of the cutting tool, the workpiece and the machine tool itself [3]. The most successful areas of in-process sensing were tool failure and tool wear. Tool wear could lead to loss of specifications of the finished component size and the surface and excessive tool forces, driving torque and motor current, while tool failure could cause catastrophic damage to the cutter tool, the workpiece and the machine tool.

Tool wear sensing was more practical because it could be applied to avoid tool failure or loss of tolerance of the workpiece. However, it was a more difficult technique to employ. With increasing focus on the development of the sensing techniques, many different methods were exported. Some of these are classified as follows:

Direct Methods

1. Use of radioactivity : The proposed method was to measure the radioactivity of the swarf and the implanting of the radioactive particles in the tool. It had been reported that continuously monitoring the radioactivity of the

tool allowed the tool wear to be measured to accuracies of 2 μm. [4].

2. Electrical resistance : The electrical parameters of the circuit of the tool, the workpiece and the machine varied with the state of the tool work junction and this could be applied to measure tool wear [5]. Another technique proposed was to print a film resistor onto the clearance surface of the tool and to insulate it. A circuit was completed through the resistor and as the tool wore out, it decreased the size of the resistor, thus changing its resistance [6].

3. Optical methods : One of the proposed methods [7] was the measurement of the reflected light from the cutting edge by a photodiode array. It was necessary to clean the cutting edge by air pressure before any measurement could take place. Another method [8] was to measure the difference between the reflectance of the worn and the unworn area of the tool flank. It has been reported that using fibre optics to direct the light to the sensor at the tool and to carry the reflected light to a photocell could measure flank wear to +/- 10 μm.

<u>Indirect Methods</u>

1. Tool size measurement : The distance between the tool point and the workpiece was monitored by ultrasonics [9] or air gauges [10] so that the wear could be measured.

2. Temperature : Methods were proposed to measure temperature including using a tool and a workpiece as the hot junction [11], an imbedded thermocouple [12] and an infra-red sensor. However, the correlation between temperature and wear was still doubtful since at high temperature, significant changes in wear corresponded to small changes in temperature.
3. Tool forces : It was agreed that there was a correlation between the tool force and wear [13]. Some reported that the feed force or the axial component was more sensitive to wear than other components [14]. However, most researchers suggested that the measurement of two or more components was necessary for a good correlation [15].
4. Vibration : The vibration of the machine tool generated by the cutting process had been used as an indirect measurement of the tool wear. Researchers [16] had measured the spectral density of the output signal from the accelerometer fixed near the cutting edge and had shown that this was proportional to the cutting speed and wear.
5. Surface finish : The surface finish of a machined component was a sensitive measure of the tool wear [17] and research in this area is still ongoing.
6. Acoustic emission : Sonic devices had been studied with respect to wear [18]. The high frequency content of the vibration was normally directly related to the frictional

rubbing of the tool flank on the workpiece; this high frequency content was compared to the low frequency content to determine a correlation with wear.

Besides, bearing forces, shaft torque, power and motor current had been studied and it was found that they did not have a good correlation with the tool wear [3]. An overview of the above methods is shown in Table 1.

Among the above techniques, the tool forces and the acoustic emission were most sensitive to tool wear [3]. Therefore, in this research, the tool forces were measured and studied. In addition, most of the techniques discussed previously have only been used on the turning operations.

As NC and CNC machines were developed, the concepts of automation and the unattended manufacturing systems were promoted. Therefore, the monitoring of on-line manufacturing process, especially the automatic detection of the cutting tool failure was very important in achieving higher productivity, and protecting the work pieces and the machine tools from any possible damage. Prior to the late 1980's, very few researchers dealt with the milling operation. This was probably due to the complexity of the operation itself. On the other hand, the turning operation was receiving more attention. Up to this time, the monitoring of the milling

TOOL WEAR SENSING METHODS			
TECHNIQUES			
Use of Radioactivity	ON-LINE	DIRECT	NON-CONTACT
Use of Electrical Resistance	ON-LINE	DIRECT	CONTACT
Use of Optical Methods	ON-LINE	DIRECT	NON-CONTACT
Tool Size Measurement	ON-LINE	INDIRECT	NON-CONTACT
Vibration Measurement	ON-LINE	INDIRECT	CONTACT
Surface Finish Measurement	OFF-LINE	INDIRECT	BOTH
Acoustic Emission Measurement	ON-LINE	INDIRECT	CONTACT
Bearing Force Measurement	ON-LINE	INDIRECT	CONTACT
Shaft Torque Measurement	ON-LINE	INDIRECT	CONTACT
Power Measurement	ON-LINE	INDIRECT	CONTACT
Motor Current Measurement	ON-LINE	INDIRECT	CONTACT
Temperature Measurement	ON-LINE	INDIRECT	BOTH
Cutting Force Measurement	ON-LINE	INDIRECT	CONTACT

TABLE 1 Tool Wear Sensing Methods

operations had been investigated by several researchers. Detection of the tool breakage and any changes in the cutting parameters were the topics that had been focused on. Also, different methods had been used. A summary of the previous work by different researchers is illustrated in Table 2. A summary of what the researchers had done is presented as follows :

Lan and Naerhein [19] developed an adaptive signal processing scheme for the cutting force signal to detect the fracture and the chipping of a cutting tool during the milling operations. The cutting force signal was modeled using a discrete autoregressive model where the parameters were estimated recursively at each sampling instant using a parameter adaption algorithm based on the model reference adaptive system approach. By comparing the predictive value and the measured value, a priori prediction error was obtained. Therefore, by observing the amount of the predictive error, the tool fracture could be detected. However, no mention was made of subsequent detection of the fracture.

Altintas, Yellowley and Tlusty [20] developed a simple and efficient algorithm for processing the milling cutting force signal to detect the cutter breakage. The basic variation per tooth was removed by calculating the average

Authors	On-line Identification				Sensor			
	m/cing cond'n	tool break-age	tool life	distin-guish ability	dynamometer strain gage	dynamometer Kistler 9257	com-ponents 2	com-ponents 3
Lan, Nearhein (1986)		*				*		
Jacobs, Hentschel Stange (1988)		T	T					
Altintas, Yellowley Tlusty (1988)	*	*		*	*			*
Tarn, Tomizuka (1989)	*	*		*		*	*	
Fussel, Srinvasan (1989)	*					*	*	
Altintas, Yellowley (1989)	*	*		*	*			*
Billatos, Tseng (1991)	*	*			*	*		
Suliman, Hassan (1991)	*							
Yien (1991)	* (process optimization)		M		Kistler 9067		*	

T == Theory
M == Model

Table 2. Summary of literature survey

force per tooth. The first difference of these forces, i.e., the difference between the force sample at a specific instant and the next instant, detected both the breakage and some sudden changes in cutting conditions. The second difference, the difference of the first difference, distinguished between the two. First, the quasi-mean resultant force was calculated, and then a first normalized difference was defined by the difference between the force at the specific instant (i) and the one at the next instant (i+1) divided by the force at that instant (i). Second, by calculating the ratio of the second to the first difference, the transient cutting condition could be segregated from the tool breakage. In addition, two thresholds were required for the first and the second difference. Only the detection of the tool breakage and the changes of parameters were presented.

Altintas and Yellowley [21] improved the existing system by introducing a method of an on-line identification of the immersion ratio and the threshold tuning. Jacobs, Hentschel and Stange [22] described the monitoring of the tool breakage, the recognition of the end of the tool life as well as the adaptive control of machining process generally. There was no specified model or method described.

Tarn and Tomizuka [23] developed an on-line monitoring system of the tool and the cutting conditions in a milling operation. The key feature was the cutting force signals extracted from the force signal pattern over one spindle revolution. The monitoring scheme combined this feature to differentiate the tool breakage from any variations in the cutting conditions. First of all, the quasi-mean resultant force was calculated and then five different features of plots were defined. They were the maximum force level, the total amplitude of the cutting force, the combined incremental force changes, the amplitude ratio and finally, the radial depth of cut. By using these five basic features of the force signal, the tool breakage and changes in cutting conditions could be both detected and separated.

Fussel and Srinivasan [24] described a method for the on-line identification of the process parameters by relating the feed rate to the cutting force. A simple model was developed by using the measured feed drive velocity and the cutting force as the input and output signals, respectively, and by choosing a sampling interval equal to the tooth delay period. The system was responsive to any changes of the axial and the radial depths of cut and the feed rate. The primary potential use of the on-line identification scheme developed was in the feedback control of the cutting force using feed rate manipulation and a parameter adaptive controller. However, no specified system was developed.

Billatos and Tseng [25] presented an adaptive control model for the tool breakage recognition. In their research, they used an adaptive control transformation and the error function to make a tool breakage recognition algorithm. The error function was actually the difference between the measured cutting force and the cutting force from the model. However, no threshold value was mentioned for evaluation.

Recently, Suliman and Hassan [26] developed the mathematical models for milling low carbon steel. The models involved surface roughness, power consumption, and vibration as the dependent variables. The independent variables were the cutting speed, the feed rate, and the depth of cut. Factorial design of experiment was applied so that only ten experiments were conducted. After formulating the models, the adequacy of the models was examined and some analysis was also performed on the effects of the independent variables on the dependent variables. Moreover, response curves were plotted to illustrate the relationships among the different variables. One of the applications was the process optimization. However, the cost function was not a complete one, because no tool life was considered. In addition, no specific conclusion could be made about model adequacy because more criteria need to be considered. The dependent variables such as vibration and power consumption might not be as a practical measure as the tool life and the cutting force which were formulated in the current research in terms of sensing the tool wear. The reasons are discussed at the beginning of this chapter.

Since tool-breakage detection algorithms have been already developed, the main objective of this research is to study the behaviour and the effects of the cutting forces and their further applications.

Chapter 3

Objectives of the research

In order to make a manufacturing system more efficient, not only should a tool breakage be detected but should also be avoided. Although many factors can lead to a tool breakage, wear is the immediate cause. Because of a relatively good correlation between tool wear and cutting force, a sound monitoring system can be based on the cutting forces alone. Due to the complexity of the milling process, it is necessary to study the behaviour of the cutting forces of the milling process, and their relationships with the other parameters such as cutting speed, feed rate, depth of cut, and tool life. It is also important to find a sound methodology to achieve that. Henceforth, the objective of this research is to determine such inter-relationships.

Despite research performed over the past decade, a predictive theory for machinability has not yet evolved. Current test procedures do not relate all the machinability criteria, such as the tool life, the power consumption, the cutting force, the cutting parameters and the economic criteria. Hence, the objectives of the proposed research as shown in Figure 2 are:

(1) to monitor the on-line cutting forces of the milling

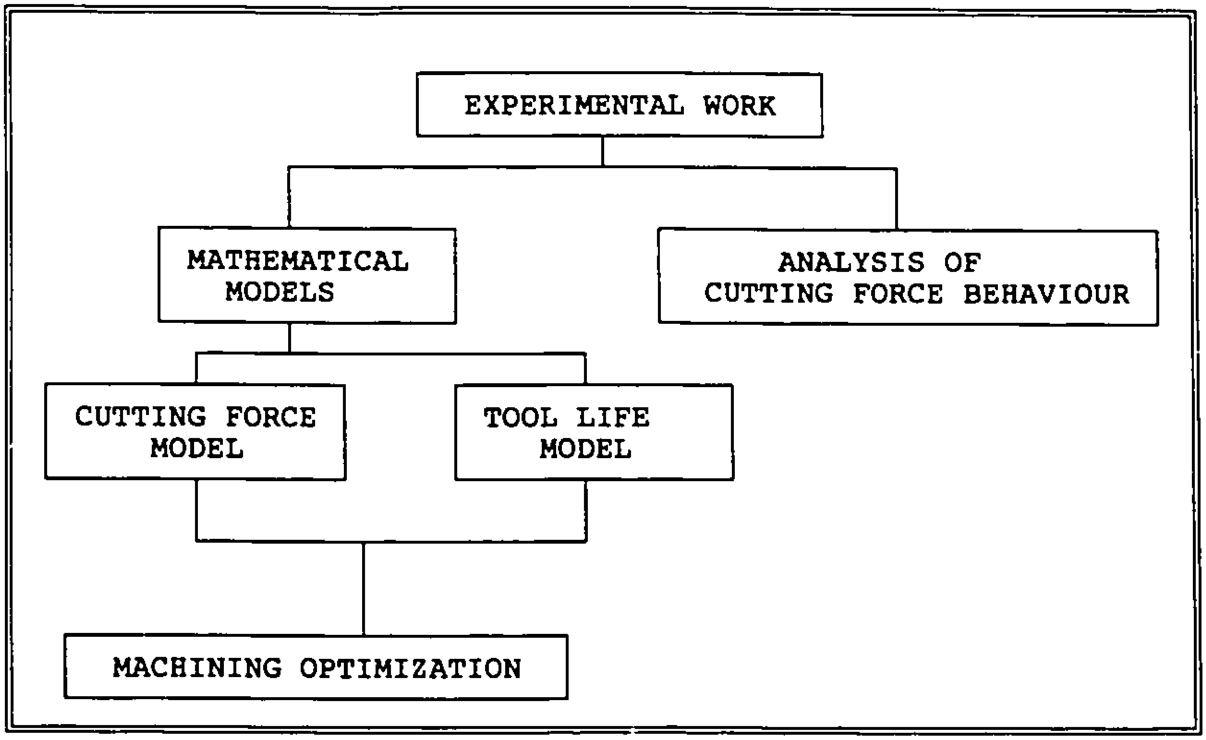

FIG. 2 Direction of the Research

operations. Since the milling operation can achieve a very high material removal rate and is one of the most common manufacturing processes, it is studied in this research;

(2) to evaluate the performance of the milling process in cutting the Aluminum Alloy 2024T by identifying and carrying out the most efficient combination of experimental and the analytical techniques. It should be noticed that the usage of aluminum has been increased due to its light weight. Obviously, this objective cannot be accomplished for all possible situations. Thus, the study will be limited to the operation of end milling;

(3) to develop and analyze the mathematical models for the cutting force and the tool life. The models are the functions of the cutting speed, the feed rate, and the depth of cut;

(4) to analyze the stochastic cutting process in terms of the behaviour of the cutting force,

(5) to perform the optimization of the metal cutting process to determine optimal cutting parameters for a practical problem by applying the above models.

In other words, the main objective of the research is to apply the appropriate monitoring technique and to develop further applications in order to achieve the goal of automated machining. The research methodology includes the following steps:

1. Current problems in tool monitoring are defined, which are then followed by a brief survey about the research done in this area.
2. Experiments on the milling operations are carried out, and the results from experiments on the cutting forces, the tool life measurements and the machining parameters are obtained.
3. A force-based model and a tool life model is developed according to these experimental data. The former model determines the independent force components due to the changes in the feed rate, the cutting speed and the depth of cut. The latter model estimates the tool life by determining the cutting conditions.
4. Machining parameters of the milling operation are analyzed to evaluate the effect of each of the machining parameters on the cutting force and the other parameters which directly reflect on the efficiency and the effectiveness of the milling operation.
5. Optimal cutting parameters will be determined based on the minimum cost. It is noted that all data have been obtained experimentally by using the force transducer. Therefore, the results reflect the real practice of the milling process.

Chapter 4

Experimental Implementation

The equipment used in the experiments consisted of hardware and software. Hardware included a 80386 IBM PC compatible microcomputer, an analog-to-digital converter board, a data input terminal box, a force transducer, a charge amplifier, a CNC milling machine, some end mill cutters, some workpieces, and a microscope. The software used included an interactive program PLOT which was written in BASIC and the vendor programs for analog-to-digital conversion.

4.1 Microcomputer

A 80386 IBM PC compatible with the speed of 25 MHz was used. It executed the software to collect, process, and store the data . As soon as the data were processed, a plot of cutting forces was displayed on the screen.

4.2 Analog-to-digital converter board

An analog-to-digital converter (ADC) is a device that converted an analog signal into digital form. Analog signals are usually continuous, and the analog-to-digital conversion consisted of three phases:

1. Sampling. The continuous signal is periodically sampled to convert it into a series of discrete-time analog signals;
2. Quantification. Each discrete-time analog value must be

assigned to one of a finite number of previously defined amplitude levels. These amplitude levels consist of discrete values of voltage ranging over the full scale of the ADC,

3. Encoding. The various amplitude levels obtained during quantization must be converted into a digital code. This involves the representation of the amplitude level by a sequence of binary digits. Besides, in selecting and applying an analog-to-digital converter, three basic characteristics have to be considered and they are the sampling rate, the conversion time and the resolution. Sampling rate is the rate at which the continuous analog signal is sampled. Conversion time of an ADC is the time required to perform its function, while the resolution of an ADC refers to the precision with which the analog signal is evaluated. In this research , a Metrabyte ADC interface with on-board memory model DAS-50 was used and installed within the microcomputer. Its features were a high conversion rate of 1 MHz and the on-board memory of 1 MB. Detailed specifications [27] are shown in Table 3.

4.3 Data input terminal box

It was a dummy device which interfaced with the DAS-50 converter board via the co-axial cable. The Metrabyte Model BNC-50 was used in the experiments.

4.4 Charge Amplifier

Kistler model 5004 dual mode amplifier was selected. It

MetraByte ADC Interface with On-Board Memory DAS-50

INPUT		
	Channels:	4 single-ended (Selectable for Sequence)
	Ranges:	0 to +5V, 0 to +10V, +/-2.5V +/-5V, +/-10V
	Max. Input:	+/- 25V
	Resistance:	100 kOhms
	Capacitance:	10 pF
	Bandwidth (-3dB):	6MHz (BW flat within 0.5dB, DC to 500 kHz)
	Channel-to-Channel: (Signal Isolation)	62 dB (500kHz Analog Input)
CONVERTER		
	Resolution:	12 bits
	Conversion Rate:	1 MHZ
ACCURACY		
	Overall:	2 LSB Max.
	Differential:	1 LSB Max.
	Integral:	1.5 LSB Max.
	No Missing Codes:	Guaranteed
TEMPERATURE DRIFT		
	Offset Coeff.:	15 ppm/deg.C typ.
	Gain Coeff.:	25 ppm/deg.C typ.
	Diff. Linearity:	1.5 ppm/deg.C typ.

TABLE 3. Specification of Analog-to-Digital Converter

served to filter the cutting force signals and amplify the signals before processing. A low pass plug-in filter of 10 kHz was used. Once it had been adapted to the connected transducer, it allowed for operations with fixed scales. The charge applied was converted by a first stage with a capacitive feedback into a proportional voltage. Final scaling of the voltage output took place in the amplifier. Detailed specifications [28] are shown in Table 4.

4.5 Force transducer

A transducer is a device that converts one type of physical quantity such as temperature, force, velocity into another type (commonly electrical voltage). The reason for making the conversion is that the converted signal can be used or evaluated more conveniently. Two types of transducers are the analog type and the digital type. Analog transducers produce a continuous analog signal such as an electrical voltage. The signal can be interpreted as the value of the measured variable. To make the interpretation, a calibration procedure is required. The calibration of the measuring device establishes the relationship between the variable that is to be measured and the converted output signal. In fact, the transducer used in this research was an analog one.
A Kistler 9067 force transducer was used to measure the three orthogonal components of the cutting forces in an arbitrary direction. The force transducer contained 3 pairs of

Kistler Model 5004 Dual Mode Charge Amplifier

Charge Amplifier		
Scale setting, 12 steps in 1 - 2 - 5 sequence		
Selectable scales, for transducer sensitivity ranges :		
0.01 to 0.11 pC or mV per M.U.	M.U./V	100 to 500,000
0.1 to 1.1 pC or mV per M.U.	M.U./V	10 to 50,000
1 to 11 pC or mV per M.U.	M.U./V	1 to 5,000
10 to 110 pC or mV per M.U.	M.U./V	0.1 to 500
0.1 to 1.1 nC or mV per M.U.	M.U./V	0.01 to 50
Accuracy, Medium time const.		
of two most sensitive ranges	%	< +/-5
of all other ranges	%	< +/-1
Linearity, of Transducer Sensitivity potentiometer	%	< +/-0.5
Calibration input, sensitivity	pC/mV	1 +/-0.5%
Input voltage, abs. max., at Charge input pulse width <0.5s	V	< +/-125
Amplitude linearity	%FS	< +/-0.05
Frequency response error, Long time const.		
without filter	%	< +/-2
with 180 kHz std. filter	%	< +/-5
with 180 kHz std. filter	%	-1 to +3
Low frequency (-5%)	Hz	0.5

TABLE 4. Specification of Charge Amplifier

Kistler Model 5004 Dual Mode Charge Amplifier

3-dB-frequency, with std. filter 180 kHz, input capacitance up to 1500 pF	kHz	180 +/-10%
Time const. resistor		
Long	Ohms	10e14
Medium	Ohms	10e11
Short	Ohms	10e9
Time const., Long	s	up to 100,000
Medium	s	1 to 5,000
Short	s	0.01 to 50
Output ,Voltage	V	+/-10
Current	mA	+/-5
Impedance	Ohm	100+/-5
Noise at the output typical value	mVrms	0.1/1
DC drift, Short time const.		
during 10 hours	mV	< +-1 / +-5
due to line power variations +/- 20%	mV	< +-1 / +-10
due to temperature variations	mV/ C	< +-0.5 / +-5
Input impedance	Ohm	70
Input cable	Ohm	10e14
Monitoring circuit		
Overload indicator, triggered by output voltage	V	+/-10.5

TABLE 4. Specification of Charge Amplifier (Cont'd)

Kistler Model 5004 Dual Mode Charge Amplifier

General data		
Operating temperature range	deg.C	0 to +50
Power supply	V	100 to 130
Frequency	Hz	60
Power consumption	VA	8
Connections		
Input	Type	BNC neg.
Output	Type	BNC neg.
Weight	Ib	3.3
	kg	1.5

TABLE 4. Specification of Charge Amplifier (Cont'd)

quartz rings that were mounted between two steel blades in the transducer case. Two quartz pairs were sensitive to shear and were used to measure the horizontal force components. The remaining quartz pair, which were sensitive to pressure, measured the vertical component of a force acting in an arbitrary direction. The electrical charges generated proportionate to the different components were led through the electrodes to the corresponding connector contacts. Moreover, the workpiece had to be mounted onto the transducer very tightly. In this research, the workpiece and the fixture were fixed together, and it was not practical and feasible to have transducers mounted on every workpiece in the performance of automation. However, many other kinds of fixture could be used and the workpiece could be loaded and unloaded from it. A sketch of the designed fixture for the application of automation is shown in Figure 3. The suggested fixture was mounted into the force transducer and the transducer itself was fixed by the vice. Therefore, the workpiece could be placed on the fixture. It should be noted that the transducer had to be calibrated with the fixture as a preload. Table 5 shows the detailed specifications [29] of the transducer.

4.6 <u>CNC milling machine</u>

A Jet CNC mill was used to perform the milling processes. It was a 1.5 hp vertical milling machine, with a spindle speed up to 2700 rpm and feed rate up to 100 ipm. All the operations

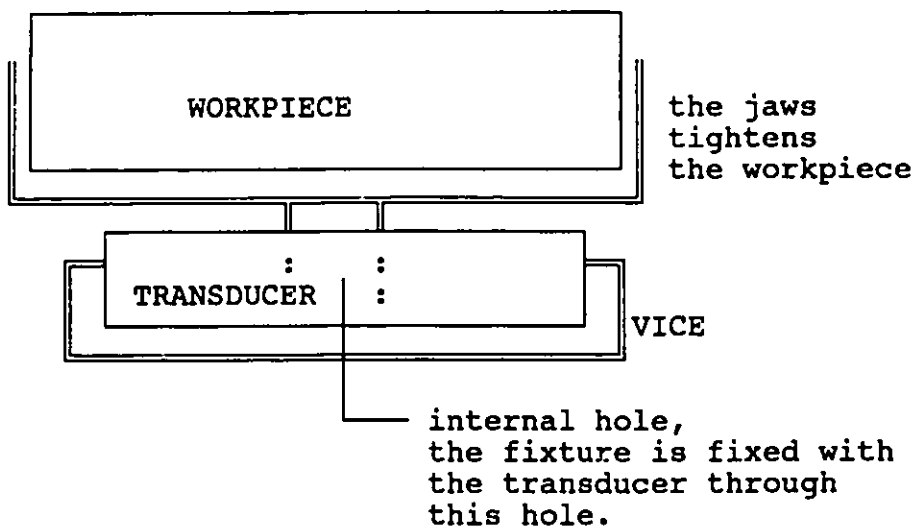

Figure 3. Sketch of Designed Fixture

Kistler 3-Component Force Transducer Type 9067

Range	Fx,Fy	kN	-20...20
	Fz	kN	-40...40
Overload	Fx,Fy	kN	-22/22
	Fz	kN	-44/44
Threshold		N	< 0.01
Sensitivity	Fx,Fy	pC/N	-8
	Fz	pC/N	-3.8
Linearity,each axis		%FSO	<+/-0.5
Hysteresis,each axis		%FSO	< 0.5
Cross talk	Fz --> Fx,Fy	%	=< +/-1
	Fx <--> Fy	%	=< +/-1
	Fx,Fy -->Fz	%	=< +/-4
Rigidity	Cx,Cy	N/um	3500
	Cz	N/um	8000
Allowed moments	Mx,My	Nm	-350/350
Operating temperature range		deg.C	-50...150
temperature coeff. of seneitivity		%/deg.C	=< +/-0.02
Insulation resistance			>10e13
Capacitance		pF	100
Connector		Type	10-32 UNF
Weight		g	270

TABLE 5. Specification of Force Transducer

were controlled by the machine controller, i.e., a 80286 IBM PC compatible microcomputer. Detailed specifications are listed in Table 6.

4.7 Milling cutter and workpiece

Two 1/2 inch flute end mills were used to perform the cutting of slots. All the end mills were constructed from high speed steel (HSS). The maximum permissible flank wear was taken to be 0.062 inches [30]; this was the value at which the tool required regrinding. The workpieces selected in this project were made from 2024T Aluminum, with a diameter of 3 inches.

4.8 Microscope

Tool wear was measured with a microscope. Generally, the tool-maker's microscope is the most common equipment for measurement of tool wear. This instrument consists of a microscope that is mounted over a base and may be adjustable. The base in turn carries a coordinate-measuring stage that is positioned by a precision scale. It also includes a movable external light source which provides magnification from 10 to 100 diameters. The fixture is another component of the tool-maker's microscope used to fix the tool to make readings consistent.

Jet CNC Mill

Spindle Motor			
Output		hp	1.5
Frequency		Hz	60
Motor RPM			1720
Phase			1
Pole			4
Heat		deg.C	60
Control Parameters			
Spindle speed		RPM	230-2520
Feed rate		IPM	up to 100
Milling Table			
Motor (x,y-dir)		RPM	3000 max.
	resistance	Ohm	2.1
Motor (z-dir)		RPM	2000 max.
	resistance	Ohm	0.8
Controller	IBM-PC/AT Compatible		

TABLE 6. Specification of CNC Milling Machine

4.9 Computer Software

Apart from the vendor software of DAS-50, an interactive program PLOT was written in BASIC to collect, process and plot the data and display it on the screen on-line. Some useful information such as the cutting parameters were stored in the data upon the request of the user. It had to be noted that the sampling rate and the number of samples were specified in the program PLOT. Simple NC part programs had also been written to carry out the cutting process, in which control variables such as the spindle speed, the feed rate, and the depth of cut were specified. Table 7 lists the values of the control variables used in the experiments. The listing of the programs is shown in Appendix A.

4.10 Experimental Set-up & System Integration

First of all, the workpiece was mounted onto the force transducer by applying a very high pressure. Though it was a very simple operation, it fixed the part very tightly. The transducer was then fixed onto the milling table with the help of a vice and was connected to the charge amplifier. The scaling of the amplifier was set up as 20 N/v. The amplifier needed at least one hour as a warm up period prior to any process. The input terminal box was the means of interfacing the charge amplifier and the analog-to-digital converter interface board. There were special cables used for all connections. The ADC interface board was calibrated

SPINDLE SPEED

S1	S2	S3
670	1420	2170
RPM		

FEED RATE

F1	F2	F3	F4
5	8	10	12
ipm			

DEPTH OF CUT

D1	D2	D3
0.0625	0.09375	0.125
in		

TABLE 7 Input Parameters of Control Variables

before application. Besides, the program PLOT and the NC part programs of the milling process were made ready for each experiment. The microscope was also set up and calibrated for the tool wear measurements. The reliability of the tool wear measurements was ensured by measuring a new tool that had no wear. A block diagram of the experimental setup is shown in Fig. 4.

4.11 <u>Data collection</u>

Since data collection in this project was important, this section is devoted to a more detailed description.

Before collecting any data, two parameters had to be determined and specified in the program PLOT. The first parameter was the sampling rate while the second one was the number of samples required. According to the sampling theorem [31], the sampling rate had to be greater than two times the frequency of the low pass filter, i.e., 10 KHz. Therefore, a sampling rate of 24000 was selected. Moreover, 1600 samples were collected in one loop, in which 400 samples per channel were collected and processed, i.e., one channel for one component. There were 600 loops in the data collection procedure. In other words, 600 signals were obtained in each milling process. Each of these 600 samples was actually the average of 400 samples within a 0.017 second period. In addition, the computer processing time for computation and the

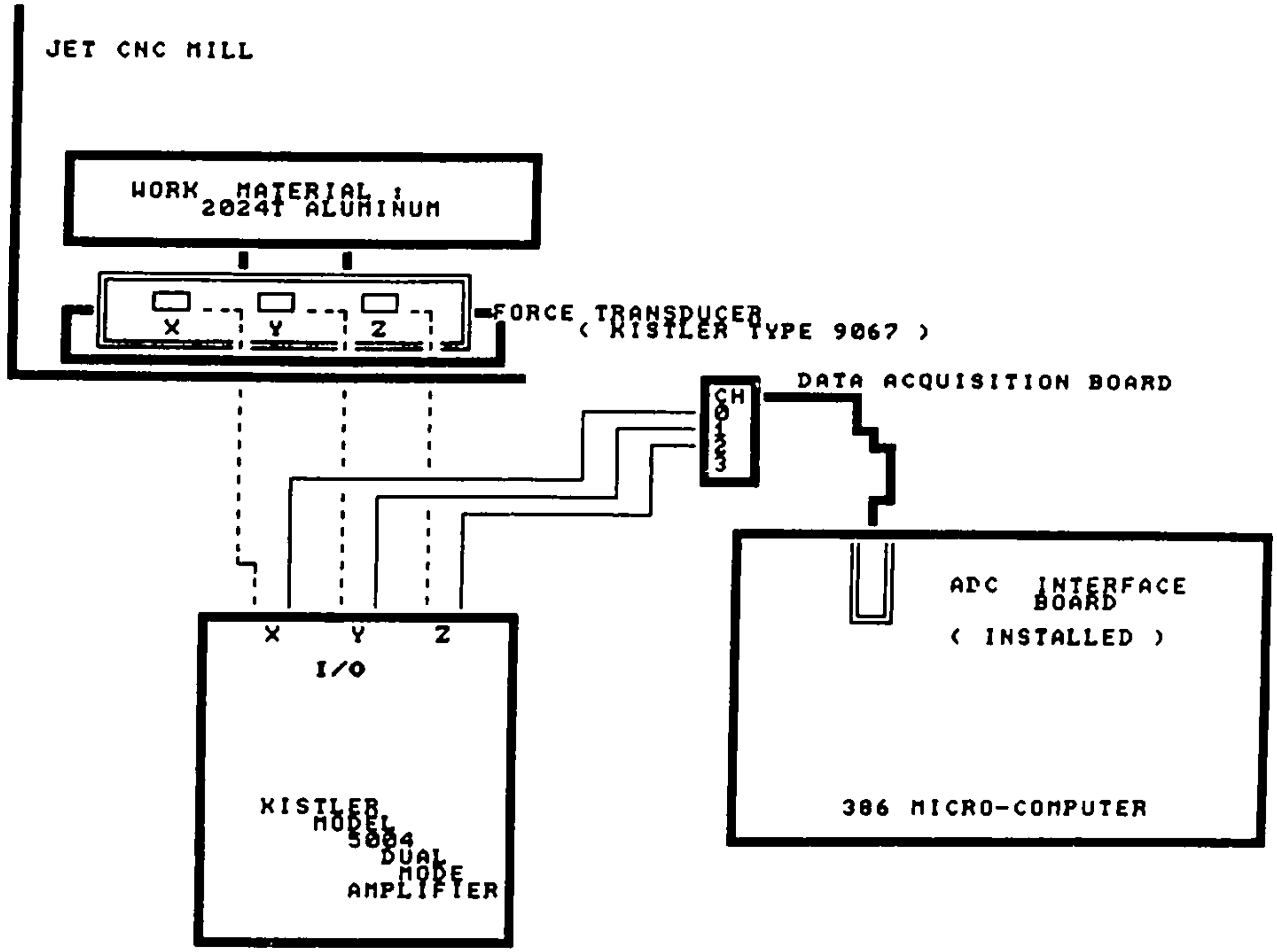

Fig. 4 Experimental Setup

on-line plotting of the signals on the screen was 0.083 second. Therefore, during the entire milling process, some signals were lost due to the limitation of the speed of the computer.

Detailed procedures for data collection are listed as follows:

1. The analog signals equivalent to the cutting forces in the three planes are measured by the force transducer.
2. These signals are then transferred to the amplifier to be filtered and amplified.
3. The three signals of the different components are then transferred through the dummy input terminal box to the ADC interface board.
4 The signals are digitized, and collected with the help of the program PLOT.
5. The digital signals are transferred to an array and stored in the computer memory as an ASCII file.
6. The data in the array are then processed and plotted on the screen immediately.
7. Step 6 is repeated until all the data is processed and plotted.

It should be noted that there were independent channels and memory buffers for each component of the cutting forces. Therefore, the three components of the cutting forces were measured at the same instant. A data flow diagram is shown in Figure 5.

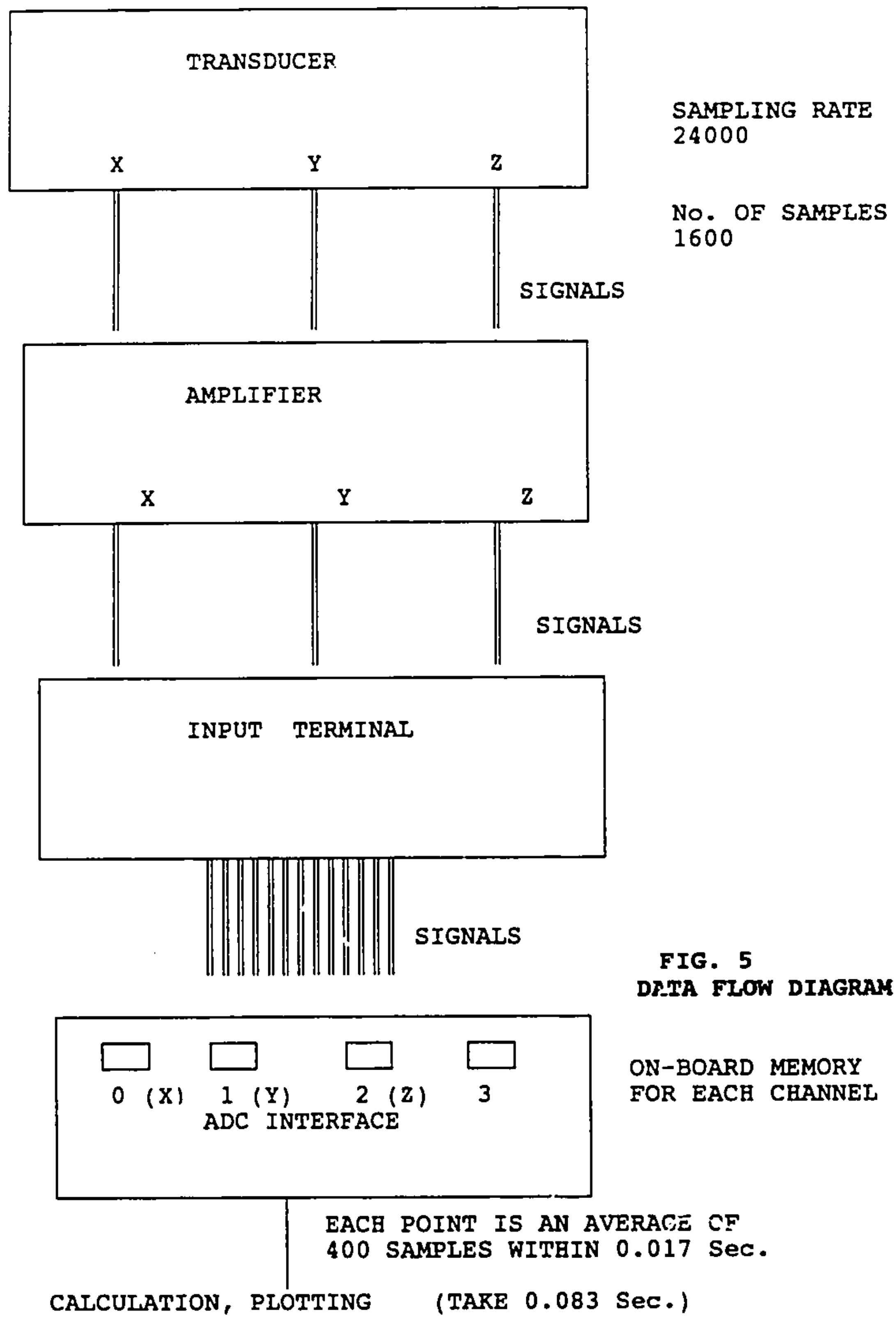

FIG. 5
DATA FLOW DIAGRAM

Chapter 5

Methodology

In order to achieve the objectives of this research, it is necessary to conduct experiments to obtain the experimental data. The cutting force and tool life models can then be formulated, from the analysis of these experimental data the behaviour of the cutting force can be found. Therefore, this chapter contains sections on the experimental design and procedures, the formulation of the mathematical models, the analysis of the cutting forces, as well as the process optimization.

5.1 Experimental Design & Procedures

5.1.1 Experimental Design

Experimental Design is necessary in order to obtain reliable results. In this research, since the mathematical models of the cutting force and the tool life are formulated according to the experimental data, how valid the models are depends directly on how the experiments are designed. A factorial design of experiments has been introduced so that the number of experiments conducted can be reduced. That is, the total number of experiments equals $2^n + 2$, where n is the number of variables, and there are two repeated central point experiments. However, in the machining processes, the results of the repeated experiments are rarely the same. This is due to the non-uniformity of the hardness of workpieces and the cutting tools, and the stochastic nature of the process. Moreover, during adaptive control, the feed rate is the most common parameter to be corrected, and it also has the most direct influence on the cutting force due to the same direction of the tool force. Hence, the experimental design used in this research was actually a modification of the factorial design.

In a milling process, there are three control parameters, that is, the spindle speed, the feed rate, and the depth of cut. These three control variables were selected to be the independent variables of the mathematical models of the cutting force and the tool life. In the factorial design, two values of each independent variable were selected and thus a cubic box was formed. Within this cubic box, the selected values of the independent variables were the vertices and the central point of this box became the set of values to be used twice. They were the $2^3 + 2$ experiments designed by the factorial method.

Because of reasons outlined earlier, this factorial design was modified as follows :

<u>selected vertices</u>

two values of spindle speed : 670, 2170 rpm

two values of depth of cut : 0.0625, 0.125 inch two values of feed rate : 5, 12 ipm

one central value of spindle speed : 1420 rpm

one central value of depth of cut : 0.09375 inch

two central values of feed rate : 8, 10 ipm

therefore a total of 36 experiments were conducted.

5.1.2 Experimental Procedures of cutting force measurement

After the experiment was set up and all the equipment was integrated, the experiments were carried out as per the following procedures:

Step 1. A new cutting tool is set up.

Step 2. The workpiece is fixed with the aid of a vice.

Step 3. The data acquisition program is ready and all necessary information is entered.

Step 4 The amplifier is set up after the half hour warm-up period.

Step 5 The CNC milling machine and the NC part program are ready.

Step 6 The data acquisition program is then actuated and the cutting process is performed.

Step 7 If there is no overload signal, then the data is saved.

5.1.3 Experimental Procedure of tool life measurement

Since the cutting process was performed prior to the tool life measurements, step 1 to step 7 remained the same as the procedure of the cutting force measurements. Having finished the cutting process finishes, the cutting tool was unloaded and the flank wear of the cutter was measured. If the flank wear of any cutting edge reached 0.062 inch, which was the maximum permissible wear, the tool life was considered as have reached its limit; otherwise, it was necessary to load the cutting tool and to perform the cutting again until the maximum flank wear was reached. The procedures of the tool life measurements consisted of the following steps:

1. The cutting tool is placed on a V-block.
2. The external light source is then turned on.
3. The scale of magnification is adjusted.
4. The initial reading is recorded before cutting, and the final reading is then recorded after each cut.
5. The tool wear is obtained by calculating the difference between the two readings made in step 4. An example of readings is listed below.

Path	Readings (cm.)	Tool Wear (mm.)
1	1.975	0.00
2	1.965	0.10
3	1.940	0.25
4	1.920	0.20
5	1.917	0.03
6	1.905	0.12
7	1.889	0.16
8	1.865	0.24
9	1.839	0.26
10	1.811	0.28
Total		1.64

Path	Readings (cm.)	Tool Wear (mm.)
1	1.761	0.00
2	1.746	0.15
3	1.722	0.24
4	1.695	0.27
5	1.683	0.12
6	1.661	0.22
7	1.653	0.08
8	1.627	0.26
9	1.617	0.10
10	1.613	0.14
		1.58

It was noticed that all the cutting edges had to be measured and the calibration was carried out simply by measuring a new tool.

5.2 Model Formulation

There are dependent variables and independent variables in the models. The cutting force (Y_1) is the dependent variable of the cutting force model, while the tool life (Y_2) is the dependent variable of the tool life model. The independent variables in both models are the control variables such as the cutting speed (X_1), the feed rate (X_2), and the depth of cut (X_3). The relationship between the dependent and independent variables can be mathematically represented as follows :

$$Y_i = X_0 * X_1^{n1} * X_2^{n2} * X_3^{n3}$$

This non-linear relationship can then be written linearly as:

$$\ln(Y_i) = \ln(X_0) + n1 * \ln(X_1) + n2 * \ln(X_2) + n3 * \ln(X_3),$$

$$y_i = x_0 + n1 * x_1 + n2 * x_2 + n3 * x_3,$$

where $y_i = \ln(Y_i)$ $i = 1, 2$

$x_0 = \ln(X_0)$

$x_1 = \ln(X_1)$

$x_2 = \ln(X_2)$

$x_3 = \ln(X_3)$

n1, n2, and n3 are the exponents

Hence, x_0, n1, n2, and n3 can be determined by using the multiple regression technique, which is the statistical technique to determine the equation of the line or the curve which minimizes the deviations between the observed data and the regression equation values. Since there is more than one independent variable, the multiple regression technique is employed.

5.3 Adequacy of Models

After the regression models are formulated, evaluation of the models has to be done to ensure adequacy. Thus, the Analysis of Variance (ANOVA) is performed. The correlation coefficient (R) and the F-test are the main output of the ANOVA. The correlation coefficient is a measure of how well a specific regression equation explains the observed variation. Hence, the higher the R value, the better the regression model. A F-test is then used to examine the adequacy of the model. The F value is actually the ratio of the regression sum of squares and the sum of squared error. The hypothesis H_0 is tested by F value, where $H_0 : B_j = B_{j0}$, $j=1,2,..,k$,

B_j is the mean of the observations. H_0 is rejected if the calculated F-value is greater than the tabulated F_a-value, and it means that the independent variables are significant with respect to the dependent variable at a specific confidence level. However, it does not confirm the adequacy of the model. Residual analysis is necessary to draw a conclusion about the regression model. Since all the above measures are based on the assumption of normality, the residual analysis is the tool to confirm this assumption. In this research, standardized residuals were calculated, the assumption of normality was confirmed if approximately 95 percent of the residuals fell into the interval (+2, -2). This implies that there is no outlier present. In addition, more analysis of residuals is required to determine whether or not there is any pattern of the residuals, and any relationship exists between each variable and the residuals. The partial correlation matrix is another measure of the functional relationship between each individual independent variable and the dependent variable. All the corresponding results are presented in the next chapter.

5.4 Seasonal Pattern Analysis

Since the milling process is an interrupted process, the cutting force is not a constant. It goes up as the cutting edges contact and cut the material, and goes down as the cutting edges leave the material. Therefore, the average cutting forces are used in the formulation of the model. It is usually assumed that the cutting force should act in a cyclic pattern because the same material is being cut under the same conditions during every revolution of the spindle. However, it is not necessarily the case in a real situation. This section describes the method which attempts to analyze the cutting force patterns of the available experimental results. Seasonal exponential smoothing forecast model (Winter's method, Winter 1960) was applied for the curves with seasonal patterns. The seasonal forecast model is presented as

$$F_t = (a + b * t)\ SN_t + e_t$$

Of these three components, SN_t was continuously updated. When performing this pattern analysis, segments of the cutting force curves were extracted for study; these would lie between the initial and the exit states of the cutting, i.e., the periods over which the cutting tool enters and leaves the material, respectively. When Winter's method is used, the three smoothing constants, alpha, beta and gamma have to be input to estimate the permanent component, the linear trend and the seasonal component. Usually, smaller smoothing constants are used for less stable data, and vice versa. Moreover, another parameter known as the season length is required. This season length is determined by observation, and it is different from curve to curve.

5.5 Non-linear Trend Analysis

Apart form the seasonal pattern, it is found that some cutting force curves are bell-shaped. The changes increase to a maximum value and then go down before entering the exit state. MathCAD (MathSoft,1989) software has been used to smooth this non-linear trend and to present this non-linear trend in a mathematical form, which is

$$F_t = a_1 - b_1 * Re((t-t_0)^k)$$

In the above model, a_1, b_1, t_0 and k are determined by minimizing the mean absolute percentage error (MAPE) between the experimental and the calculated value, i.e., sum of the absolute percentage deviation between these two values divided by the number of samples. Moreover, the parameters in the model have their physical meaning. The value of a is the maximum level of the smoothed curve determined by the above model; t, the only variable in the model, is the sample number and is proportional to the cutting time, t_0 is the sample (or instant) at which the smoothed curve reaches the maximum, and finally the value of b and the exponent k determine the width of the smoothed curve. The "Re" in the model means the real part of the complex value. An analysis was performed to find out if there was any relationship between the cutting conditions and the trend. This can be done by the comparison of the parameters of the models.

5.6 Process Optimization

One of the applications of the cutting force and the tool life models is process optimization, necessary to achieve economic machining in mass production. The efficiency of a metal-cutting process can be judged from the main criteria of the life of the cutting tool, the forces and power, the surface finish and dimensional accuracy, and the rate of material removal. The first two considerations determine the costs while the last two measure the output. There are three fundamental evaluation criteria used in the process optimization. They are the maximum production rate, the minimum cost criterion, and the maximum profit rate criterion. In this research, the criterion of the minimum cost was used. In fact, the factors within an operation that may be revised to change the costs and the results are the cutting speed, the feed rate, the depth of cut, the work material, the tool material and the tool form and shape and the cutting fluid. However, in a system that is capable of optimization, there are various controllable variables and uncontrollable parameters. Once work material, the cutting tool, and the operative worker have been reasonably determined, these are considered as uncontrollable parameters. Then, the typical controllable variables are the machining conditions, i.e., the cutting speed, the feed rate, and the depth of cut. Therefore, these controllable variables were optimized to achieve the minimum part production cost.

The part production cost consists of (1) the cost of workpiece, C_w, (2) the set-up cost, C_s, (3) the machining cost, C_m, (4) the tool cost, C_t, (5) the tool replacement cost, C_r, and (6) the overhead cost of the whole cutting process, C_o.

(1) The cost of workpiece is the cost of the machining component.

(2) The set-up cost includes the part loading and unloading cost and the machine set-up cost.

(3) The machining cost is the cost of the cutting process, in which the power consumption and the machine depreciation costs are included.

(4) The tool cost covers both the cutting tool and the regrinding cost.

(5) The tool-replacement cost is actually the cost for an operator or an automatic tool changer to replace a worn-out tool.

(6) The overhead cost of the whole process is the cost for an operator or a machining cell controller allocated to overheads over the entire process.

Therefore,

(PC) Production cost = $C_w + C_s + C_m + C_t + C_r + C_o$.

$$PC = C_w + (U_s + U_o) * t_s + (U_m + U_o) * t_m + (U_t + U_r * t_r + U_o * t_r) * t_m/T \quad \text{, eqn.1}$$

$$t_m = (L + D) * d_0 / (f * d), \quad \text{eqn.2}$$

It should be noted that the cutting time t_m (eqn.2) is not only for one pass; the number of passes is also considered, i.e., d_0/d. The term t_m/T represents the number of cutting tools used. The tool life model developed in this research is used and it is substituted into the cost objective function to replace the term T. Hence, it is found that only the third and fourth terms are to be minimized because the remaining terms are constants.

In fact, it is not practical to minimize the cost unrestrictedly. Constrained optimization has to be performed. The constraints are the allowable and practical range of the cutting speed, the feed rate, the depth of cut, the cutting force, and the maximum surface roughness . They are listed as follows :

(1) cutting speed constraint $v_{min} =< v =< v_{max}$

(2) feed rate constraint $f_{min} =< f =< f_{max}$

(3) depth of cut constraint $d_{min} =< d =< d_{max}$

(4) cutting force constraint $F_{min} =< F =< F_{max}$

(5) surface roughness $R_{max} =< (f/(n * N))^2/(4 * D)$

The ranges of the variables are determined by the machine specifications, the material of the workpiece, and practical experience. Practical experience does not mean subjective perception, but the recommended range from the related handbooks. The minimum values of the constraints are usually determined from the machine tool specifications, i.e., the minimum available values, while the maximum values are obtained from the handbook. However, due to diverse capacities of different machine tools, not all the values can be used. For instance, the range of the cutting speed mainly depends on the machine tool because a small machine does not have a high spindle speed available. On the other hand, the maximum feed rate and the maximum depth of cut can always be obtained from handbooks. The range of the cutting force is derived from the maximum power available from the machine tool while the surface roughness is specified by the machinist. In fact, the surface roughness constraint actually restricts the cutting speed and the feed rate. Otherwise, the lowest speed and the highest feed rate always obtain the lowest cost.

The process optimization presented above is actually a typical non-linear constrained optimization. Due to its special nature [32], the feed rate is always the variable with the highest priority for maximization. The cutting speed is then determined from the surface roughness constraint, from which the tight relationship between the cutting speed and the feed rate is shown. Since different machine tools have different ranges of spindle speed, if the cutting speed obtained from the surface roughness constraint is less than or equal to the maximum allowable cutting speed , it is taken to be the optimal value. In cases where the calculated speed exceeds the maximum allowable speed, the optimal feed rate has to be decreased and coupled with the maximum speed to meet the surface roughness requirement. The depth of cut should be as high as possible so as to reduce the number of passes, as long as the machine tool is not overloaded. It is because the cutting force generated from such a heavy cut is quite high.

In short, the following procedure can be used to obtain the optimal cutting conditions at the lowest cost.

Step 1. Set the maximum feed rate (f_{max}) to be the optimal feed rate (f_{opt}).

Step 2. Calculate the cutting speed (v') according to the relationship from the surface roughness constraint.

Step 3. If v' is less than or equal to the maximum cutting speed (v_{max}), v' is the optimal cutting speed (v_{opt}).

Step 4. If v' is higher than the maximum available cutting speed, v_{max} is the optimal speed, and f_{opt} is then determined by the surface roughness constraint.

Step 5. Obtain the depth of cut (d') from the cutting force constraint.

Step 6. If d' is less than or equal to the maximum depth of cut (d_{max}), d' is the optimal depth of cut (d_{opt}). Otherwise, d_{max} is the optimal depth of cut.

Chapter 6

Analysis of Results

6.1 Cutting force model

The cutting force measurements of the 36 experiments are shown in Table 8, in which the minimum, the maximum and the average forces are listed. It should be noted that each sample is the resultant force of its three orthogonal components. The average cutting forces of each experiment are used in the formulation of the model. After applying the regression technique, the constant x_0 and the exponents n1, n2, and n3 are determined, and the cutting force model is thus written as

$$y_1 = 8.33 - 0.632 * x_1 + 0.831 * x_2 + 1.158 * x_3,$$

where $y_1 = \ln(Y_1)$, Y_1 = Force , N

$x_1 = \ln(X_1)$, X_1 = cutting speed , ipm

$x_2 = \ln(X_2)$, X_2 = feed rate ,ipm

$x_3 = \ln(X_3)$, X_3 = depth of cut, inch

or

$$Y_i = 4147.4 * X1^{-0.632} * X2^{0.831} * X3^{1.158}$$

The adequacy of the linear model is examined by the analysis of variance. First of all, the correlation coefficient of 91% shows the independent variables (cutting speed, feed rate and depth of cut) that are closely related to the dependent variable (cutting force). The F value of 51.684

S	f---	d=0.0625" 5	8	10	12	d=0.09375" 5	8	10	12	d=0.125" 5	8	10	12
v	MIN	1.74	1.16	1.86	4.25	1.8	2.6	4.55	2.55	1.85	4.25	4.3	2.05
87.7	AVG	6.29	7.92	9.19	19.2	11.6	18.9	21.4	25.2	15.6	26.5	33.6	34.6
	MAX	27.6	32.0	47.4	59.9	34.5	46.6	59.4	87.4	54.7	88.4	94.7	99.5
	MIN	0.73	1.0	2.24	1.9	2.02	4.2	1.38	2.18	2.48	2.82	4.94	4.2
186	AVG	5.54	6.4	8.36	13.9	11.2	16.8	18.1	19.5	13.2	21.6	27.5	31.6
	MAX	19.0	25.6	32.1	34.3	30.5	36.0	39.0	40.1	31.8	49.6	60.5	79.2
	MIN	0.51	0.61	0.98	0.9	0.9	1.07	1.22	1.72	1.1	1.02	1.16	1.82
284	AVG	4.49	5.62	6.89	8.63	5.[illegible]2	7.86	8.51	9.01	6.41	9.18	10.0	11.0
	MAX	9.76	15.1	19.9	21.8	10.2	15.7	22.9	29.5	12.5	29.6	46.2	59.3

S = Cutting Speed ,fpm
f = Feed Rate ,ipm
d = Depth of Cut ,inch

Table 8. Experimental Data for the Cutting Force

of the model is much greater than the tabulated $F_{0.01,3,32}$ value of 4.4. This implies that the dependent variables are greatly significant in the model. In addition, the residual analysis has been conducted to prove the adequacy of the model. The assumption of normality is confirmed since approximately 95% of the standardized residuals fall in the interval (-2, +2). Therefore it can be concluded that there is no outlier. Table 9 shows the standardized residuals of the cutting force model.

Furthermore, there is no evidence that any trend of the dependent or independent variables will affect the residuals. That is, no pattern of variances is shown. According to the correlation matrix, it is found that 29 (square of .54) percent of the variation is explained by the cutting speed, 23 percent of the variation is explained by the feed rate, and 31 percent of the variation is explained by the depth of cut, while a total of 83 percent (R^2) of the variation is explained by all the independent variables. The results of ANOVA and the correlation matrix are shown in Table 10. The comparison between the experimental and the predicted values is illustrated in Figure 6.

According to the functional relationship revealed in the model, it is necessary to note that the cutting force increases as the cutting speed decreases, or the feed rate or the depth of cut increases. Therefore, in order to keep the

Experiment Number	Experimental Value (N)	Predicted Value	Residual	Std. Res.
1	6.29	7.8	-1.51	-0.44
2	5.54	4.9	0.64	0.187
3	4.49	3.74	0.75	0.219
4	7.92	11.5	-3.58	-1.04
5	6.4	7.17	-0.77	-0.22
6	5.62	5.53	0.09	0.026
7	9.19	13.8	-4.61	-1.35
8	8.36	8.67	-0.31	-0.09
9	6.89	6.62	0.27	0.079
10	19.2	16.2	3	0.876
11	13.9	10.1	3.8	1.109
12	8.63	7.7	0.93	0.271
13	11.6	12.4	-0.8	-0.23
14	11.2	7.8	3.4	0.992
15	5.52	5.9	-0.38	-0.11
16	18.9	18.4	0.5	0.146
17	16.8	11.5	5.3	1.547
18	7.86	8.7	-0.84	-0.25
19	21.4	22	-0.6	-0.18
20	18.1	13.8	4.3	1.255
21	8.51	10.5	-1.99	-0.58
22	25.2	25.5	-0.3	-0.09
23	19.5	16	3.5	1.022
24	9.01	12.1	-3.09	-0.9
25	15.6	17.4	-1.8	-0.53
26	13.2	10.8	2.4	0.701
27	6.41	8.3	-1.89	-0.55
28	26.5	25.8	0.7	0.204
29	21.6	16	5.6	1.635
30	9.18	12.3	-3.12	-0.91
31	33.6	30.9	2.7	0.788
32	27.5	19.3	8.2	2.393
33	10	14.7	-4.7	-1.37
34	34.6	35.8	-1.2	-0.35
35	31.6	22.4	9.2	2.685
36	11	17.1	-6.1	-1.78

Appox. 95 % of Standardized Residuals fall into (+2,-2)

Table 9. Standardized Residuals of Cutting Force Model

Cutting Force Equation

$$Force = X_0 * Speed^{n1} * (Feed\ rate)^{n2} * (Depth\ of\ cut)^{n3}$$

where $X_0 = 4147.4$

$n1 = -0.632$

$n2 = 0.831$

$n3 = 1.158$

Therefore, the equation can be written as :

$$\ln(F) = x_0 + n1 * \ln(v) + n2 * \ln(f) + n3 * \ln(d)$$

where $x_0 = \ln(X_0) = 8.33$

Analysis Of Variance for the equation

Source of Variation	Sum of Squares	Degree of Freedom	Mean Square	Fo
Regression	9.862404	3	3.287468	51.68403
Error	2.035425	32	6.360E-02	
Total	11.89783	35		

Determination Coefficient (R^2) = 0.83
Correlation Coefficient (R) = 0.91

Correlation Matrix

F	1			
v	-0.54	1		
f	0.47	-0.01	1	
d	0.56	0	0	1
	F	v	f	d

Table 10. ANOVA of Cutting Force Model

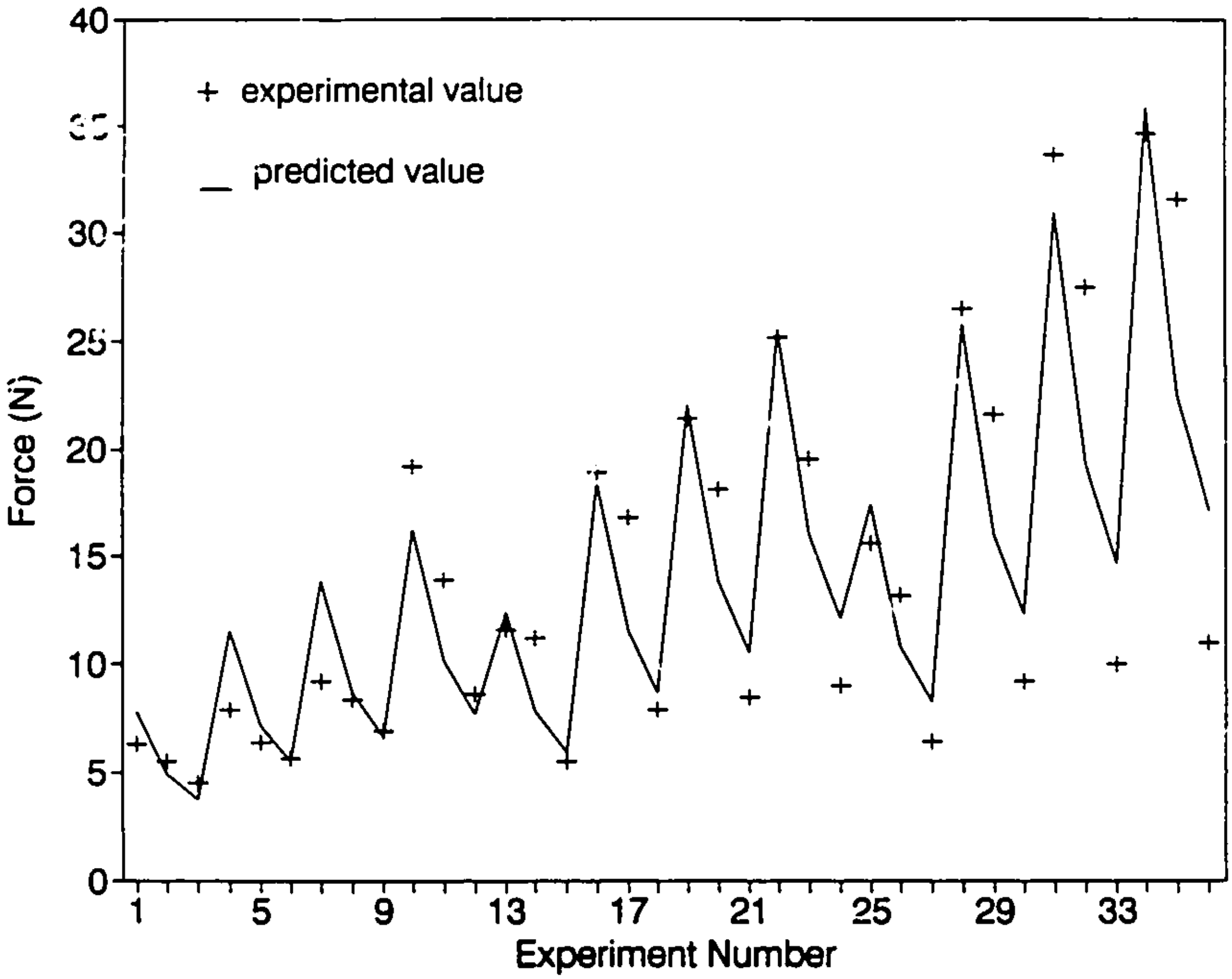

Fig. 6 Experimental & Predicted Cutting Force

cutting force within the maximum allowable level, the feed rate and the depth of cut cannot be too high while the cutting speed cannot be too low. Response curves of cutting forces at a depth of cut of 0.02 inch are shown in Figure 7. Other curves for different depths of cut from 0.04" to 0.2" are shown in Appendix C. It is found that at a specific feed rate the cutting speed increases significantly for a reduction of the cutting force under 10 N, while only a small change of the speed is adequate to cause the changes in the cutting force above 10 N. On the contrary, at the higher force level, a larger decrease in feed rate is needed to reduce the cutting force, and the higher the cutting speed, the larger the change in the feed rate needed to maintain the same level of force.

Moreover, since the cutting speed is used as one of the independent variables, it is actually a function of the spindle speed and the diameter of a cutting tool. Therefore, selections of the spindle speed and the cutting tool are to be considered to obtain the desirable cutting force level.

6.2 Tool life model

The experimental data of the tool life measurements are shown in Table 11. After applying the regression technique, the constant X_0 and the exponents n1, n2, and n3 are determined, and the tool life model is thus written as

$$y_2 = 9.64 - 1.02 * x_1 - 0.30 * x_2 - 0.85 * x_3,$$

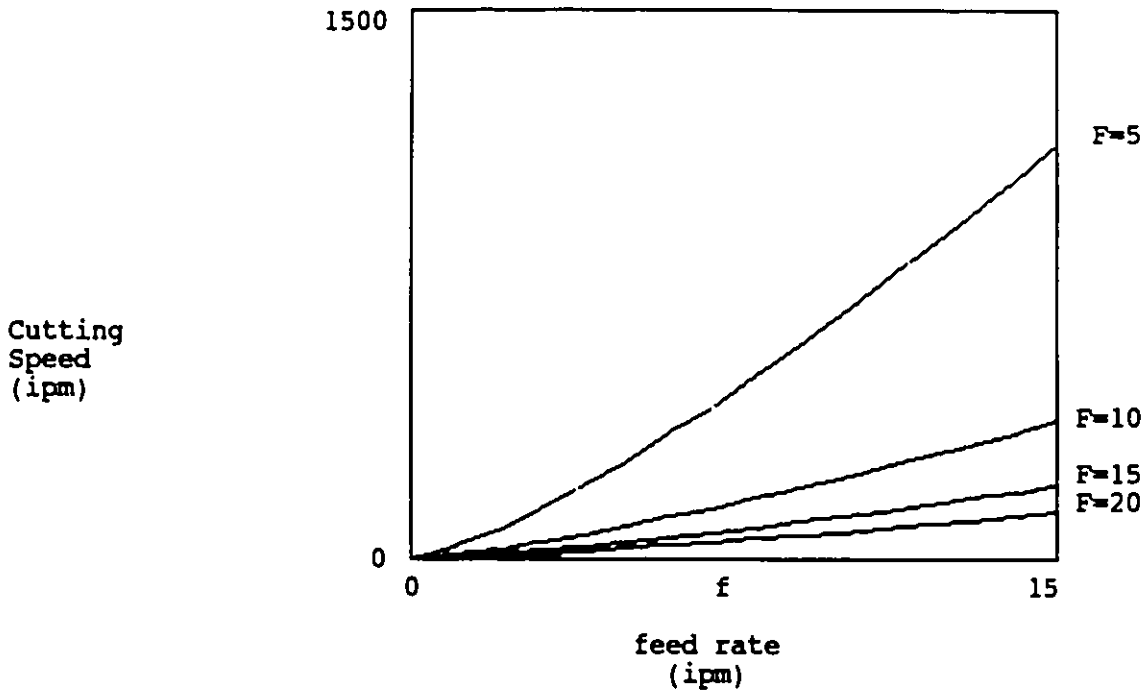

F = Cutting Force , N
d = Depth of Cut , in

Fig. 7 Response Curve of Cutting Force
depth of cut =0.02"

Experiments	Speed (fpm)	Feed rate (ipm)	depth of cut (in.)	Force (N)	Tool life (min.)
1	87.7	5	0.0625	30	88.8
2	185.9	5	0.0625	23	39.1
3	284	5	0.0625	10.76	29
4	87.7	8	0.0625	36.8	75.6
5	185.9	8	0.0625	28.36	27.9
6	284	8	0.0625	15.7	32.7
7	87.7	10	0.0625	49.7	75
8	185.9	10	0.0625	33.6	24.1
9	284	10	0.0625	22.4	24.8
10	87.7	8	0.09375	68.3	32.8
11	185.9	8	0.09375	36	23.2
12	284	8	0.09375	17.8	33.2
13	87.7	12	0.09375	87	46
14	185.9	12	0.09375	42.4	14.3
15	284	12	0.09375	31.6	30
16	87.7	8	0.125	85.3	25.4
17	185.9	8	0.125	52.7	7.9
18	284	8	0.125	30.3	11.6
19	87.7	12	0.125	104.3	36
20	185.9	12	0.125	86.2	15.8
21	284	12	0.125	62.9	11.9

Table 11. Experimental data of tool life measurements

where $y_2 = \ln(Y_2)$, Y_2 = Tool life , min.

$x_1 = \ln(X1)$, X_1 = cutting speed , ipm

$x_2 = \ln(X_2)$, X_2 = feed rate , ipm

$x_3 = \ln(X_3)$, X_3 = depth of cut, inch

or

$$Y_2 = 15367.3 * X1^{-1.02} * X2^{-0.3} * X3^{-0.85}$$

The adequacy of the linear model is examined by the analysis of variance. First, the correlation coefficient of 91% shows that the independent variables (cutting speed, feed rate and depth of cut) are closely related to the dependent variable (tool life). The F value of 26.93 for the model is much greater than the tabulated $F_{0.01,3,17}$ value of 5.14. This again implies that the independent variables are greatly significant for the models. Moreover, the assumption of normality is confirmed because a hundred percent of the standardized residuals fall in the interval (-2, +2), shown in Table 12; thereby, no outlier is present. As observed for the cutting force model, no pattern of variance is shown here too. Detailed analysis of variance and the correlation matrix are presented in Table 13. Figure 8 shows the experimental and the predicted values of the tool life. Observations from the correlation matrix show that only 0.36 percent of the variation of the tool life is explained by the feed rate. This implies that the feed rate does not affect the tool life as much as the other variables.

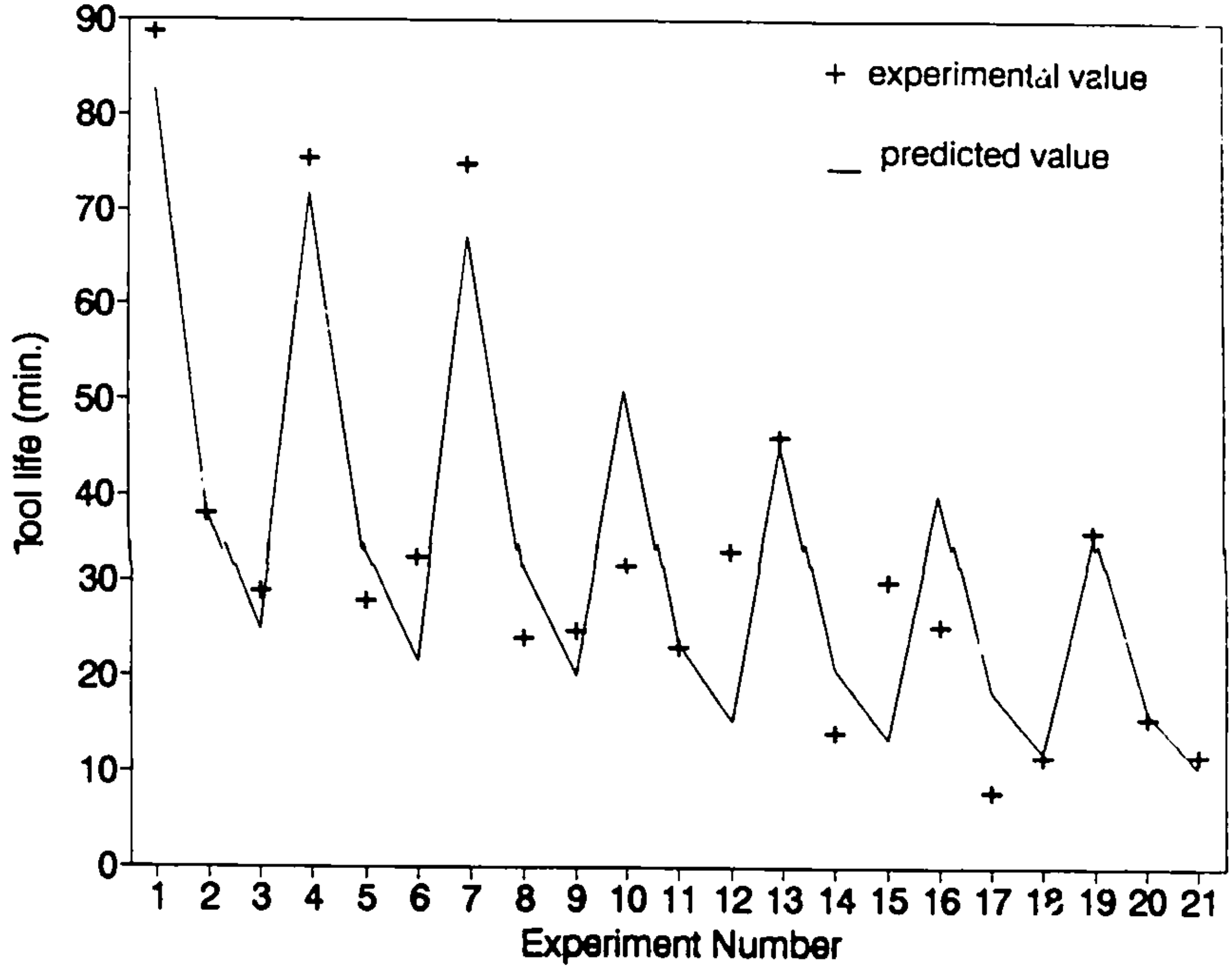

Fig. 8 Experimental & Predicted Tool LIfe

Experiment Number	Experimental Value (min)	Predicted Value	Residual	Std. Res.
1	88.7	82.6	6.1	0.054
2	38.1	38.5	-0.4	-0.00
3	29	25	4	0.035
4	75.6	71.9	3.7	0.033
5	27.9	33.4	-5.5	-0.04
6	32.7	21.7	11	0.098
7	75	67.2	7.8	0.070
8	24.1	31.2	-7.1	-0.06
9	24.8	20.3	4.5	0.040
10	31.8	50.9	-19.1	-0.17
11	23.2	23.7	-0.5	-0.00
12	33.2	15.4	17.8	0.159
13	46	45.1	0.9	0.008
14	14.3	21	-6.7	-0.06
15	30	13.6	16.4	0.147
16	25.4	39.9	-14.5	-0.13
17	7.9	18.5	-10.6	-0.09
18	11.6	12	-0.4	-0.00
19	36	35.3	0.7	0.006
20	15.8	16.4	-0.6	-0.00
21	11.9	10.7	1.2	0.010

100 % of Standardized Residuals fall into (+2,-2)

Table 12. Standardized Residuals of Tool life Model

Tool Life Equation

Tool Life = X_0 * Speed ^{n1} * (Feed rate) ^{n2} * (Depth of cut) ^{n3}

where $X_0 = e^{9.64}$

$n1 = -1.02$

$n2 = -0.30$

$n3 = -0.85$

Therefore, the equation can be written as :

$\ln(F) = x_0 + n1 * \ln(v) + n2 * \ln(f) + n3 * \ln(d)$

where $x_0 = \ln(X_0) = 9.64$

Analysis Of Variance for the equation

Source of Variation	Sum of Squares	Degree of Freedom	Mean Square	Fo
Regression	13.6757	3	4.558567	26.92506
Error	2.878197	17	0.1693057	
Total	16.5539	20		

Determination Coefficient (R^2) = 0.83
Correlation Coefficient (R) = 0.91

Correlation Matrix

Tool life (T)	1			
Speed (v)	-0.32	1		
Feed rate (f)	0.06	-0.92	1	
Depth of cut (d)	-0.23	-0.83	0.86	1

Table 13. ANOVA of Tool Life Model

According to the functional relationship revealed in the model, it is found that the tool life is decreased by increasing either the cutting speed, the feed rate or the depth of cut. Furthermore, the cutting speed is the chief variable that affects the tool life, while the feed rate affects the tool life the least. Therefore, it can be conjectured that, among the cutting conditions, it is the feed rate, not the cutting speed, that should be increased to the restricted maximum in order to improve the material removal rate. Figure 9 presents the response curves of the tool life, and the remaining curves for different cutting conditions are shown in Appendix D.

It is also observed that, just as for the cutting forces, a larger increase in the cutting speed is required in order to achieve a longer tool life. As previously mentioned, when the cutting speed is reduced to a certain level, the length of the tool life does not change much even though the feed rate is very high. Besides, approximately half of the length of the tool life is reduced when the depth of cut is doubled.

6.3 Seasonal cutting force pattern

Winter's method is applied and the parameters of the model are obtained and shown in Appendix E. In order to visualize the seasonal pattern, a forecasted pattern is plotted in Figure 10. Other plots for different cutting

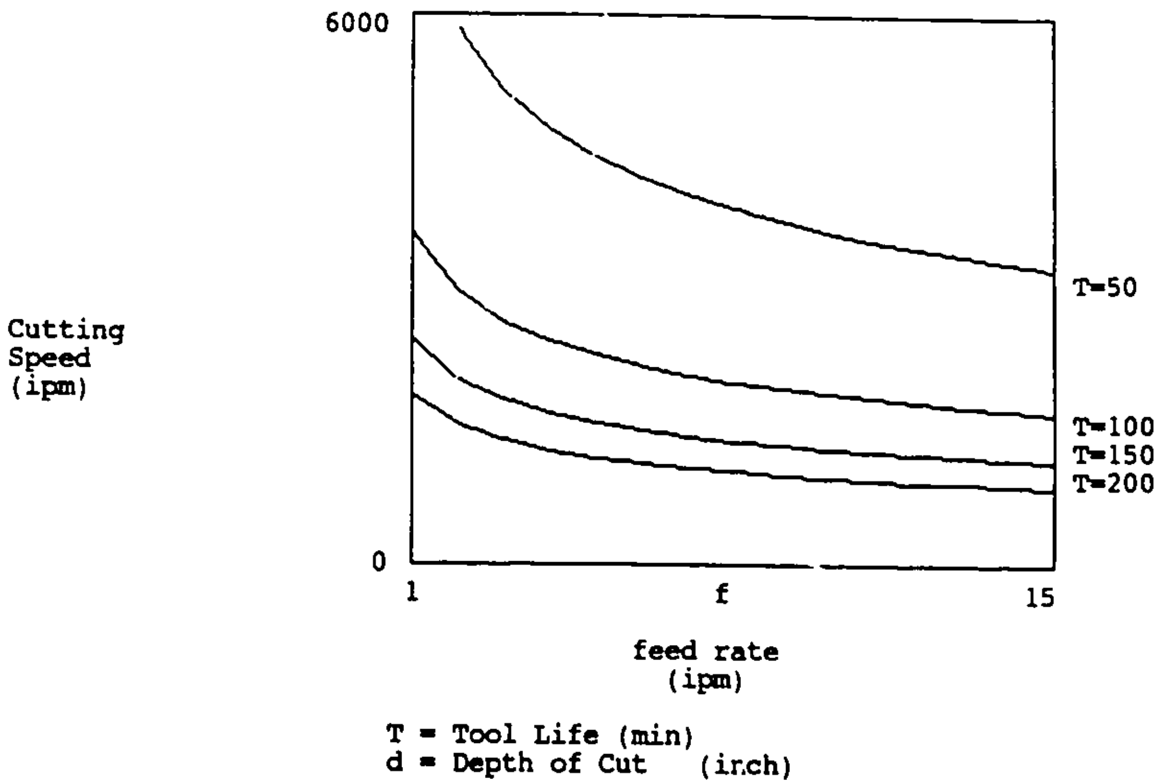

Fig. 9 Response Curve of Tool Life
depth of cut =0.02 inch

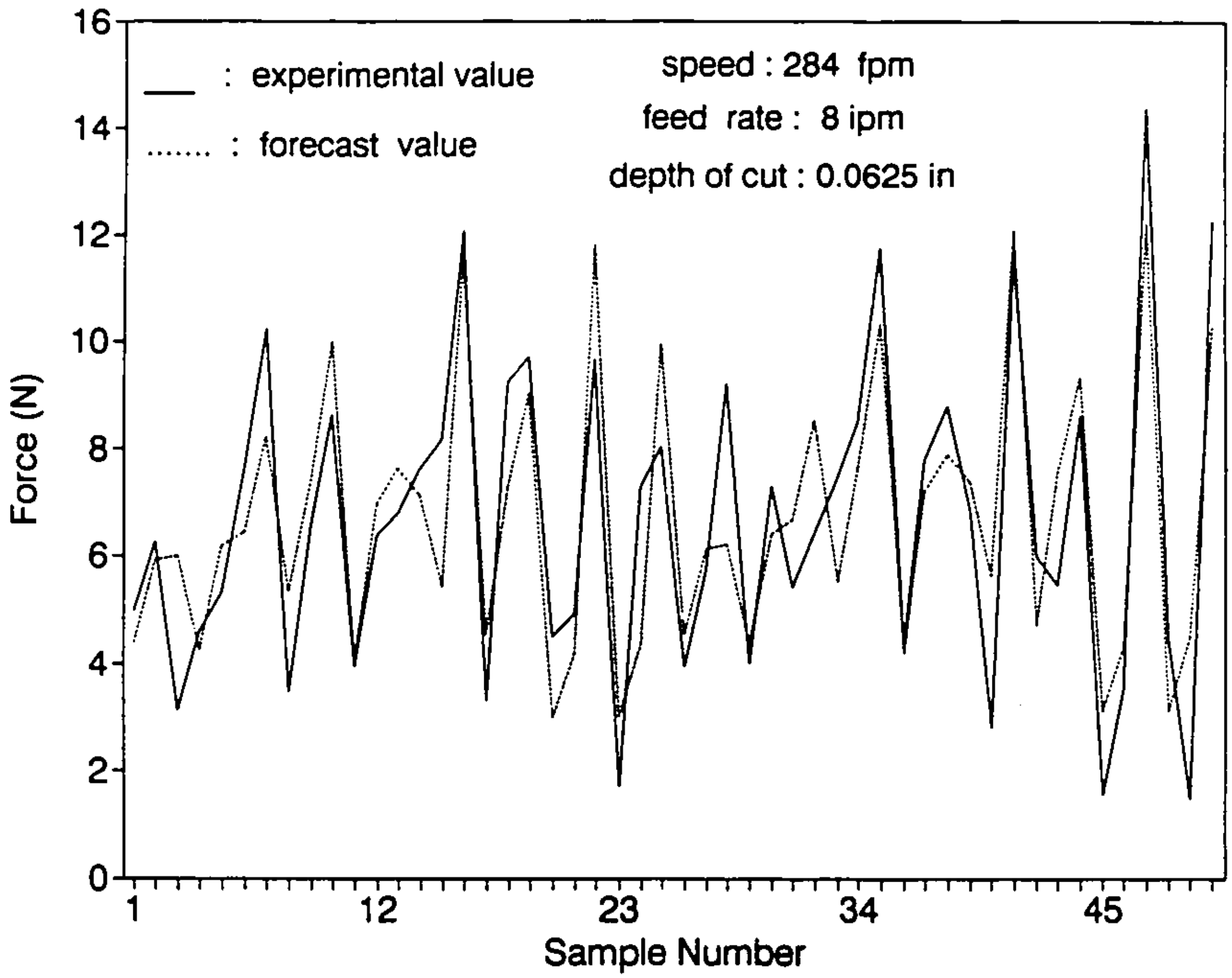

Fig. 10 Experimental & Forecasted Seasonal Pattern

conditions are presented in Appendix F.

According to the figures, most of the forecast samples follow the trend of the experimental samples. However, the exact force level cannot be estimated. This shows the stochastic nature of the cutting process. In addition, during each revolution of the spindle, any changes of the tool or the cutting conditions can change the pattern of the forces. Chipping is one of the possible causes. Therefore, the average variance of 20 percent is explainable.

6.4 Non-linear trend analysis

MathCAD has been used to smooth the non-linear trend of the bell-shaped curves, and the non-linear trend is presented in the mathematical form as

$$F_t = a_1 - b_1 * Re((t-t_0)^k)$$

In the above model, a_1, b_1, t_0 and k are determined by minimizing the mean absolute percentage error (MAPE), and the results are summarized in Table 14. Figure 11 shows some of the results while the rest are presented in the Appendix G. In the figures, the smooth curves are those determined by the model while the fluctuations are the actual cutting forces.

According to Table 14, there are some interesting observations. It is found that higher the feed rate or larger the depth of cut , the higher the value of a_1. Also, larger

$F = a - b * Re((t - t0)^k)$

cutting speed	feed rate	depth of cut	a	b	t_0	k	MAPE
185.9	12	0.125	63	0.009	50	2.26	0.19
185.9	10	0.125	38	0.004	57	2.25	0.16
185.9	12	0.09375	25	0.006	39	2.15	0.236
87.7	8	0.09375	26	0.002	71	2.23	0.20
87.7	10	0.09375	32	0.004	54	2.21	0.227
87.7	10	0.125	38	0.005	60	2.15	0.208
87.7	12	0.125	40	0.005	60	2.15	0.205
fpm	ipm	inch	N	N	--	--	---

Table 14. Parameter values of non-linear trends of force curves

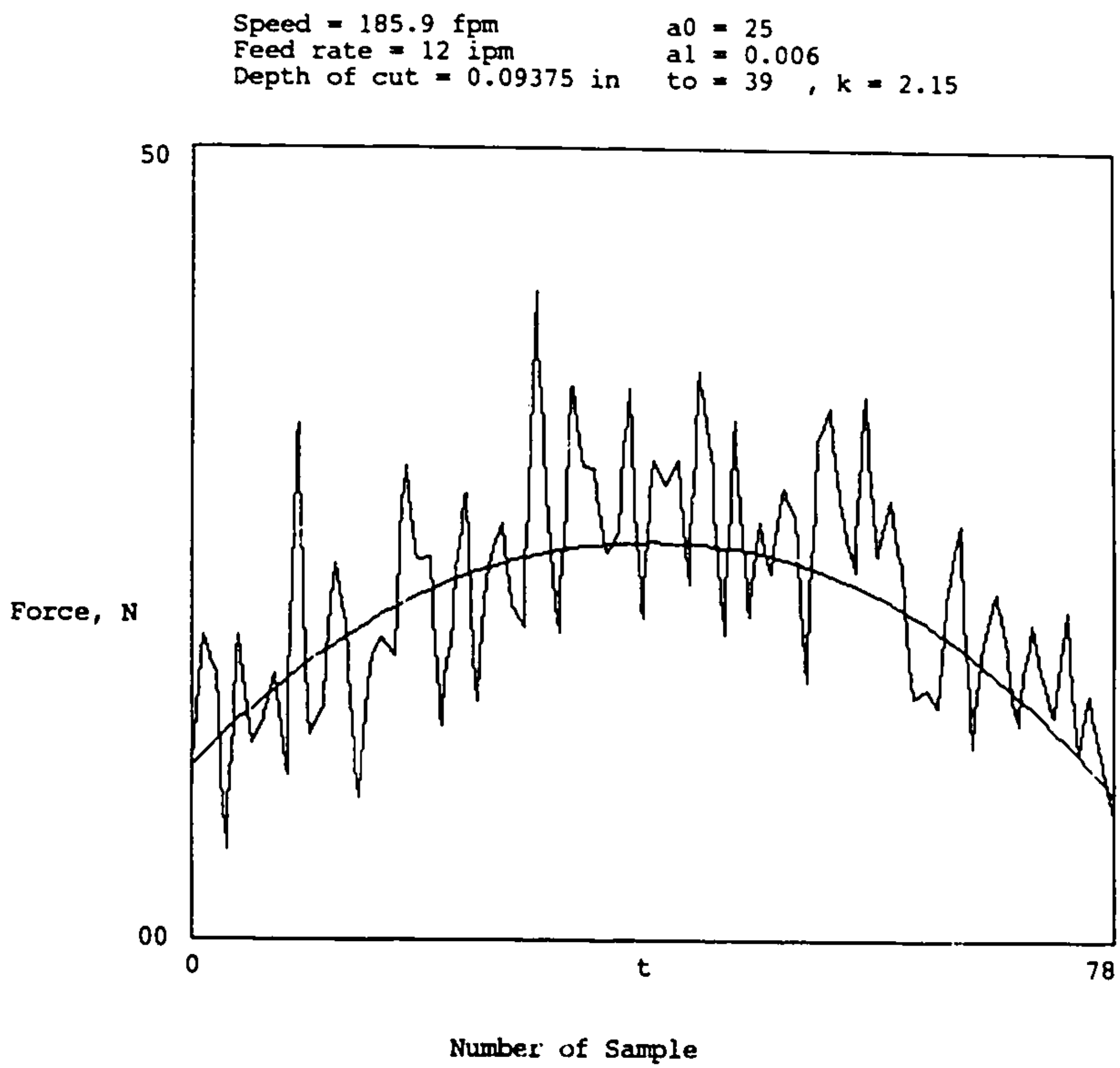

Fig. 11 Non-linear Trend Smoothing

the depth of cut, the higher the value of b_1. The value t_0 decreases when the feed rate is increased. In addition, the smaller the depth of cut, the higher the value of the MAPE. Furthermore, the non-linear trend in the cutting force does not occur under conditions of a small depth of cut, a low feed rate or a high speed. It should be noted that a high feed rate and a large depth of cut can lead to a high cutting force and a large tool wear. Thus, the force is developed and reaches a maximum, and drops when the cutting tool is leaving the workpiece. Another possible reason is that the tool wear or chipping is developed rapidly on the cutting tool. This increases the reaction force exerted on the tool. Thus, the feed rate decreases. As the feed rate decreases, the cutting force decreases too.

6.5 Tool Life/Force model

It is more practical to estimate the tool life in reference to the cutting force rather than the cutting time. Since the cutting time is definitely an independent variable, the tool life can be estimated when the cutting force changes according to tool and cutting conditions. The relationship between the tool life and the cutting force has been presented mathematically, and it is formulated and written as

$$Y_2 = 2.18 + 1.385/X$$

where Y_2 = Tool life ,min

X = Force ,N

A correlation coefficient of 0.965 shows that the cutting force can reasonably explain the tool life. It should be noted that according to the cutting force model, the higher the speed, the lower the force. Also, according to the tool life model, the higher the speed, the smaller the tool life. However, the tool life/ force model shows that the higher the force, the smaller the tool life. It is because both the feed rate and the depth of cut are affecting the tool life and the cutting force, and are compensating for the effect of the cutting speed. Table 15 presents the result of ANOVA. The experimental and the predicted tool life are shown in Figure 12.

6.6 Process optimization

Practical numerical values are used to formulate the cost objective function and the constraints. The tool life and the cutting force models are also applied. The numerical values are listed as follows :

C_w = \$ 3,	U_r = \$ 0.45/min,
U_o = \$ 0.3/min,	U_s = \$ 0.2/min,
U_m = \$ 0.2/min,	U_t = \$ 5/piece,
t_s = 3 min,	t_r = 2 min,
D = 0.5 in.,	d_0 = 1 in.,
L = 5 in,	n = 2,
v_{max} = 330 fpm,	v_{min} = 30 fpm,
f_{max} = 10 ipm,	f_{min} = 1 ipm,

Tool Life Equation

Three possible models are presented in the following :

1) Tool Life = 2.18 + 1.385 / Cutting Force

Analysis Of Variance for the model

	SS-Regr	SS-Error	SS-Total	Fo
	95824.19	7075.813	102900.0	257.3075
D. O. F.	1	19	20	

Determination Coefficient (R^2) = 0.931236
Correlation Coefficient (R) = 0.965006

* Cutting force > 0

Table 15. ANOVA table of Tool Life/ Cutting Force Model

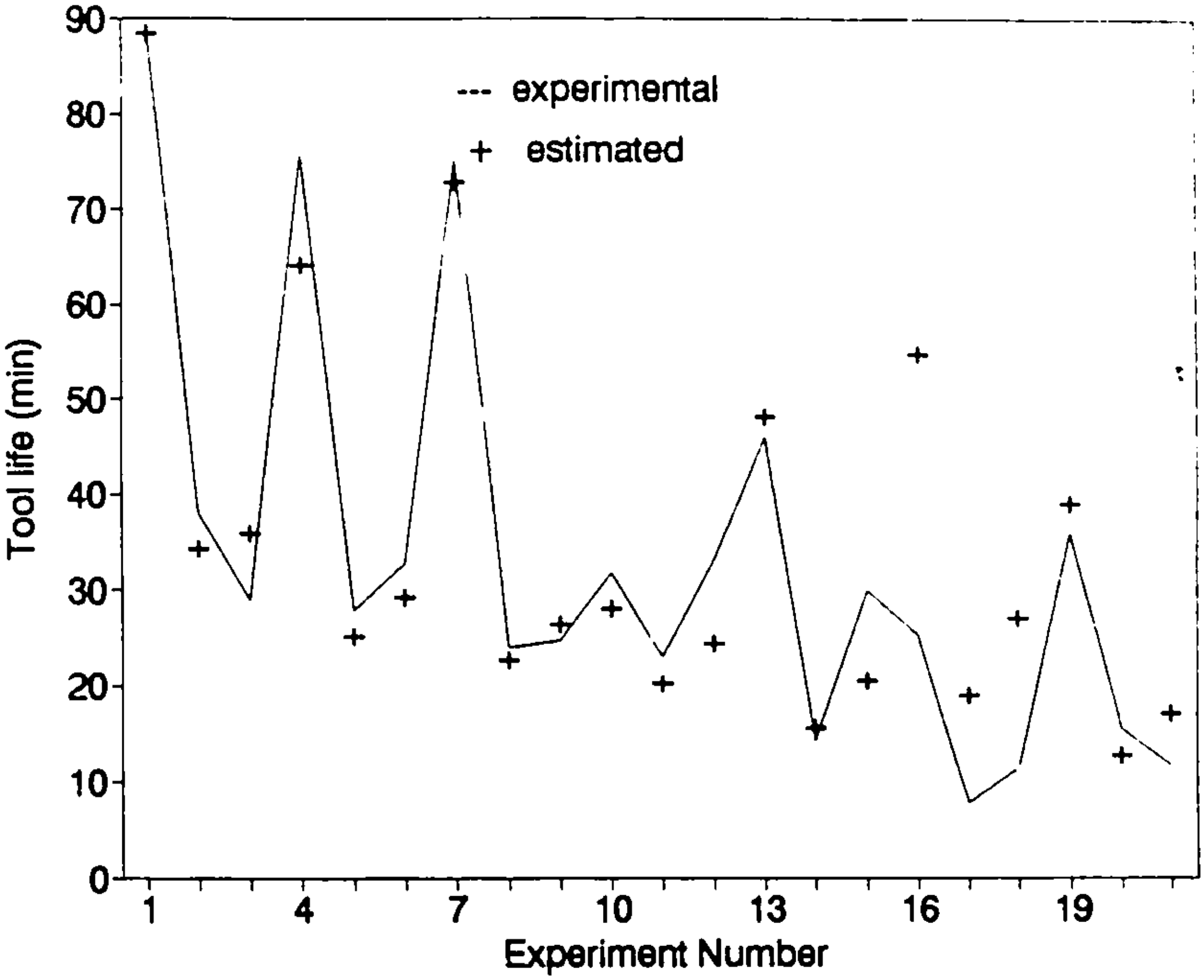

Fig. 12 Experimental & Predicted Tool Life

d_{max} = 0.02 in., d_{min} = 0.00001 in.,

P_{max} = 1.5 hp, eff = 0.8,

R_{max} = 10 microinch,

It should be noticed that the d_{max} and the f_{max} are obtained from the handbook [33], while the other parameters are determined based on machine capability. According to the experimental results, the maximum cutting force is approximately 150 percent of the average force level. Therefore, a safety factor of 1.5 is used to adjust the average value obtained from the cutting force model. This factor ensures that the power required is less than the power available. The optimal cutting conditions are then determined by following the procedures discussed previously in chapter 5, and the results are as follows:

feed rate = 10 ipm,

cutting speed = 146 fpm,

depth of cut =0.2 in.

total cost = $ 8.08

Figure 13 shows the effects of the different conditions on the cost.

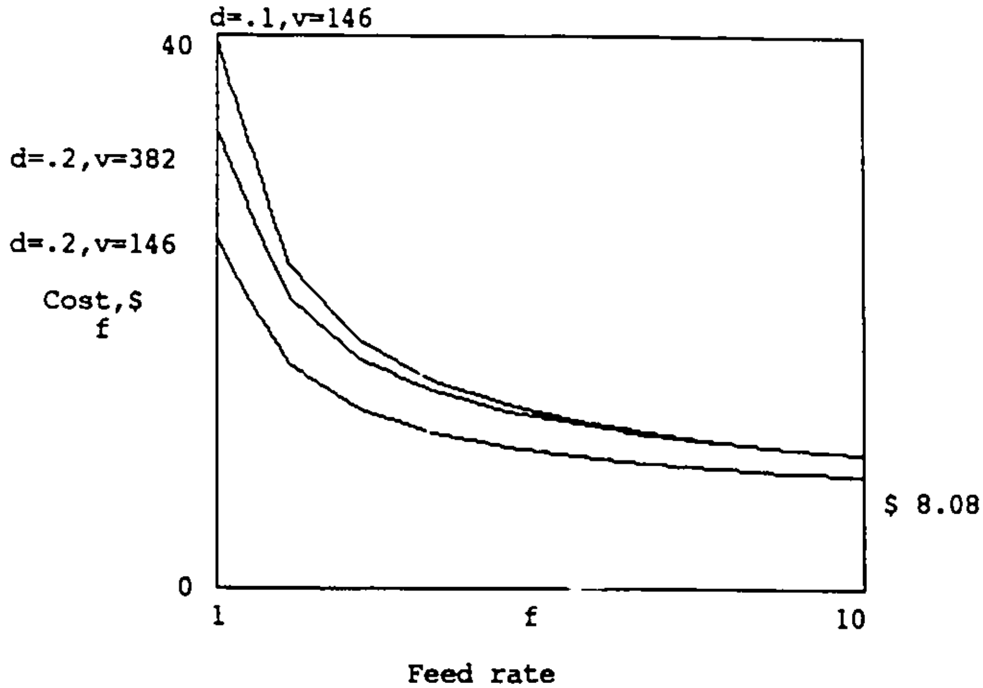

d = depth of cut (0.2 in.is the max.)
v = cutting speed (146 is the max. speed restricted by surface roughness constraint at f=10),(fpm)

Table 13. Effects of different cutting conditions on cost

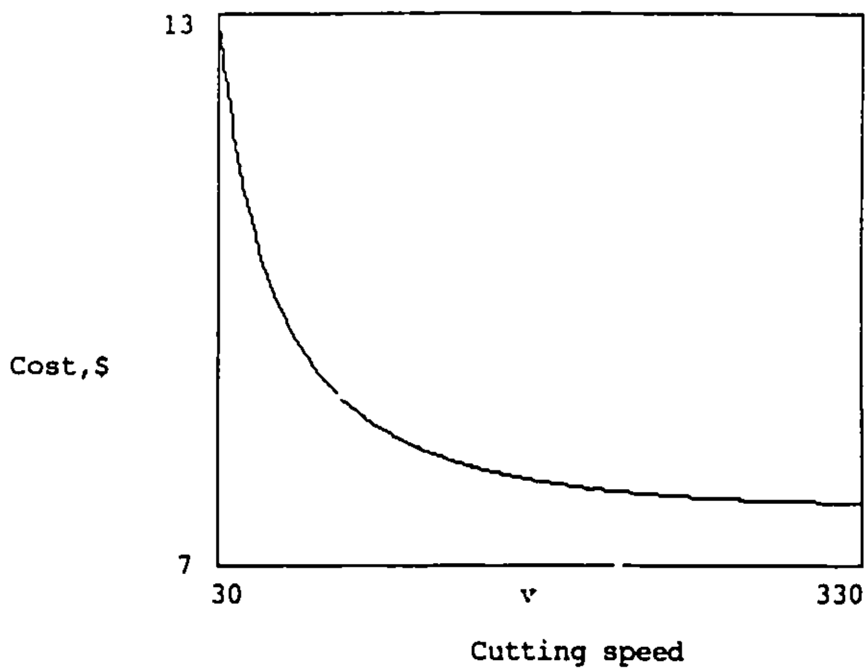

d = depth of cut (0.2 in.is the max.)
v = cutting speed (146 is the max. speed restricted by surface roughness constraint at f=10),(fpm)

Table 13. (cont'd) Effects of different cutting conditions on cost

Chapter 7

Conclusions

On-line cutting rorce measurements for milling an aluminum alloy and the tool life measurements of the HSS cutting tool were carried out in this research under different cutting conditions. According to the experimental results, analyses were performed and presented in the study. During the experiments, the necessary equipment were integrated, and an on-line cutting force monitoring system was designed. Since the cutting speed, the feed rate and the depth of cut were the controllable variables that affect the state of the cutting tool and the cutting process, their relationships with the cutting force, the tool life, and the total part production cost were investigated. The work achieved in this research can be summarized as follows:

1. The adequacy of the mathematical models of the cutting force and the tool life developed in this research was established.
2. The effects of the cutting parameters on the cutting forces were studied and it was shown that the cutting speed, the feed rate and the depth of cut affected the cutting process and the cutting tool significantly.
3. According to the ANOVA results of the tool life and tool life/force models, the cutting force was more related to the tool life than to other cutting parameters.

4. Based on the previous observation, one or more unknown factor(s) might be included in the cutting force model.
5. A bell-shaped curve of cutting force was formed under the condition of a low cutting speed and a high feed rate and a large depth of cut. It was found that the cutting parameters were affecting the shape of the curve.
6. The optimal cutting condition was obtained by formulating a non-linear constrained optimization based on the minimum cost, in which the cutting force and the tool life models were applied. The higher the feed rate and the lower the cutting speed, the lower was the cost.

However, the cutting force pattern could not be estimated perfectly. It is because of the stochastic nature of the cutting process.

Finally, some suggestions for further studies are recommended, and they are as follows:

1. A higher sampling rate should be used to collect the cutting force signals, and a more advanced microprocessor which can process the data at a higher speed should be used to perform the on-line monitoring.
2. More experiments of the cutting process under the conditions causing the bell-shaped cutting force pattern should be conducted and analyzed.
3. A tool breakage prediction system can be studied and developed by using an effective tool life-cutting force

model.

4. The relationship between the cutting force and the surface roughness should be studied and thus an on-line surface roughness monitoring system can be developed.

5. An adaptive control optimization system should be studied and developed to control the tool wear rate and the surface roughness.

The direction of future research is presented in Table 14.

Finally, it should be noted that in reporting the results, 3, 4, 5 and even 6 significant figures are shown in the data. However, it is the author's opinion that probably only two significant figures can be justified.

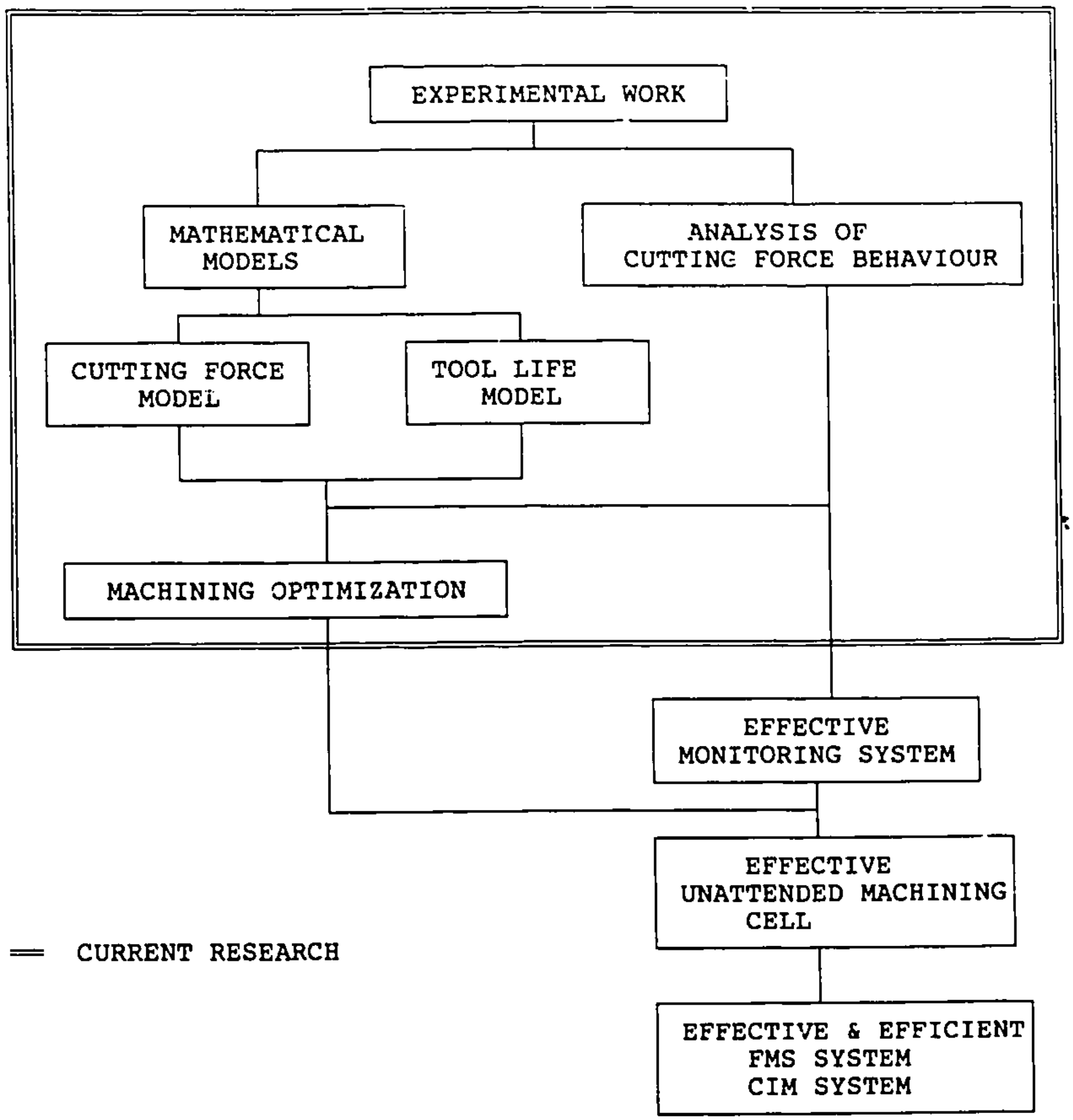

FIG. 14 Direction of Future Research

References

1. Koren, Y. "Computer control of manufacturing system", McGraw Hill, p.249, 1985.

2. Wright, P.K. "physical models of tool wear for adaptive control in flexible machining cells" CIM-PED-Vol 8, p.19-31, 1984.

3. Martin, K.F.,Brandon, J.A., Grosvenor, R., Owen, A. "A comparison of in-process tool wear measurement methods in turning", Proceedings of the 26th International machine tool design and research conference", p.289-296, 1986.

4. Arosorski, S.M., "Wear sensors in the adaptive control of machine tools", Int.J.Prod.Research Vol 21 no.3, p.347-356, 1983.

5. Wilkinson, A.J., "Construction-resistance concept applied to wear measurement of metal cutting tools", Proc.IEE Vol.118,no.2, 1971.

6. Uehara, K., "New attempts for short time tool life testing", Annals of the CIRP 22(1), 1973

7. Novak, A., "Monitoring of the tool conditions by means of photodiode arrays", Manuf.System Vol.12,no.3, p.245-255, 1983.

8. Essel, K.,Otto, F., Kirchner, W., "Sensor zum erfassen des frei-flachenverschleises an drehwerkzeugen", VDI-Z 116,no.17, p.1427-1429, 1974.

9. Spur, G., Lenards, F., "Sensoren zur erfassung von prozesskenngrossen bei der krehbearbeitung", Annals of the CIRP Vol. 24(1), 1973.

10. Essel, K., Hansel, W., "Development of sensors for process control systems in the field of production engineering", PDV-Rep KFK-PDV 41, Gesellschaft fur Kernforschung mbH, Karlsruhe, 1975.

11. Shillman, N.F., "The on-line control of cutting conditions using direct feedback", Proc. 12th Int.MTDR Conference, 1971,

12. Solaja, V., Vukelja, "Identification of tool wear rate by temperature variation of a carbide tip", Annals of the CIRP Vol. 22(1), p.117-119, 1973.

13. Micheletti, G.F., "Relationship between cutting forces and tool wear in steel turning", 7th Int.MTDR Conference

Birmingham, 1966.

14. Tlusty, J., Andrews, G.C., "A critical review of sensors for unmanned machining, Annals of CIRP Vol.32(2) p.563-572, 1983.

15. Takeyama, H., "Automation developments in Japan", 3rd North Metalworking Research Conference, p.672-785, 1975.

16. Martin, P., Mutels, B., Drapier, J.P., "Influence of lathe tool wear on the vibrations sustained in cutting", Proc. of the 15th MTDR Conf, p.251-257, 1974.

17. Hingle, T.H., Rakels, J.H., "The practical application of diffraction techniques to assess surface finish of diamond turned parts", Annals of CIRP Vol.32(1), p.499-501, 1983.

18. Weller, E.J., Schrier, H.M., Welchbrodt, B., "What sound can be expected from a worn tool?", Trans ASME J Eng.Ind Vol.91 no.3, p.525-534, 1969.

19. Lan, M.S., Naerheim, Y., "In-process detection of tool breakage in milling", ASME J Eng.Ind., Vol. 108, 1986.

20. Altintas, Y., Yellowley, I., Tlusty, J., "The detection of tool breakage in milling operations", ASME J Eng.Ind., Vol. 110, 1988.

21. Altintas, Y., Yellowley, I., "In-process detection of tool failure in milling using cutting force models", ASME J. Eng.Ind.,Vol. 111, 1989.

22. Jacobs, H. J., Hentschel, B., Stange, B., "Intelligent tool monitoring for machining", INT. J. PROD. RES., Vol. 26, No. 10. 1988.

23. Tarn, J. H., Tomizuka, M., "On-line monitoring of tool and cutting conditions in milling", ASME J. Eng. Ind., Vol. 111, 1989.

24. Fussell, B. K., Srinivasan, K., "On-line identification of end milling process parameters", ASME J. Eng. Ind., Vol. 111, 1989.

25. Billatos, S.B., Tseng, P.C., "Knowledge based optimization for intelligent machining", SME J. Manfa.System Vol.10 no.6, 1991

26. Suliman, S.M.A., Hassan, G.A., " Modelling, optimization and response curves of milling low carbon steel", Int. J. Prod. Res., Vol.29, no.4, p.725-737, 1991.

27. "User manual for MetraByte ADC interface board DAS-50", MetraByte Cor..

28. "User manual for Model 5004 dual mode amplifier", Kistler Instrument Cor..

29. "User guide for transducer type 9067", Kistler Instrument Cor..

30. Wakil, El., Sherif, D., "Process and design for manufacturing", Prentice-Hall, p.299, 1989.

31. "Applied fourier analysis", HBJ college outline series, p.137.

32. Hitomi, "Manufacturing systems engineering", Taylor & Francis, Ltd., p.177-183, 1979.

33. "Machining Aluminum", Aluminum company of Canada, Ltd., p.48, 1953.

Appendix A

Program Listing

of

PLOT.BAS & Sample NC part program

Porgram listing of PLOT.BAS

```
10 CLEAR : KEY OFF
20 REM ***************************************************
30  REM *         SIMPLE PROGRAM "PLOT" WRITTEN BY JASON
40  REM *                         TO
50  REM *    COLLECT DATA FROM THE FORCE TRANSDUCER THRU' THE
60  REM *    ADC BOARD BY USING THE CHARGE AMPLIFIER AND PLOT
70  REM *    THE DATA ON SCREEN. ALSO THE DATA CAN BE STORED
80  REM *    INTO DATA FILE 240000 SAMPLES ARE COLLECTED AND
90  REM *    THERE ARE 60 POINTS WHICH ARE THE AVERAGES OF
100 REM *    EVERY 40 SAMPLES, THUS 600 POINTS ARE SHOWN ON
110 REM *    SCREEN.
115 REM ***************************************************
120 CLS : LOCATE 1,1,0 : INPUT "ENTER THE DATE (MM-DD-YYYY)
    " , D$
130 INPUT "ENTER THE TIME (HH:MM)  " , T$
140 CLS
150 INPUT "ENTER THE FEEDRATE        (ipm)      ",F
160 INPUT "ENTER THE SPINDLE SPEED   (rpm)      ",S
170 INPUT "ENTER THE DOC             (in)       ",D
180 INPUT "ENTER THE SCALE           (N/V)      ",SC
190 INPUT "ENTER THE NAME OF THE DATA FILE (with the
    extention)",DATNAME$
200 LOCATE 20,10 : PRINT "PRESS C TO CORRECT THE ABOVE
    PARAMETERS OR "
210 LOCATE 21,10 : PRINT "PRESS ANY KEY TO CONTINUE ------
    THANK YOU !"
220 C$=INKEY$ : IF C$="" THEN 220
230 IF (C$="c" OR C$="C") THEN 140
240 DIM SUM%(10,65), PT%(10,65), D%(1605), FX(605), FY(605),
    FZ(605),FR(605)
250 OPEN "$DAS50" FOR OUTPUT AS #1
260 PRINT #1,"CLEAR"
270 OPEN "$DAS50" FOR INPUT AS #2
280 KEY OFF : CLS :COLOR 15,0
290 PRINT "PRESS RETURN WHEN READY TO COLLECT DATA"
300 V$=INKEY$
310 IF V$<>CHR$(13) THEN GOTO 300
320 'customized plot routine
330 KEY OFF
340 SCREEN 2
350 LINE (30,0)-(30,140)         'vert.-axis
360 LINE (30,140)-(630,140)      'hori.-axis
370 FOR I=0 TO 9                 'INSERT MARKERS   FOR Y-AXIS
380 LINE (29,I*14)-(31,I*14)
390 NEXT I
400 FOR I=0 TO 10                'INSERT MARKERS FOR X-AXIS
410 LINE (30+I*60,139)-(30+I*60,141)
420 NEXT I
430 LOCATE 1,1 :PRINT "20X"
440 LOCATE 1,7 : PRINT "X=";SC
```

```
450 LOCATE 9,1 : PRINT "10X"
460 LOCATE 18,3 : PRINT "0"
470 LOCATE 19,4 : PRINT "0        1       2       3       4
     5       6       7       8       9      10"
480 LOCATE 21,30 : PRINT "TIME    (Sec.)"
490 LOCATE 1,79,0
500 'PLOT POINTS
510 FOR N=1 TO 600
520 PRINT #1, "SA 1600 RATE INT 2.4E4 ch 0&1&2&3 +-10v tm 0
     ACquire"
530 FOR II=1 TO 850 : NEXT II
540 PRINT #1, "Set ADdress 0"
550 PRINT #1, "transfer ";-1;VARPTR(D%(0));1600
560 FX(N)=(D%(0)+D%(396)+D%(796)+D%(1196)+D%(1596))/5
570 FY(N)=(D%(1)+D%(397)+D%(797)+D%(1197)+D%(1597))/5
580 FZ(N)=(D%(2)+D%(398)+D%(798)+D%(1198)+D%(1598))/5
590 FR(N)=((FX(N))^2+(FY(N))^2+(FZ(N))^2)^.5
600 GOSUB 960
610 NEXT N
620 LOCATE 23,6 : PRINT "PRESS Y TO STORE THOSE DATA "
630 FOR N=1 TO 600
640 FX(N)=FX(N)*10!/2048                                    :
650 FY(N)=FY(N)*10!/2048
660 FZ(N)=FZ(N)*10!/2048
670 FR(N)=FR(N)*10!/2048
680 NEXT N
690 Y$=INKEY$ : IF Y$="" THEN 690
700 IF (Y$<>"Y" AND Y$<>"y") THEN GOTO 880
710 'WRITE DATA INTO FILE
720 OPEN DATNAME$ FOR APPEND AS #3
730 PRINT #3, "Date  :",D$,"      Time   :",T$
740 PRINT #3,
750 PRINT #3, "Feedrate           (in)     = ", F
760 PRINT #3, "Spindle speed      (rpm)    = ", S
770 PRINT #3, "Doc                (in)     = ", D
780 PRINT #3, "Scale              (N/V)    = ", SC
8    0    0    P    R    I    N    T    #    3    ,
"-------------------------------------------------------
----------------"
810 PRINT #3, "TIME _sec","F-R _N","Fx _N","Fy _N","Fz _N"
8    2    0    P    R    I    N    T    #    3    ,
"-------------------------------------------------------
----------------"
830 FOR N=1 TO 600
840 PRINT #3, USING"####.###    "; N/60, FR(N), FX(N), FY(N),
FZ(N)
850 NEXT N
8    6    0    P    R    I    N    T    #    3    ,
"=======================================================
================"
870 CLOSE #3
880 SCREEN 0 : CLS : PRINT "PRESS ANY KEY TO CONTINUE OR PRESS
     Q TO QUIT"
890 Q$=INKEY$ : IF Q$="" THEN 890
```

```
900 IF (Q$<>"Q" AND Q$<>"q") THEN GOTO 980
910 PRINT
920 PRINT "ARE YOU SURE (Y/N)"
930 N$=INKEY$ : IF N$="" THEN 930
940 IF (N$<>"N" AND N$<>"n") THEN SYSTEM
950 GOTO 880
960 LINE (30+N,OLD)-(30+N,140!-(FR(N)*70!/2048))
970 OLD=140!-(FR(N)*70!/2048) : RETURN
980 CLOSE
990 GOTO 10
```

Program Listing

Sample NC part program

G90	Absolute coordinat.
G94	Set the dimension (inch)
F5	Set the feed rate to 5 ipm
G01X0Y0Z-0.0625	Position the cutting tool
M03	Start the spindle
G01X-4	Cut a slot
G01Z0.2	Back to home
G01X0Y0	Back to home
M30	Stop the spindle

Appendix B

Curves of Cutting Forces

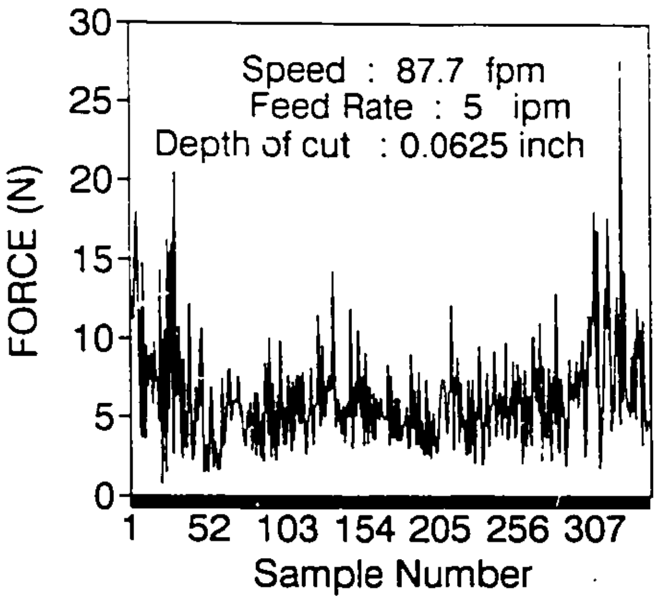
Speed : 87.7 fpm
Feed Rate : 5 ipm
Depth of cut : 0.0625 inch
FORCE (N)
0
5
10
15
20
25
30
1
52
103
154
205
256
307
Sample Number

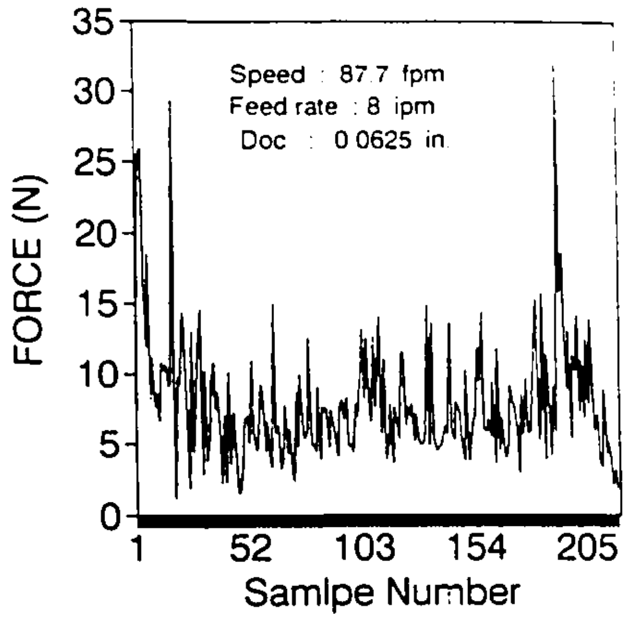
Speed : 87.7 fpm
Feed rate : 8 ipm
Doc : 0.0625 in.
FORCE (N)
0
5
10
15
20
25
30
35
1
52
103
154
205
Samlpe Number

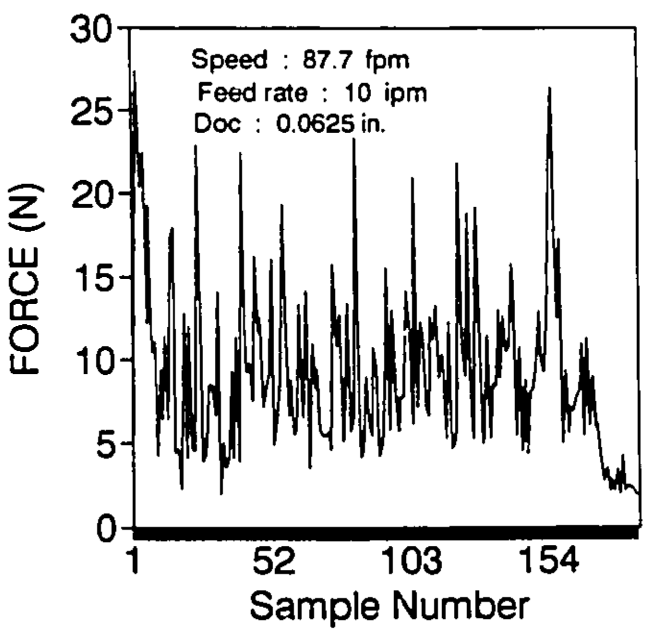
Speed : 87.7 fpm
Feed rate : 10 ipm
Doc : 0.0625 in.
FORCE (N)
0
5
10
15
20
25
30
1
52
103
154
Sample Number

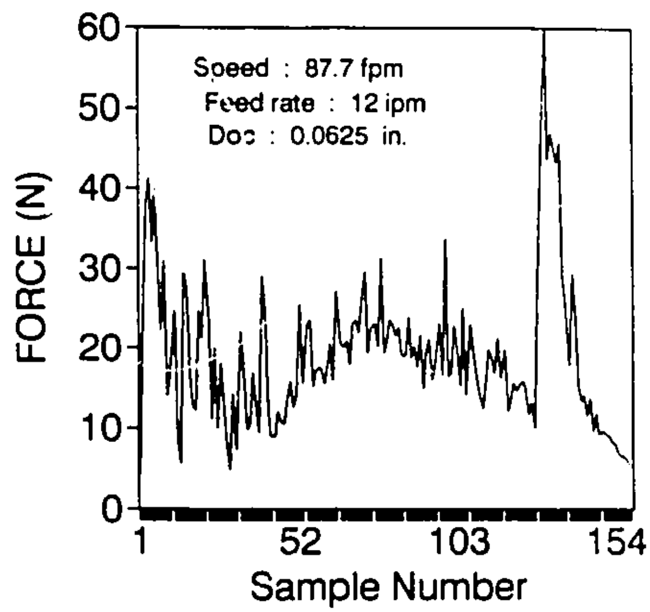
Speed : 87.7 fpm
Feed rate : 12 ipm
Doc : 0.0625 in.
FORCE (N)
0
10
20
30
40
50
60
1
52
103
154
Sample Number

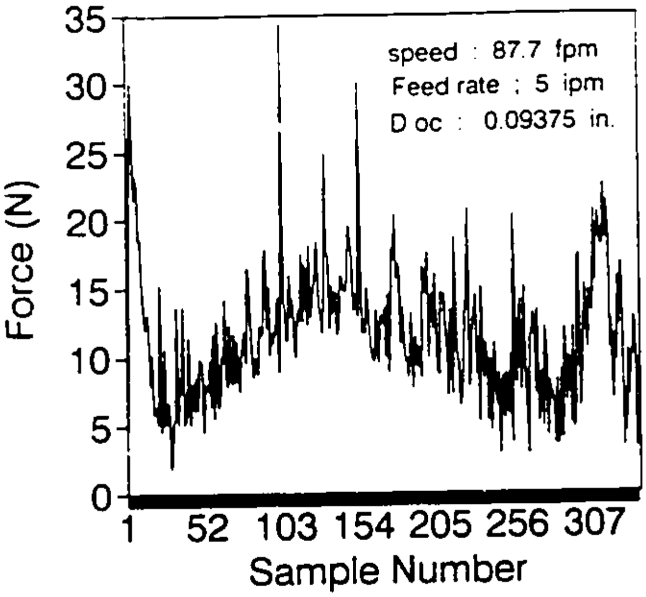
speed : 87.7 fpm
Feed rate ; 5 ipm
D oc : 0.09375 in.
Force (N)
0
5
10
15
20
25
30
35
1
52
103
154
205
256
307
Sample Number

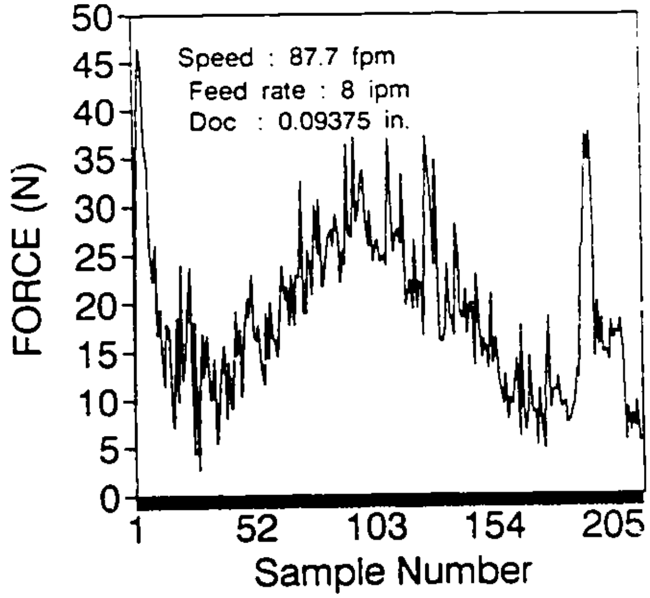
Speed : 87.7 fpm
Feed rate : 8 ipm
Doc : 0.09375 in.
FORCE (N)
0
5
10
15
20
25
30
35
40
45
50
1
52
103
154
205
Sample Number

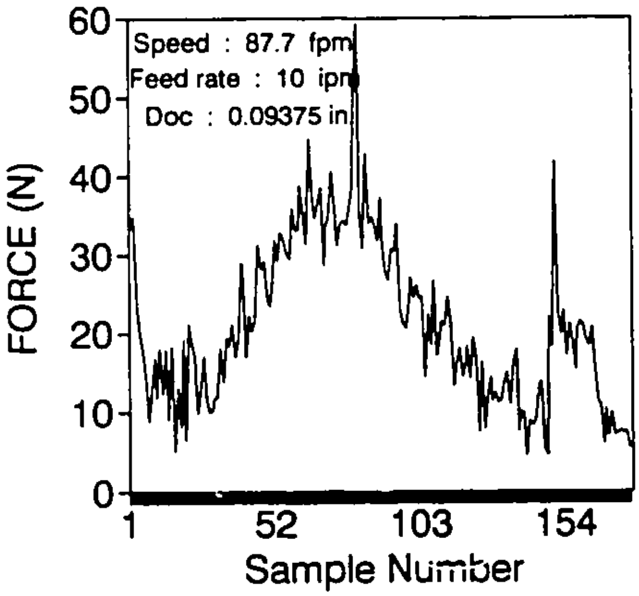
Speed : 87.7 fpm
Feed rate : 10 ipm
Doc : 0.09375 in.
FORCE (N)
0
10
20
30
40
50
60
1
52
103
154
Sample Number

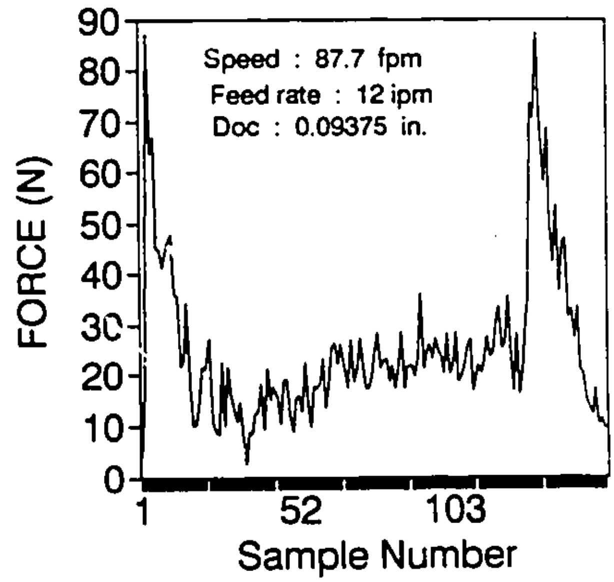
Speed : 87.7 fpm
Feed rate : 12 ipm
Doc : 0.09375 in.
FORCE (N)
0
10
20
30
40
50
60
70
80
90
1
52
103
Sample Number

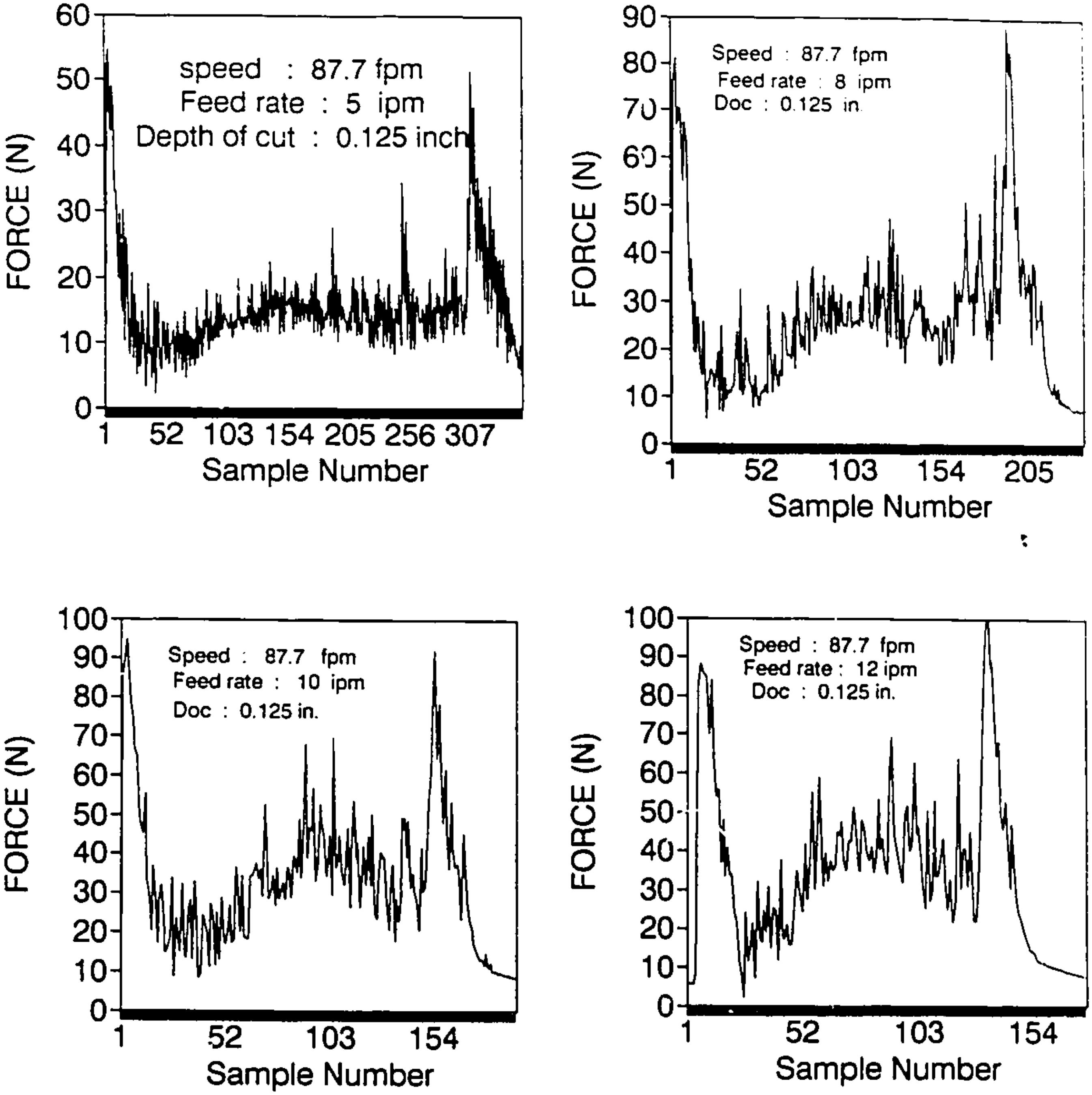
speed : 87.7 fpm
Feed rate : 5 ipm
Depth of cut : 0.125 inch
FORCE (N)
Sample Number
Speed : 87.7 fpm
Feed rate : 8 ipm
Doc : 0.125 in.
FORCE (N)
Sample Number
Speed : 87.7 fpm
Feed rate : 10 ipm
Doc : 0.125 in.
FORCE (N)
Sample Number
Speed : 87.7 fpm
Feed rate : 12 ipm
Doc : 0.125 in.
FORCE (N)
Sample Number

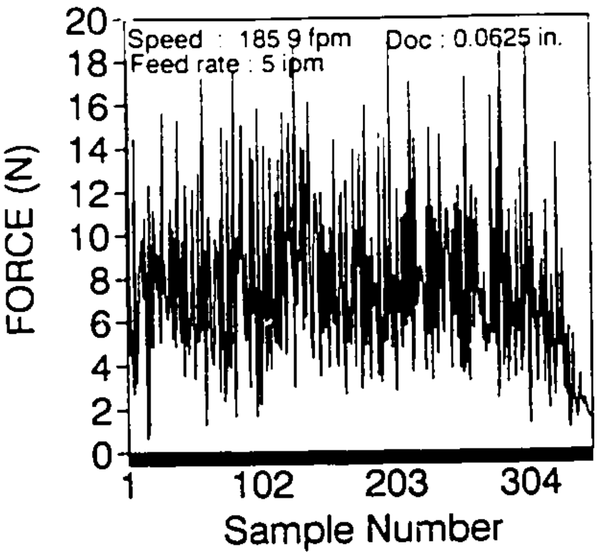
Speed : 185.9 fpm
Doc : 0.0625 in.
Feed rate : 5 ipm
FORCE (N)
Sample Number

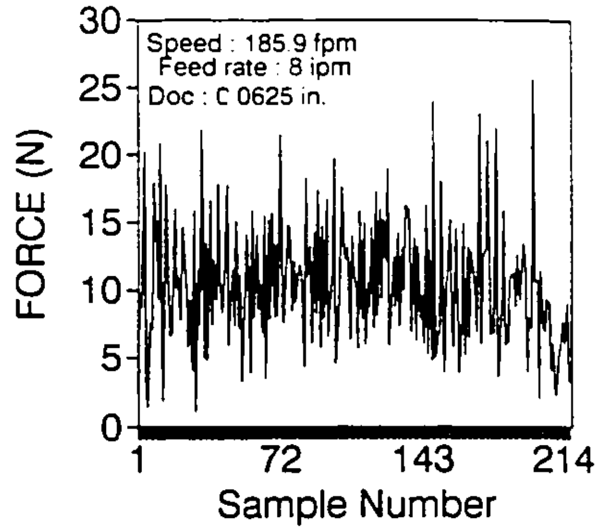
Speed : 185.9 fpm
Feed rate : 8 ipm
Doc : 0.0625 in.
FORCE (N)
Sample Number

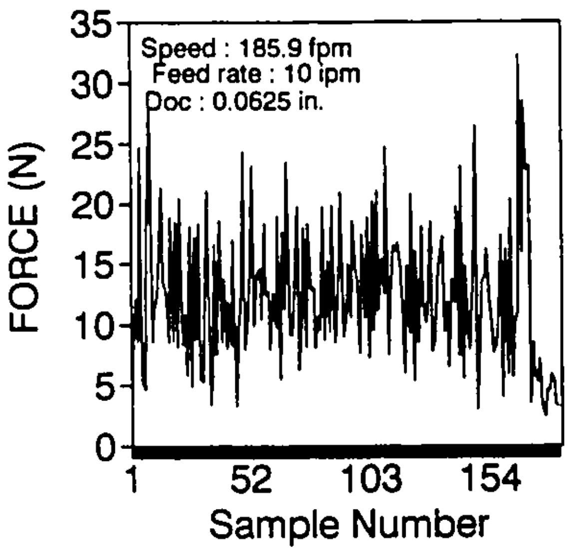
Speed : 185.9 fpm
Feed rate : 10 ipm
Doc : 0.0625 in.
FORCE (N)
Sample Number

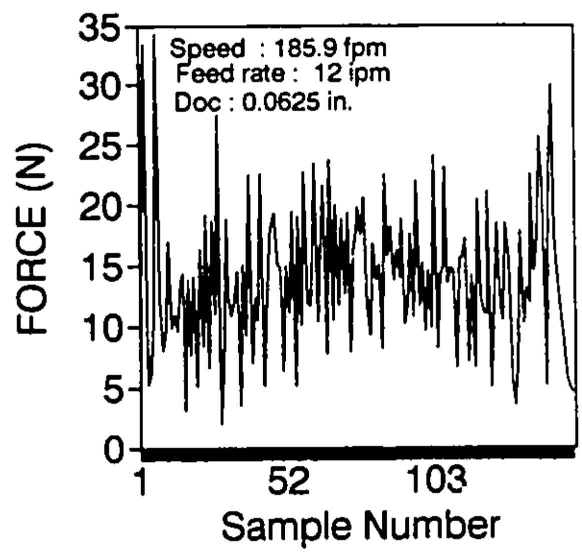
Speed : 185.9 fpm
Feed rate : 12 ipm
Doc : 0.0625 in.
FORCE (N)
Sample Number

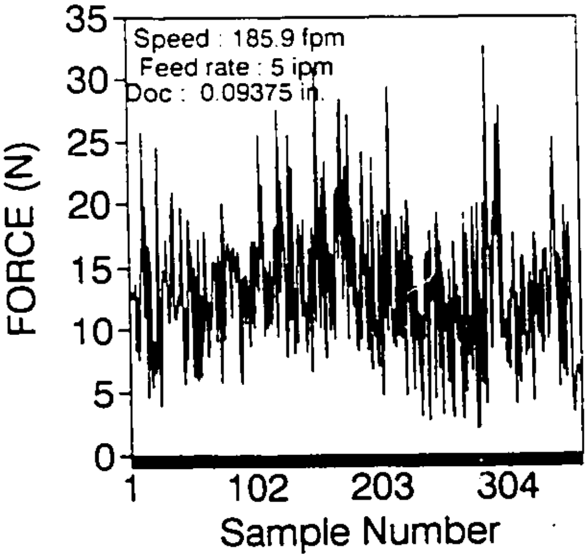
Speed : 185.9 fpm
Feed rate : 5 ipm
Doc : 0.09375 in.
FORCE (N)
Sample Number
35
30
25
20
15
10
5
0
1
102
203
304

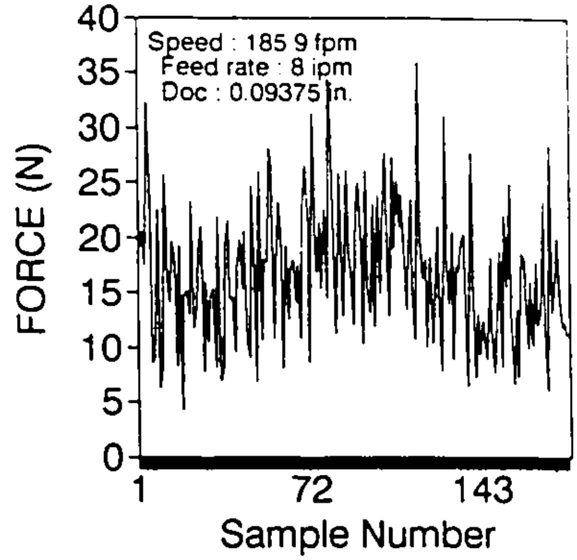
Speed : 185.9 fpm
Feed rate : 8 ipm
Doc : 0.09375 in.
FORCE (N)
Sample Number
40
35
30
25
20
15
10
5
0
1
72
143

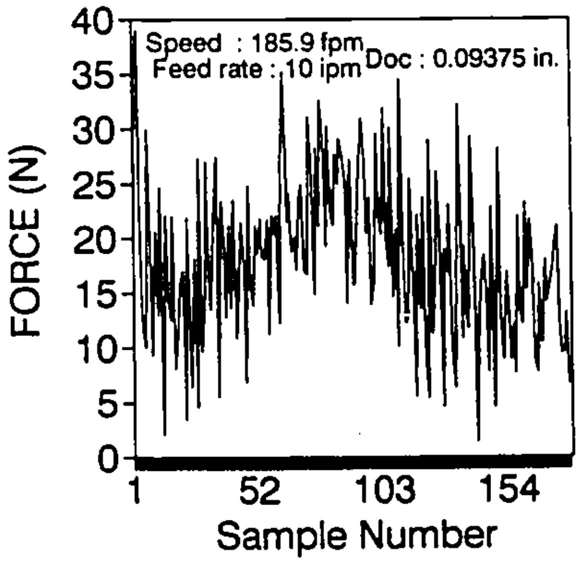
Speed : 185.9 fpm
Feed rate : 10 ipm
Doc : 0.09375 in.
FORCE (N)
Sample Number
40
35
30
25
20
15
10
5
0
1
52
103
154

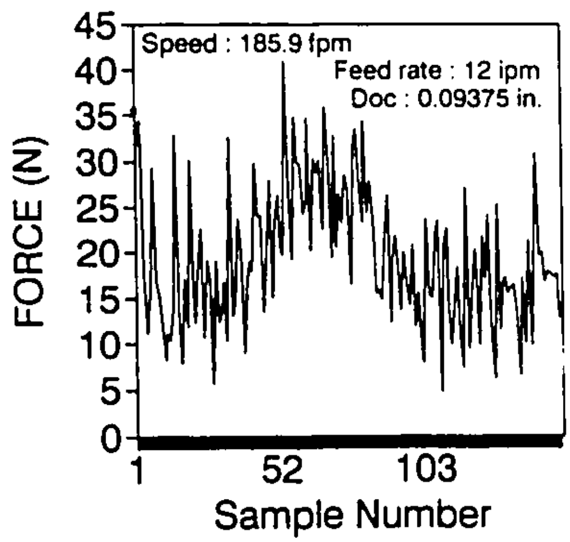
Speed : 185.9 fpm
Feed rate : 12 ipm
Doc : 0.09375 in.
FORCE (N)
Sample Number
45
40
35
30
25
20
15
10
5
0
1
52
103

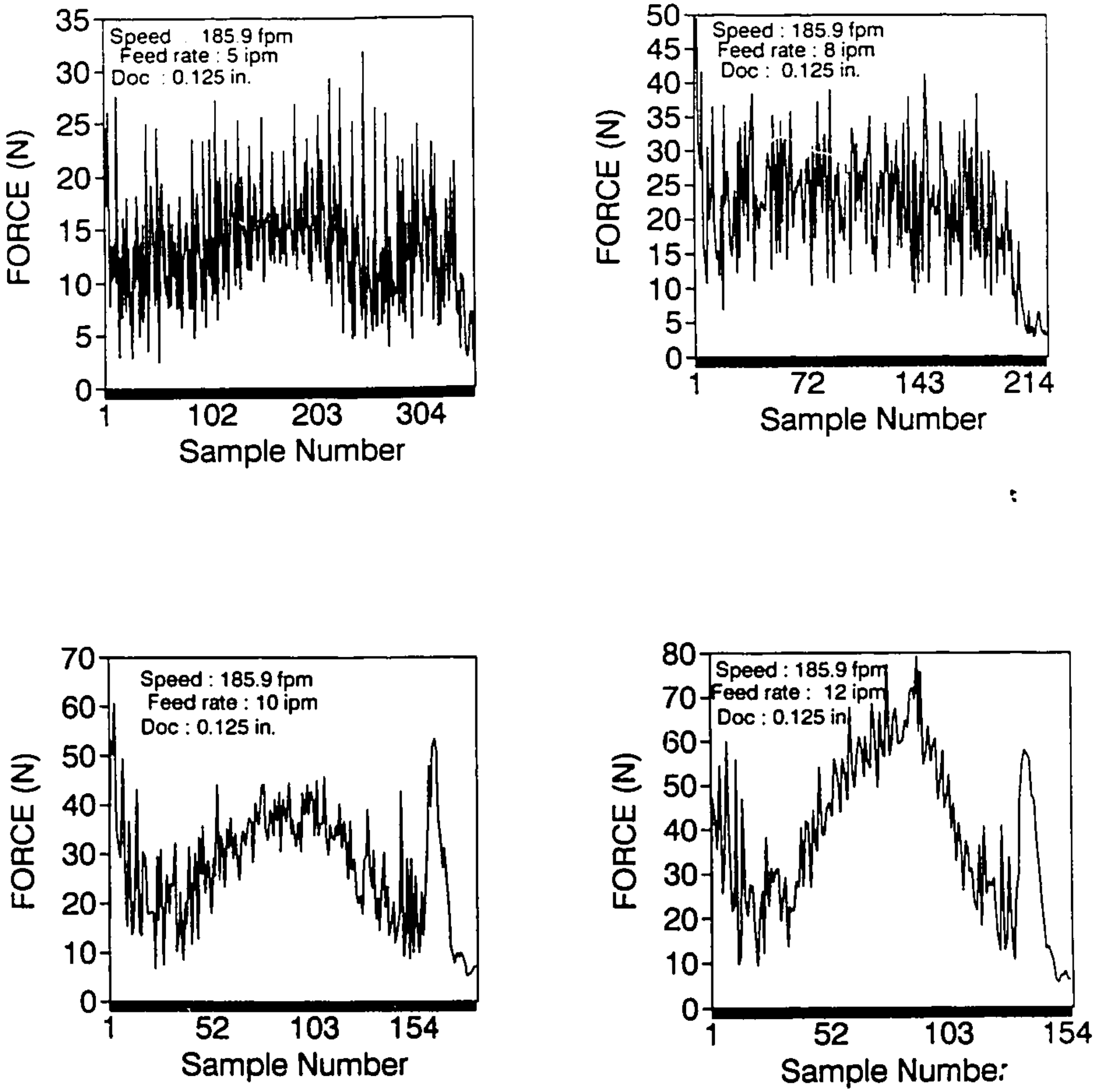
Speed : 185.9 fpm
Feed rate : 5 ipm
Doc : 0.125 in.
FORCE (N)
Sample Number
Speed : 185.9 fpm
Feed rate : 8 ipm
Doc : 0.125 in.
FORCE (N)
Sample Number
Speed : 185.9 fpm
Feed rate : 10 ipm
Doc : 0.125 in.
FORCE (N)
Sample Number
Speed : 185.9 fpm
Feed rate : 12 ipm
Doc : 0.125 in
FORCE (N)
Sample Number

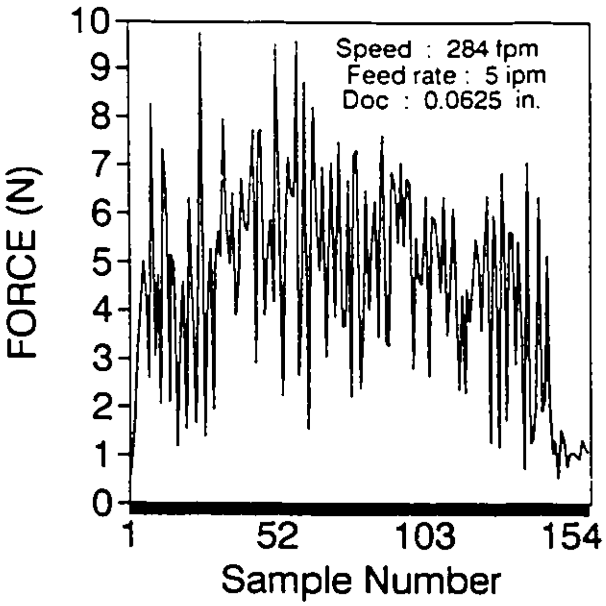

Speed : 284 fpm
Feed rate : 5 ipm
Doc : 0.0625 in.
FORCE (N)
Sample Number

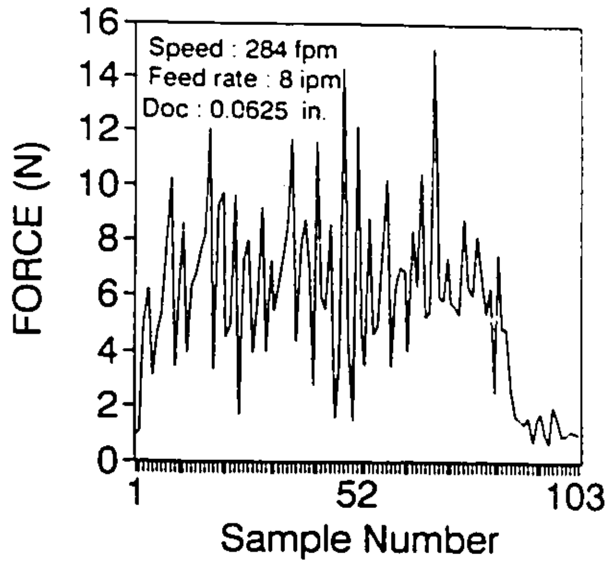

Speed : 284 fpm
Feed rate : 8 ipm
Doc : 0.0625 in.
FORCE (N)
Sample Number

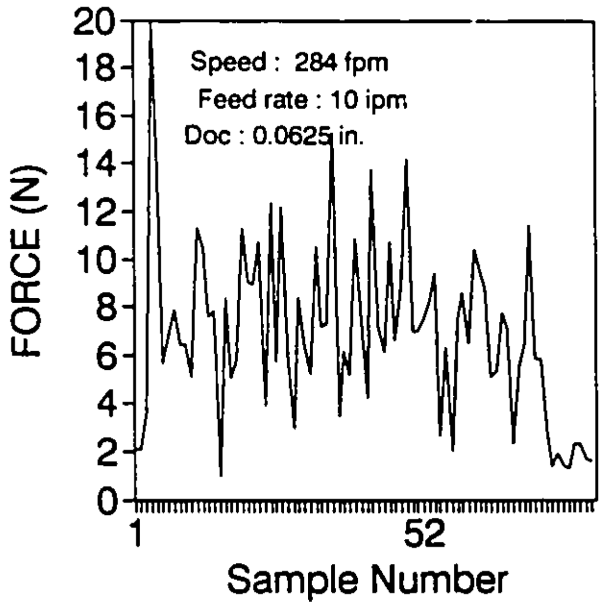

Speed : 284 fpm
Feed rate : 10 ipm
Doc : 0.0625 in.
FORCE (N)
Sample Number

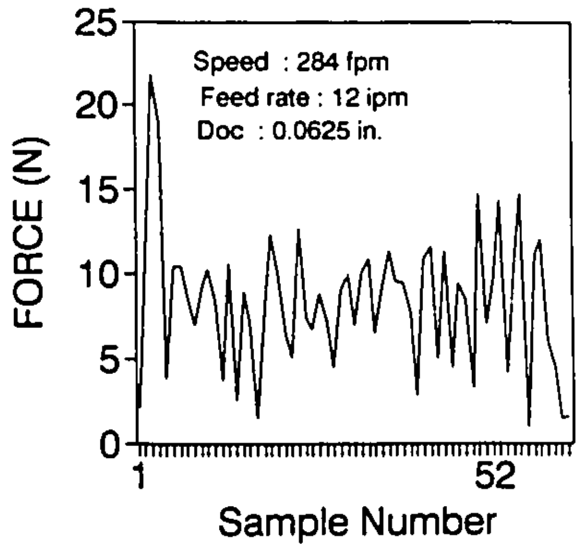

Speed : 284 fpm
Feed rate : 12 ipm
Doc : 0.0625 in.
FORCE (N)
Sample Number

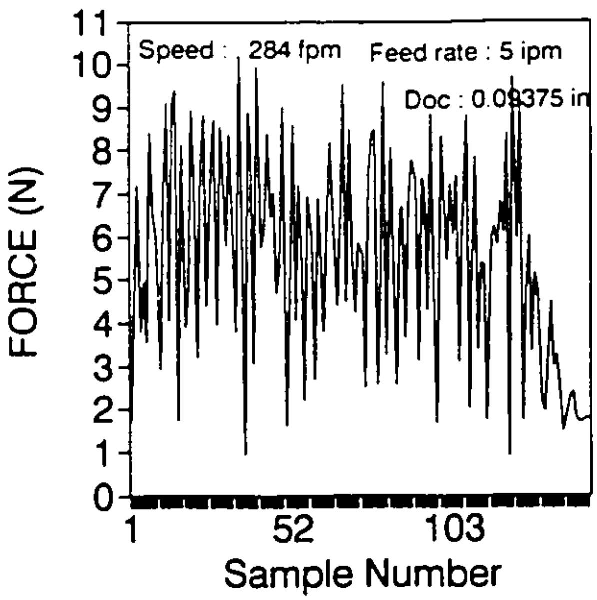
Speed : 284 fpm
Feed rate : 5 ipm
Doc : 0.09375 in
FORCE (N)
Sample Number

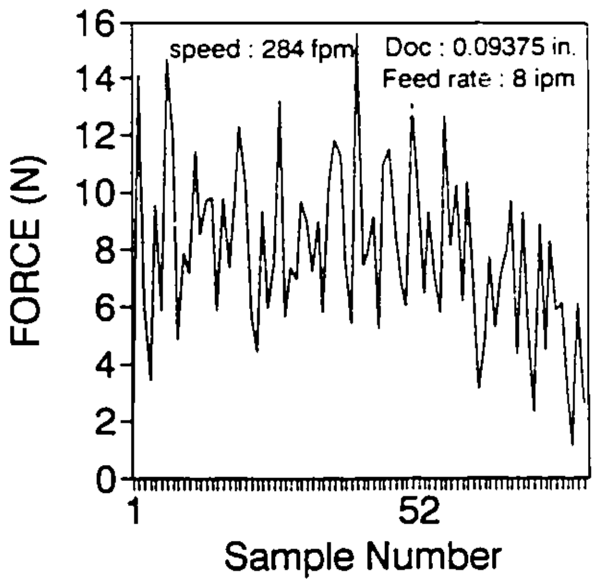
speed : 284 fpm
Doc : 0.09375 in.
Feed rate : 8 ipm
FORCE (N)
Sample Number

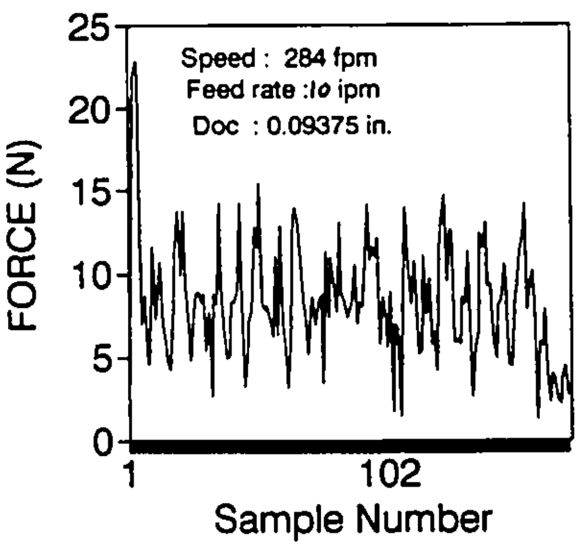
Speed : 284 fpm
Feed rate :10 ipm
Doc : 0.09375 in.
FORCE (N)
Sample Number

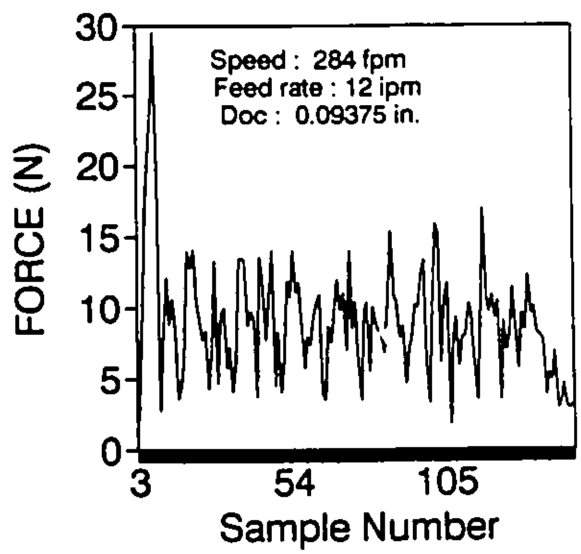
Speed : 284 fpm
Feed rate : 12 ipm
Doc : 0.09375 in.
FORCE (N)
Sample Number

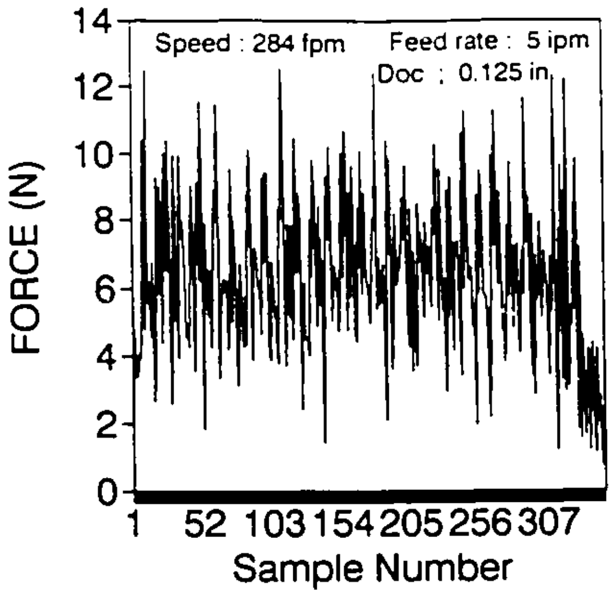
Speed : 284 fpm
Feed rate : 5 ipm
Doc : 0.125 in
FORCE (N)
Sample Number
14
12
10
8
6
4
2
0
1
52
103
154
205
256
307

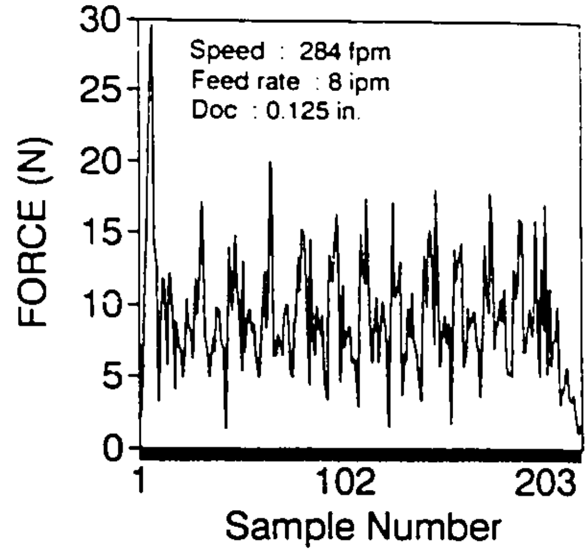
Speed : 284 fpm
Feed rate : 8 ipm
Doc : 0.125 in.
FORCE (N)
Sample Number
30
25
20
15
10
5
0
1
102
203

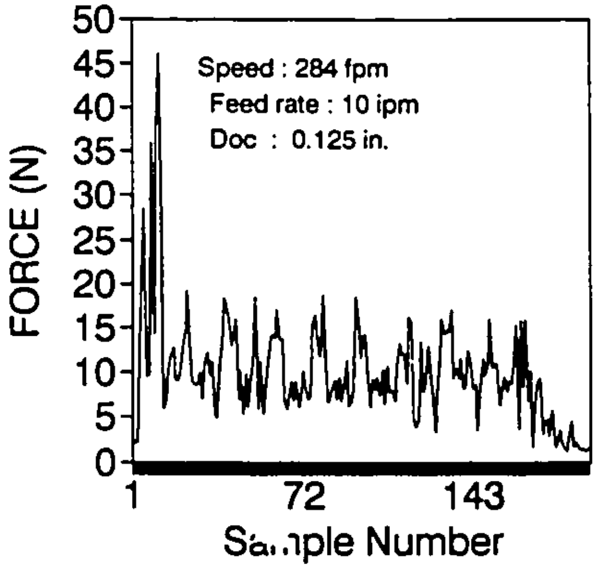
Speed : 284 fpm
Feed rate : 10 ipm
Doc : 0.125 in.
FORCE (N)
Sample Number
50
45
40
35
30
25
20
15
10
5
0
1
72
143

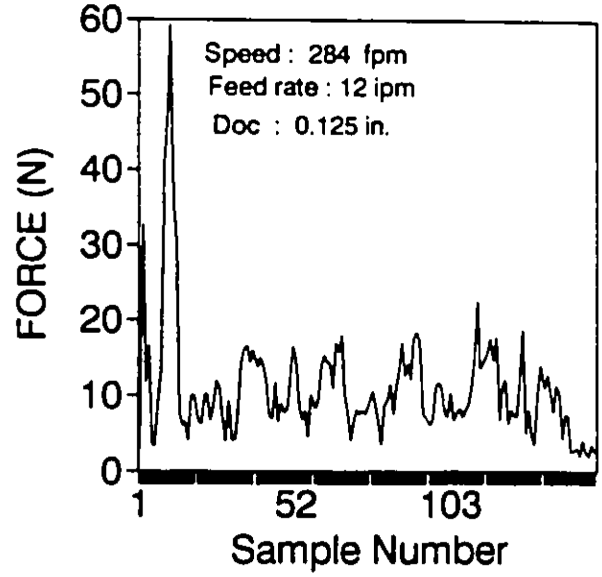
Speed : 284 fpm
Feed rate : 12 ipm
Doc : 0.125 in.
FORCE (N)
Sample Number
60
50
40
30
20
10
0
1
52
103

Appendix C

Response curves of cutting force under different cutting conditions

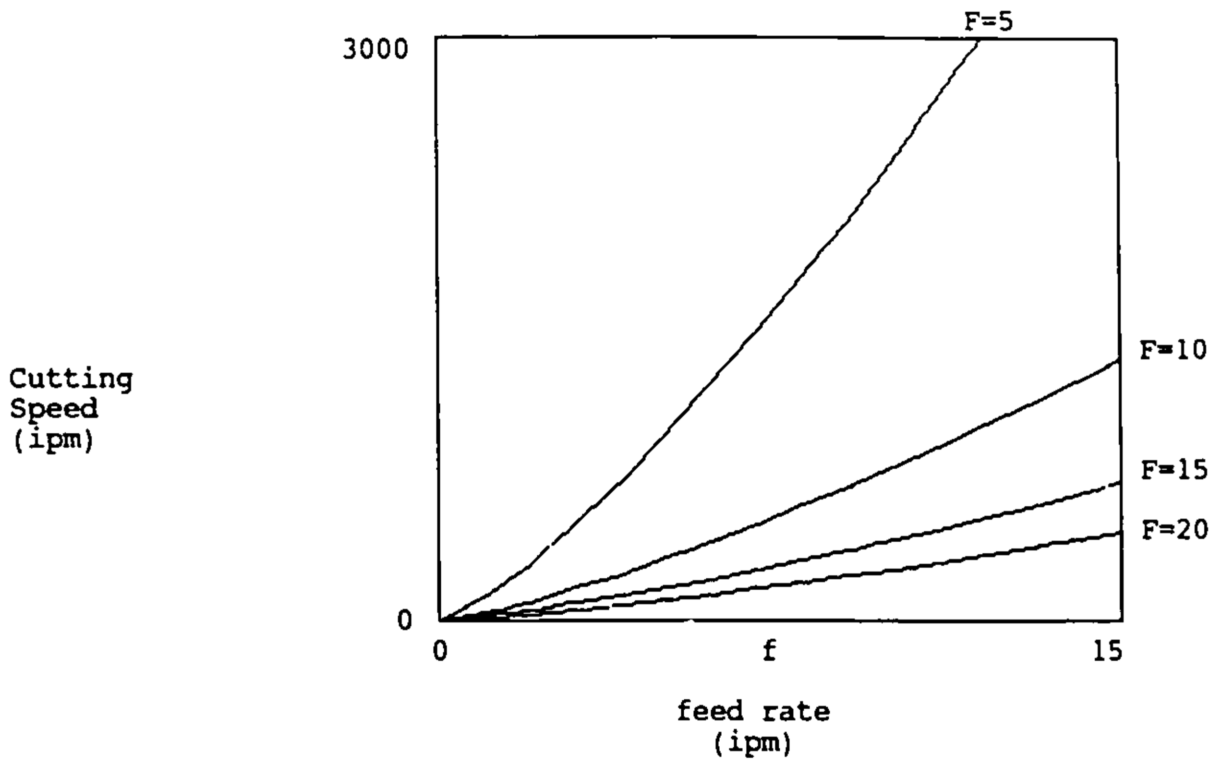

F = Cutting Force , N
d = Depth of Cut , in

Response Curve of Cutting Force
depth of cut =0.04"

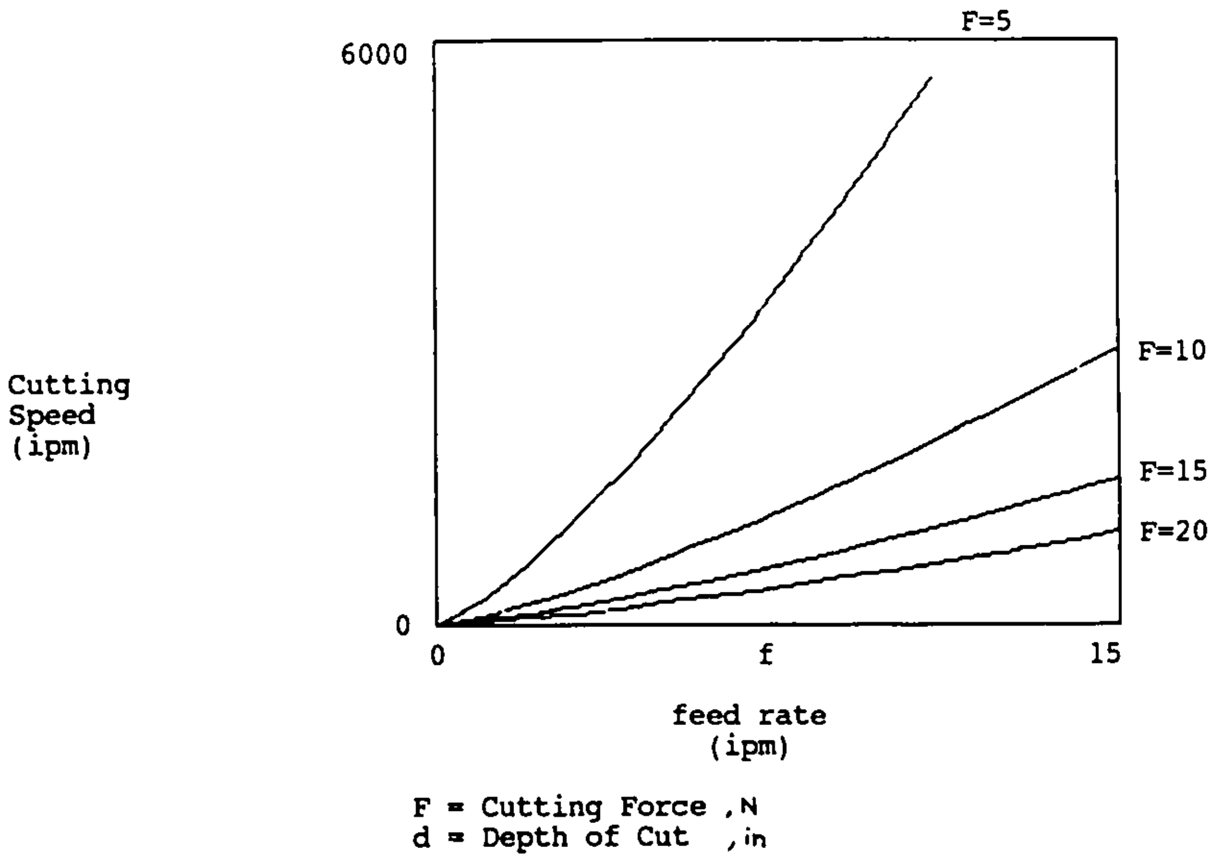

Response Curve of Cutting Force
depth of cut =0.06"

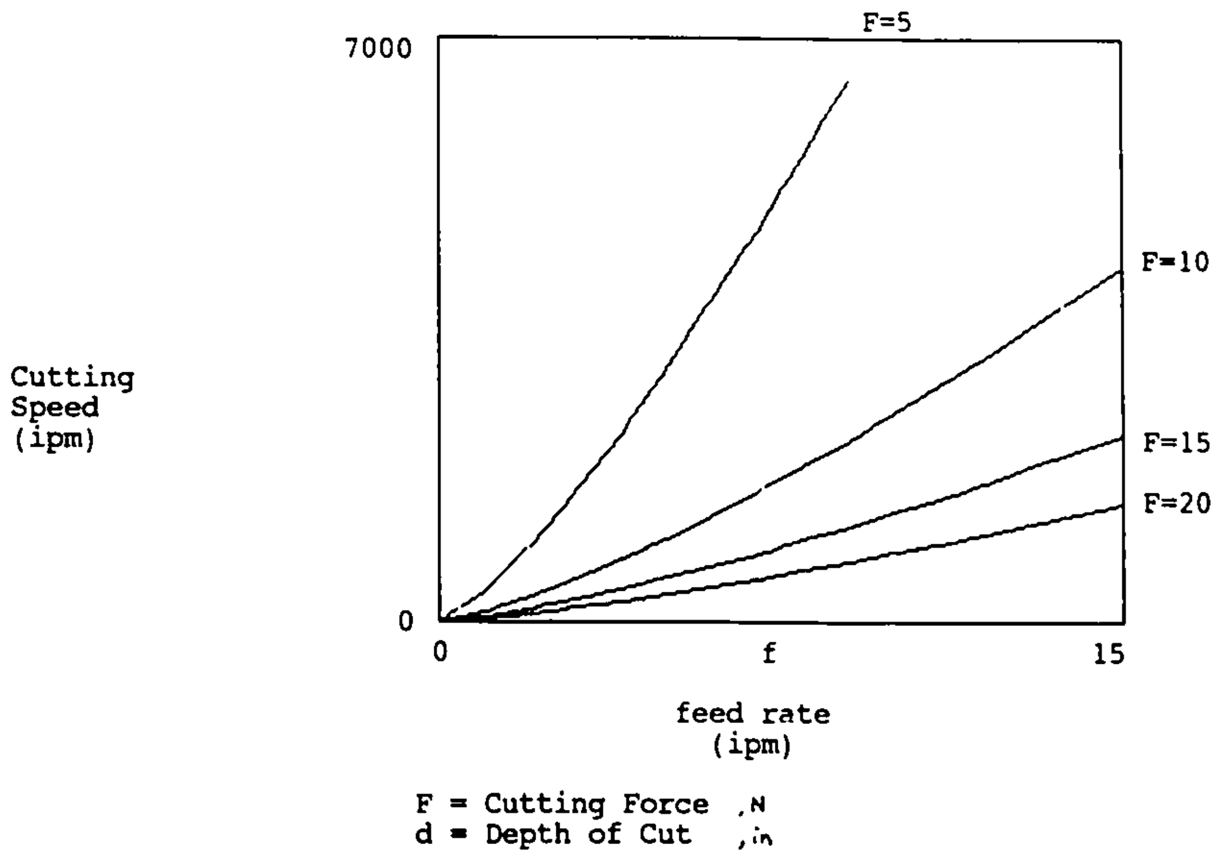

Response Curve of Cutting Force
depth of cut =0.075"

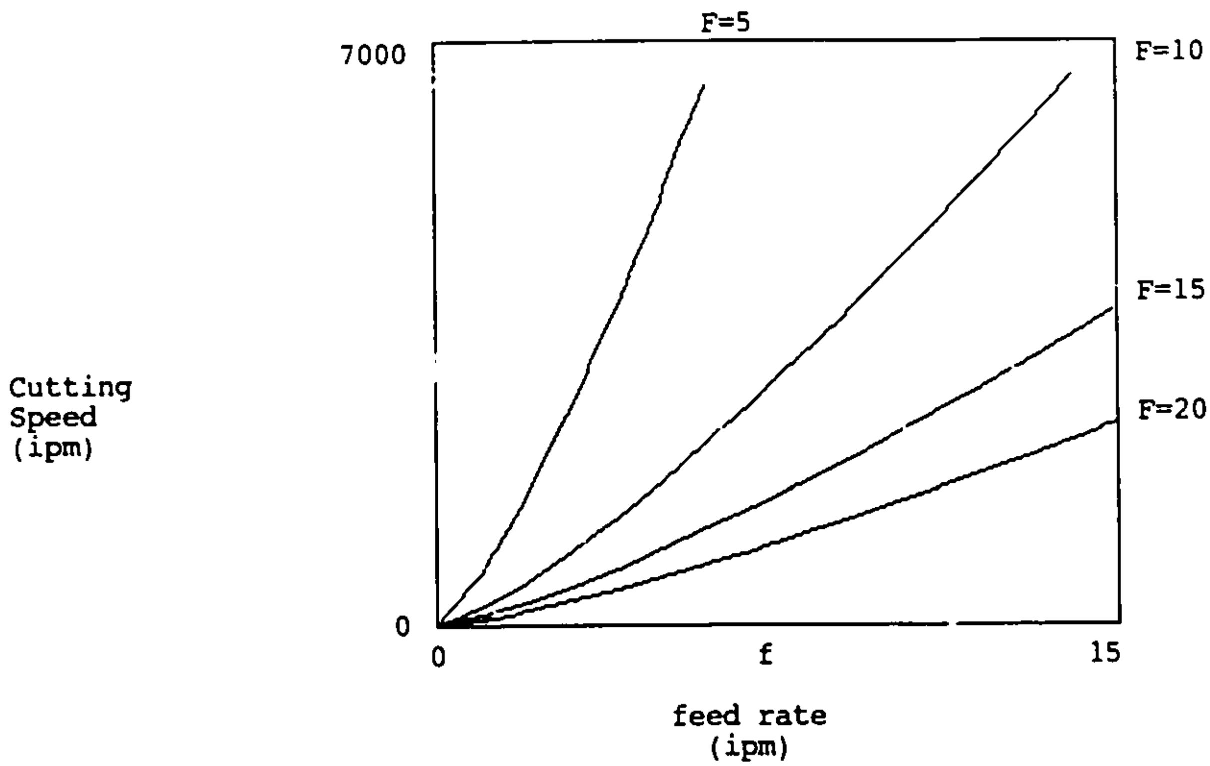

F = Cutting Force ,N
d = Depth of Cut ,in

Response Curve of Cutting Force
depth of cut =0.1"

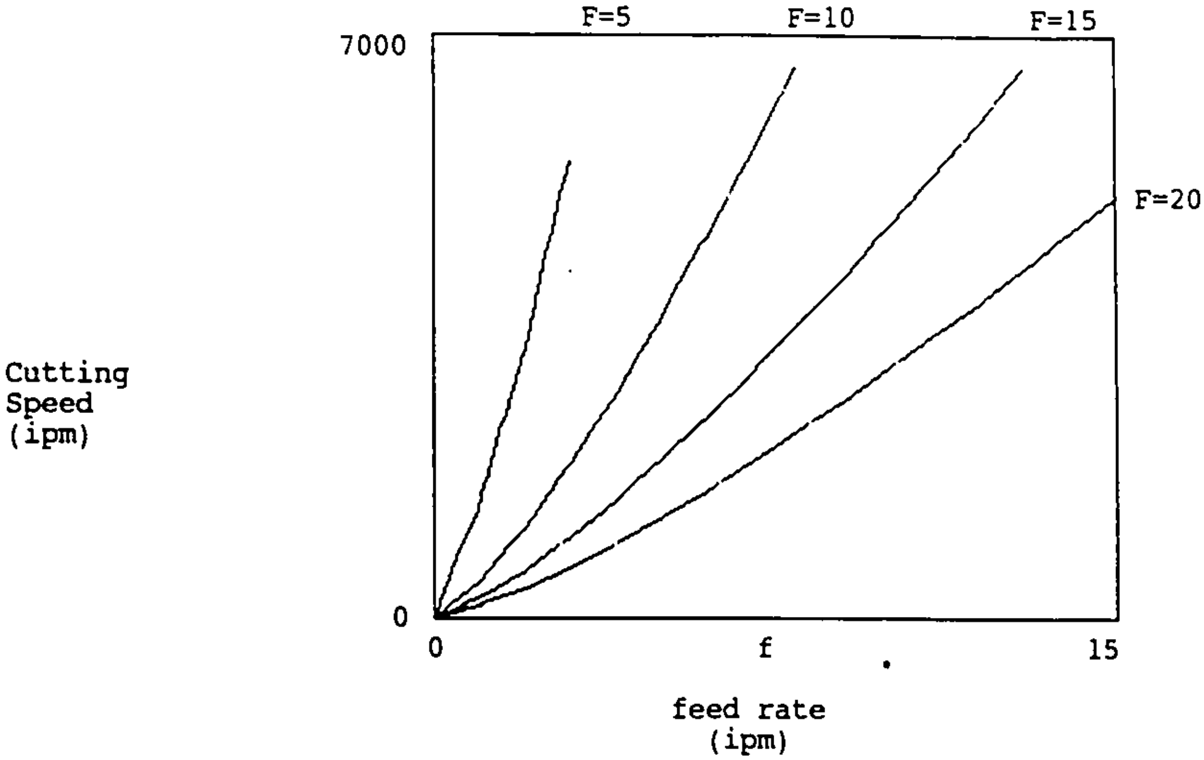

F = Cutting Force ,N
d = Depth of Cut ,in

Response Curve of Cutting Force
depth of cut =0.15"

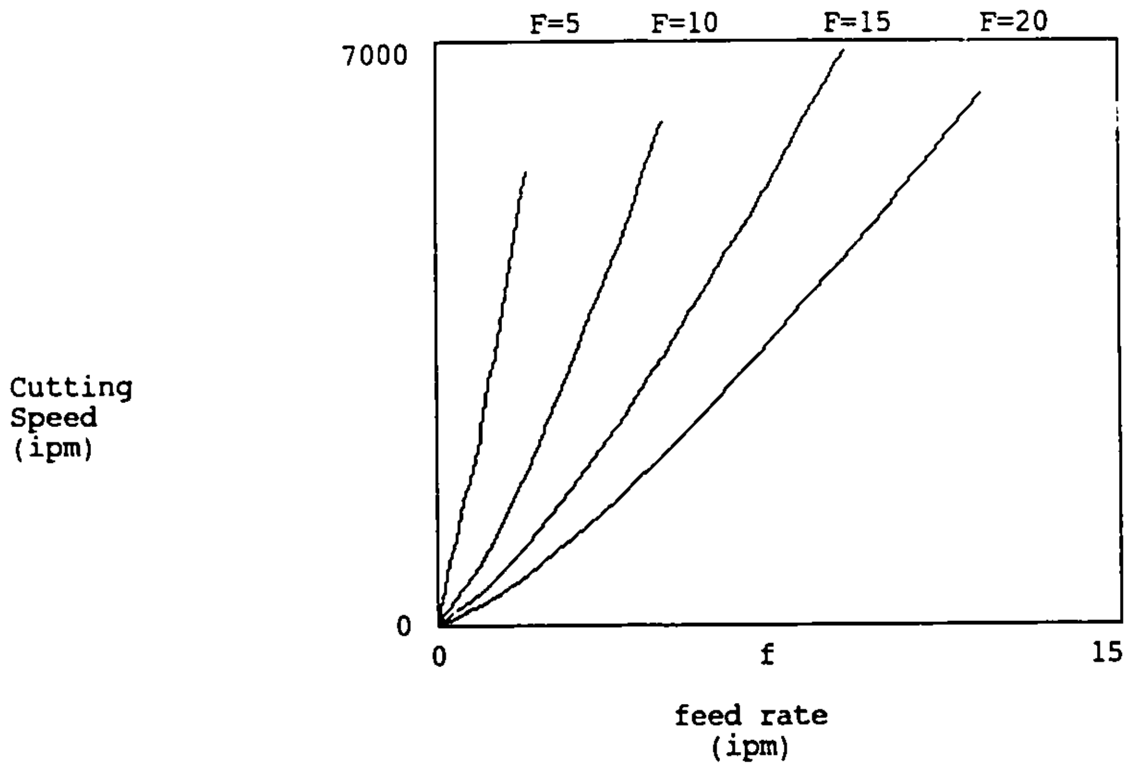

F = Cutting Force , N
d = Depth of Cut , in

Response Curve of Cutting Force
depth of cut =0.2″

Appendix D

Response curves of tool life under different cutting conditions

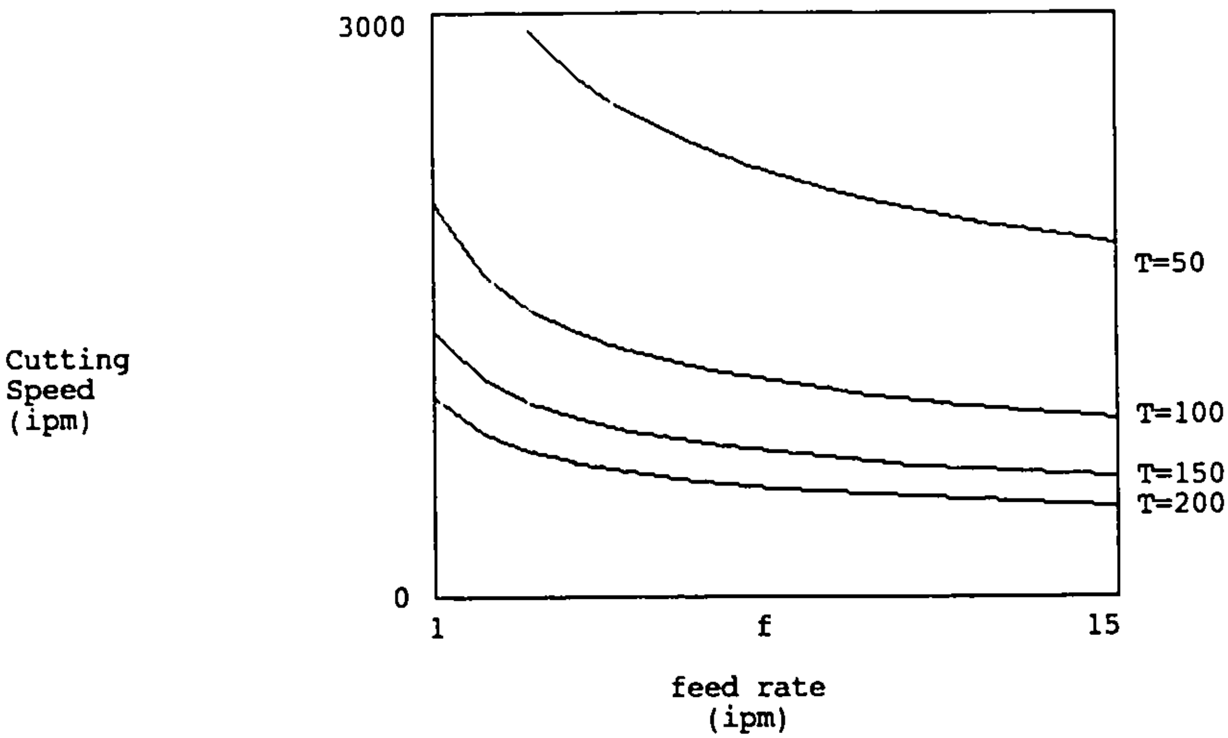

T = Tool Life (min)
d = Depth of Cut (inch)

Response Curve of Tool Life
depth of cut =0.04 inch

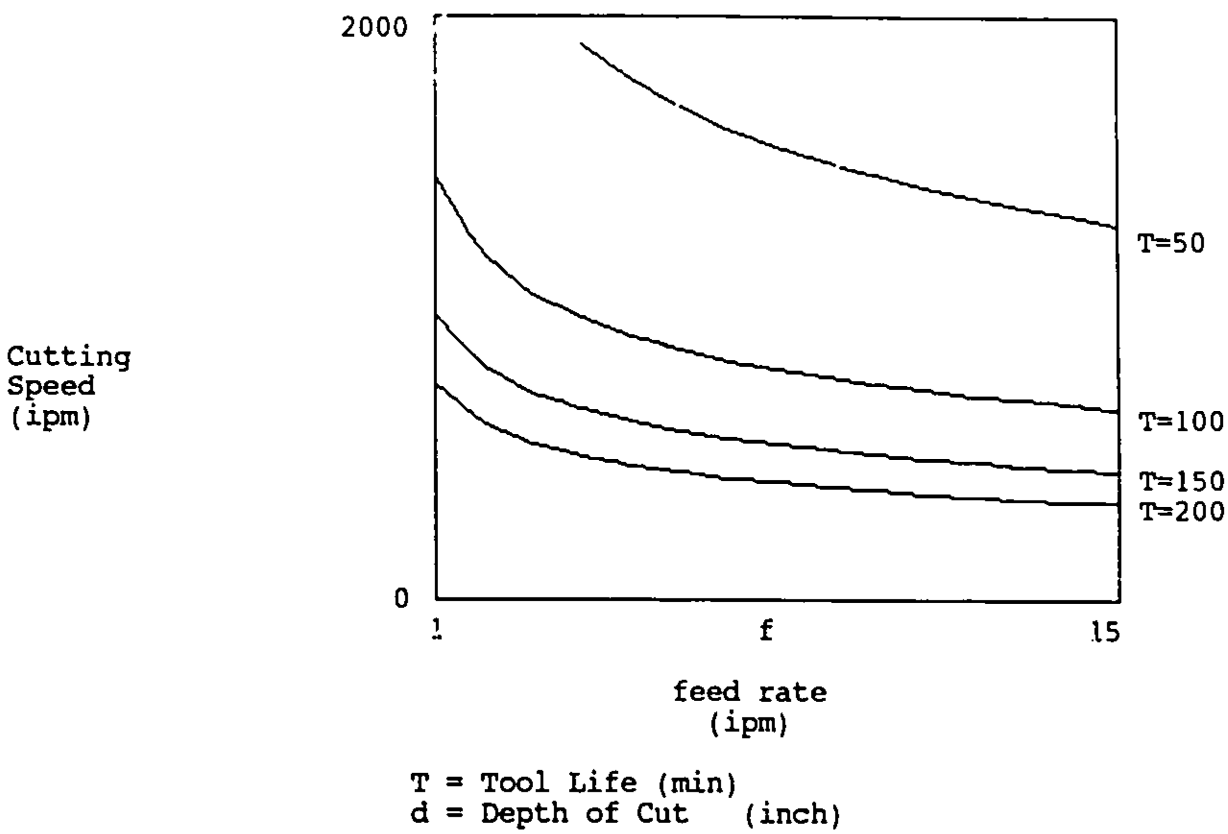

Response Curve of Tool Life
depth of cut =0.06 inch

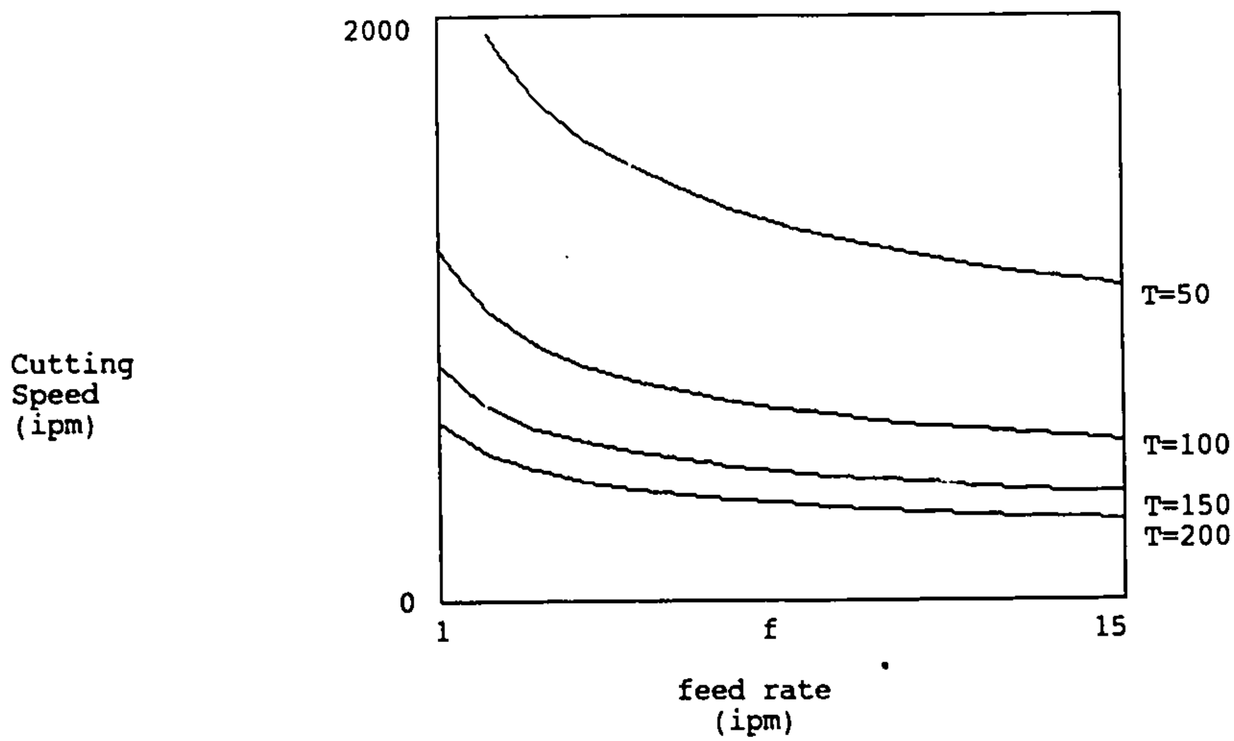

T = Tool Life (min)
d = Depth of Cut (inch)

Response Curve of Tool Life
depth of cut =0.075 inch

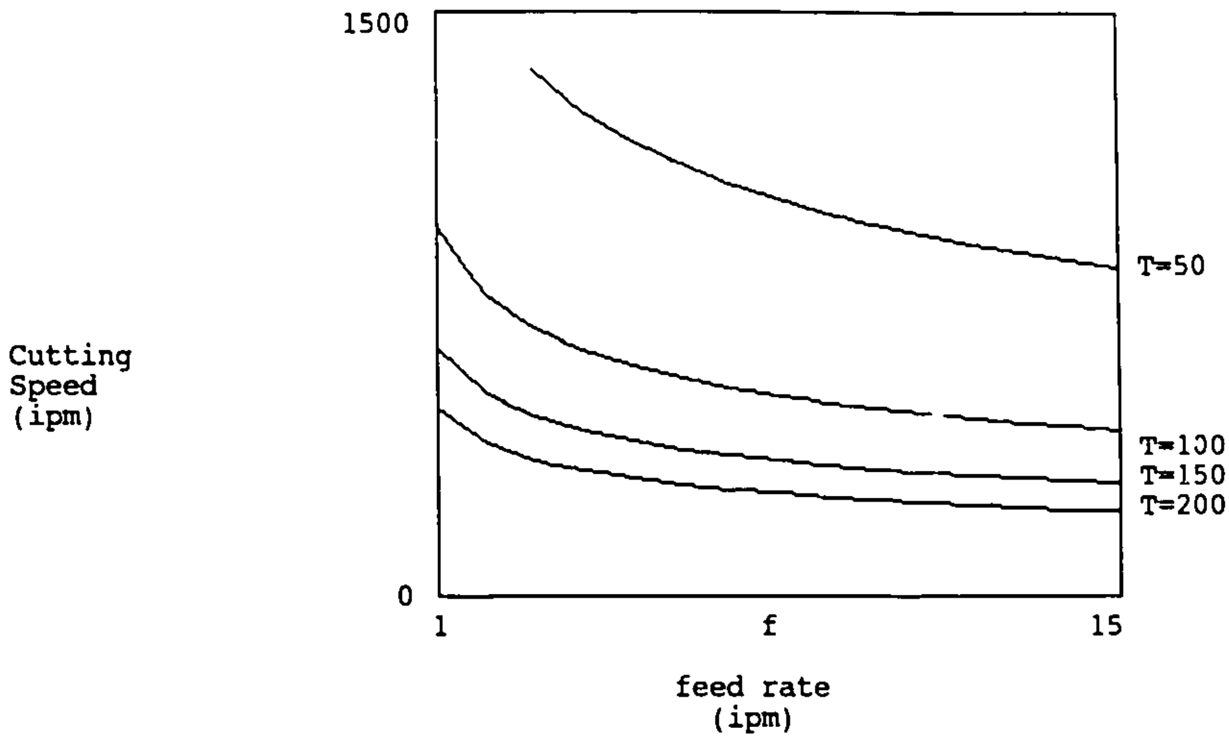

T = Tool Life (min)
d = Depth of Cut (inch)

Response Curve of Tool Life
depth of cut =0.1 inch

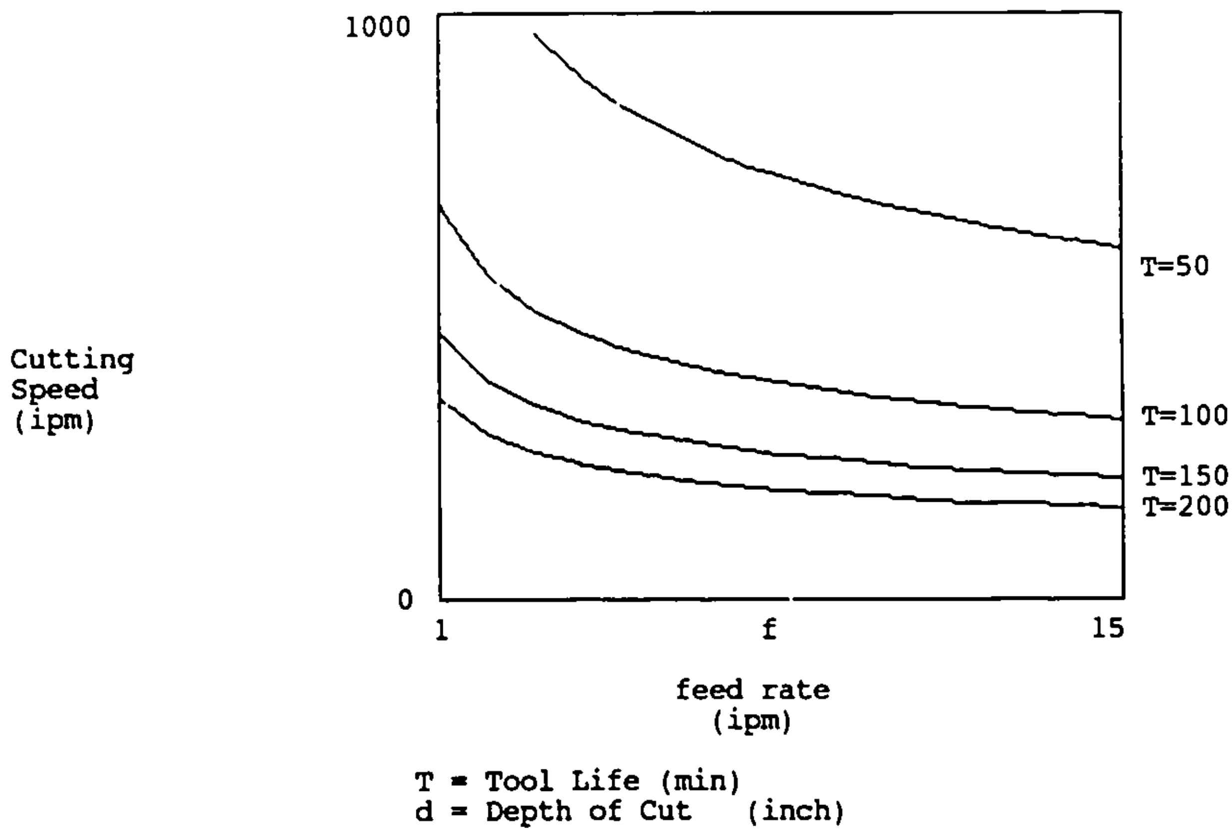

Response Curve of Tool Life
depth of cut =0.15 inch

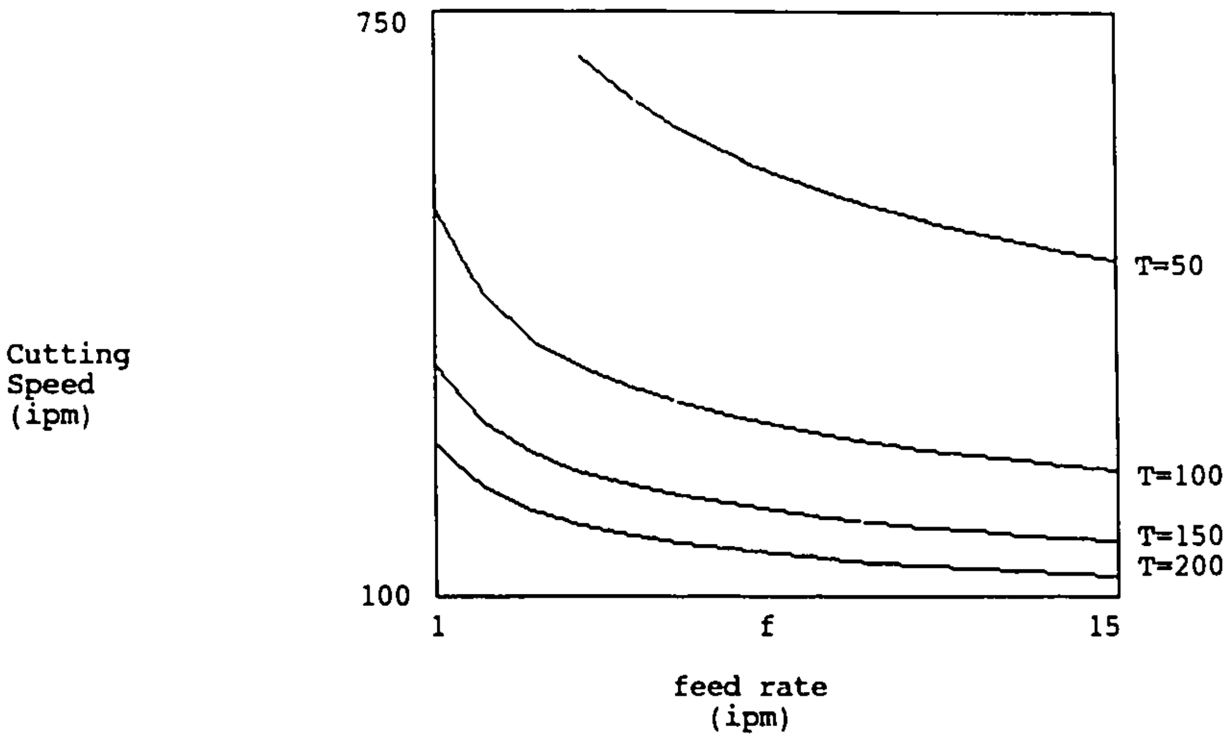

T = Tool Life (min)
d = Depth of Cut (inch)

Response Curve of Tool Life
depth of cut =0.2 inch

Appendix E

Parameter values of seasonal forecast models of cutting forces under different cutting conditions

Seasonal Forecast Model

Cutting Speed : 284 fpm

Feed Rate : 10 ipm $F(t) = (a + b * t)SN(t) + e(t)$

Depth of Cut : 0.125 in

a = 6.028

Length of Season : 19 samples b = -0.27

smoothing constants

apha = 0.35
beta = 0.07
gamma = 0.05

MSE = 5.28
MAD = 1.69
MAPE = 18.19

t	SN(t)
1	0.69
2	0.72
3	0.81
4	0.81
5	0.83
6	0.80
7	0.74
8	0.94
9	0.83
10	0.76
11	0.76
12	1.33
13	1.57
14	1.42
15	1.44
16	1.32
17	1.42
18	1.00
19	0.82

seasonal Forecast Model

Cutting Speed : 284 fpm

Feed Rate : 5 ipm $F(t) = (a + b * t)SN(t) + e(t)$

Depth of Cut : 0.125 in

a = 7.31
b = 0.005

Length of Season : 61 samples

smoothing constants

apha = 0.01
beta = 0.1
gamma = 0.05

MSE = 2.13
MAD = 1.2
MAPE = 21.9

t	SN(t)	t	SN(t)
1	1.73	31	0.50
2	1.03	32	0.76
3	0.58	33	1.12
4	0.90	34	0.87
5	1.01	35	1.42
6	1.05	36	1.10
7	0.99	37	1.14
8	0.84	38	1.10
9	0.85	39	0.78
10	1.25	40	0.99
11	1.18	41	0.99
12	1.28	42	0.87
13	1.51	43	0.89
14	0.70	44	1.18
15	0.69	45	0.84
16	0.86	46	1.13
17	0.79	47	1.47
18	0.82	48	0.98
19	0.79	49	1.06
20	0.78	50	1.35
21	0.92	51	0.74
22	0.89	52	0.99
23	1.46	53	1.09
24	1.02	54	0.81
25	1.07	55	0.71
26	0.93	56	1.01
27	1.12	57	0.84
28	0.64	58	1.01
29	0.92	59	1.13
30	0.97	60	1.02
		61	1.57

Seasonal Forecast Model

Cutting Speed : 284 fpm

Feed Rate : 8 ipm $F(t) = (a + b * t)SN(t) + e(t)$

Depth of Cut : 0.0625 in

Length of Season : 25 samples

a = 7.13
b = 0.0009

smoothing constants

apha = 0.01
beta = 0.1
gamma = 0.05

MSE = 2.46
MAD = 1.3
MAPE = 27.3

t	SN(t)
1	0.68
2	0.92
3	0.93
4	0.65
5	0.95
6	0.99
7	1.27
8	0.82
9	1.13
10	1.53
11	0.62
12	1.06
13	1.17
14	1.08
15	0.83
16	1.77
17	0.69
18	1.10
19	1.36
20	0.45
21	0.63
22	1.78
23	0.45
24	0.65
25	1.49

Seasonal Forecast Model

Cutting Speed : 87.7 fpm

Feed Rate : 5 ipm $F(t) = (a + b * t)SN(t) + e(t)$

Depth of Cut : 0.125 in

Length of Season : 50 samples

a = 14.58
b = -0.163

smoothing constants

apha = 0.5
beta = 0.2
gamma = 0.9

MSE = 6.13
MAD = 1.95
MAPE = 18.9

t	SN(t)	t	SN(t)
1	1.46	26	1.08
2	0.86	27	1.03
3	1.14	28	1.00
4	0.73	29	0.77
5	0.93	30	0.99
6	1.44	31	1.19
7	0.54	32	0.71
8	1.45	33	0.99
9	1.33	34	1.14
10	0.85	35	0.81
11	1.03	36	0.90
12	0.78	37	1.16
13	1.19	38	0.75
14	1.25	39	0.98
15	0.91	40	0.77
16	0.95	41	0.80
17	1.15	42	1.20
18	0.80	43	0.83
19	0.97	44	0.93
20	1.04	45	1.16
21	0.93	46	0.87
22	1.06	47	0.99
23	0.77	48	1.08
24	0.93	49	1.10
25	1.16	50	1.14

Seasonal Forecast Model

Cutting Speed : 87.7 fpm

Feed Rate : 10 ipm

$F(t) = (a + b * t)SN(t) + e(t)$

Depth of Cut : 0.0625 in

Length of Season : 30 samples

a = 9.17
b = 0.004

smoothing constants

apha = 0.01
beta = 0.1
gamma = 0.05

MSE = 10.01
MAD = 2.30
MAPE = 29.8

t	SN(t)
1	1.32
2	1.53
3	1.37
4	1.00
5	0.75
6	1.21
7	0.83
8	1.28
9	1.58
10	0.77
11	0.72
12	1.35
13	1.14
14	0.72
15	0.79
16	0.90
17	0.86
18	0.99
19	0.67
20	0.81
21	1.67
22	0.52
23	1.34
24	0.91
25	0.85
26	0.75
27	0.73
28	1.09
29	0.96
30	0.60

Appendix F

Experimental & forecasted values of seasonal pattern of cutting forces under different conditions

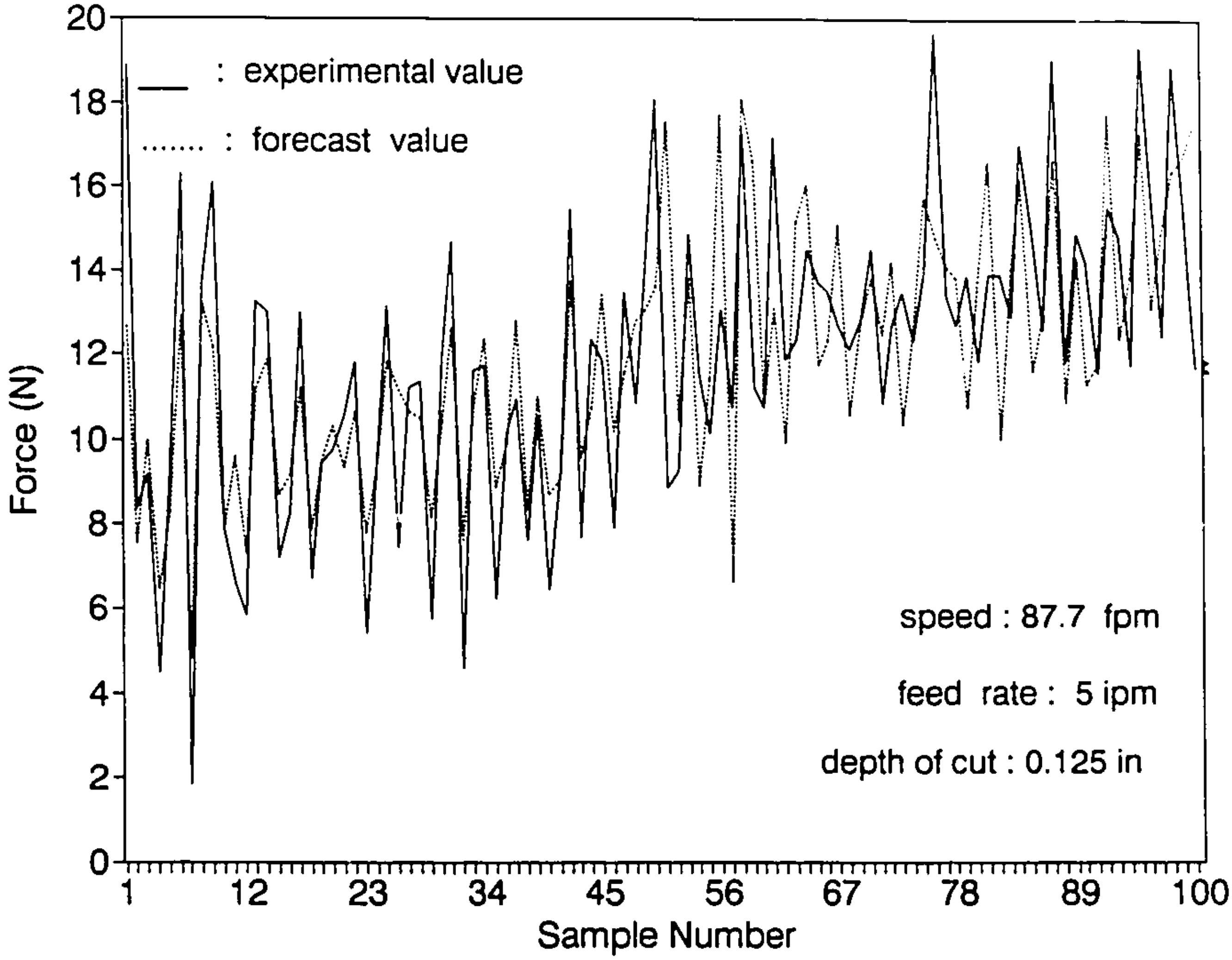

: experimental value
.... : forecast value
speed : 87.7 fpm
feed rate : 5 ipm
depth of cut : 0.125 in
Force (N)
Sample Number

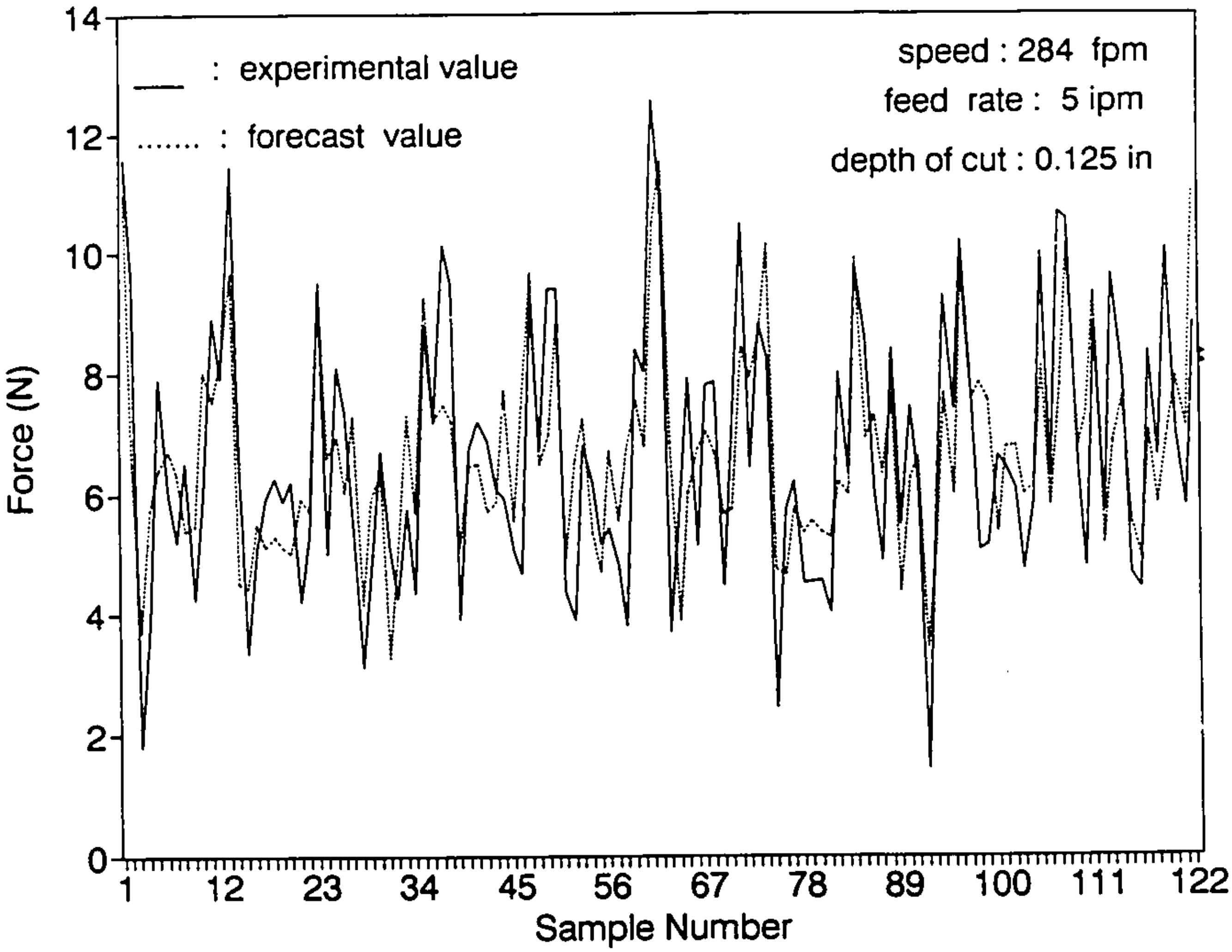

14
12
10
8
6
4
2
0
Force (N)
— : experimental value
.... : forecast value
speed : 284 fpm
feed rate : 5 ipm
depth of cut : 0.125 in
1
12
23
34
45
56
67
78
89
100
111
122
Sample Number

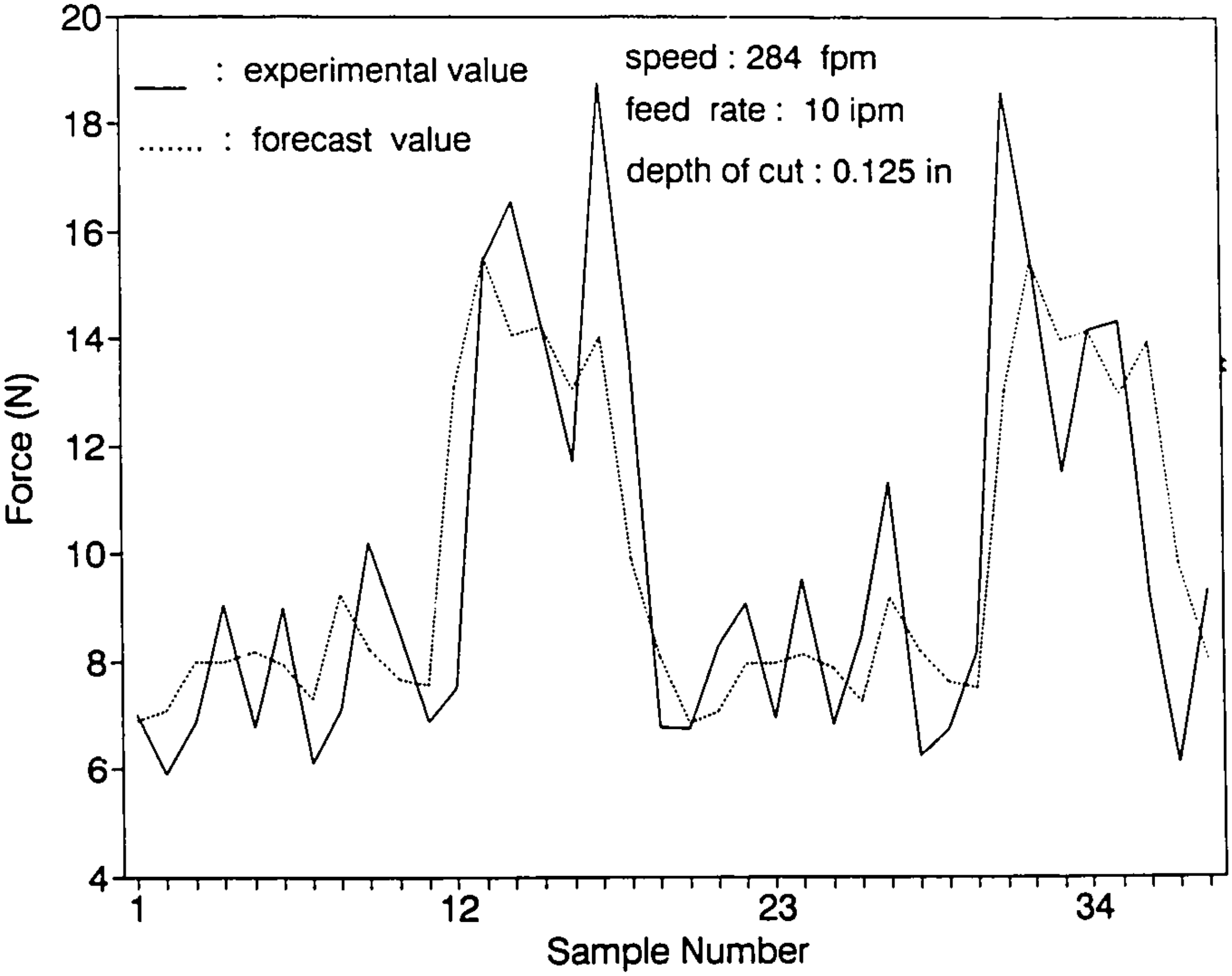

: experimental value
.... : forecast value
speed : 284 fpm
feed rate : 10 ipm
depth of cut : 0.125 in
Force (N)
20
18
16
14
12
10
8
6
4
1
12
23
34
Sample Number

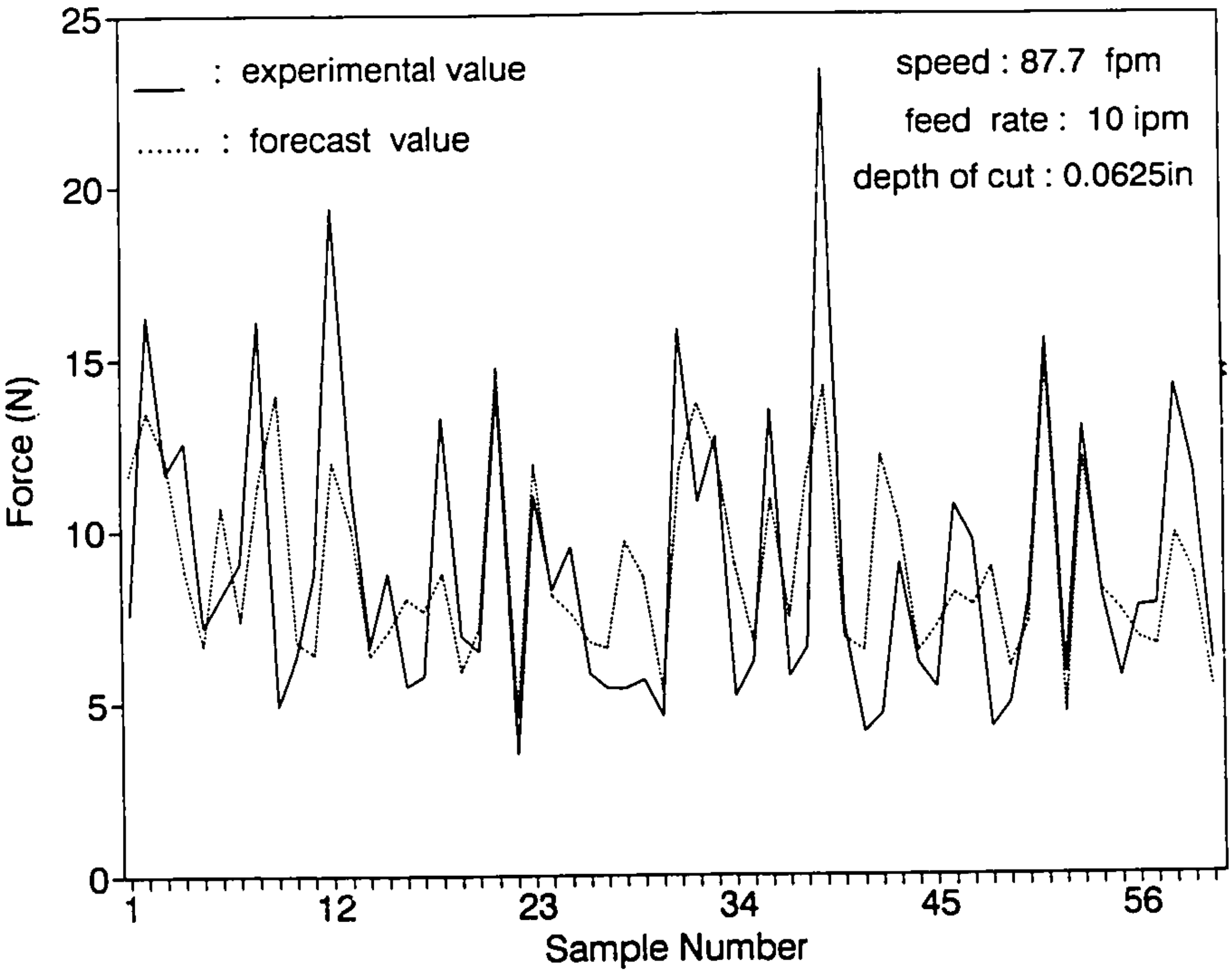

25
20
15
10
5
0
Force (N)
—— : experimental value
.... : forecast value
speed : 87.7 fpm
feed rate : 10 ipm
depth of cut : 0.0625in
1
12
23
34
45
56
Sample Number

Appendix G

Figures of non-linear trend cutting force smoothing

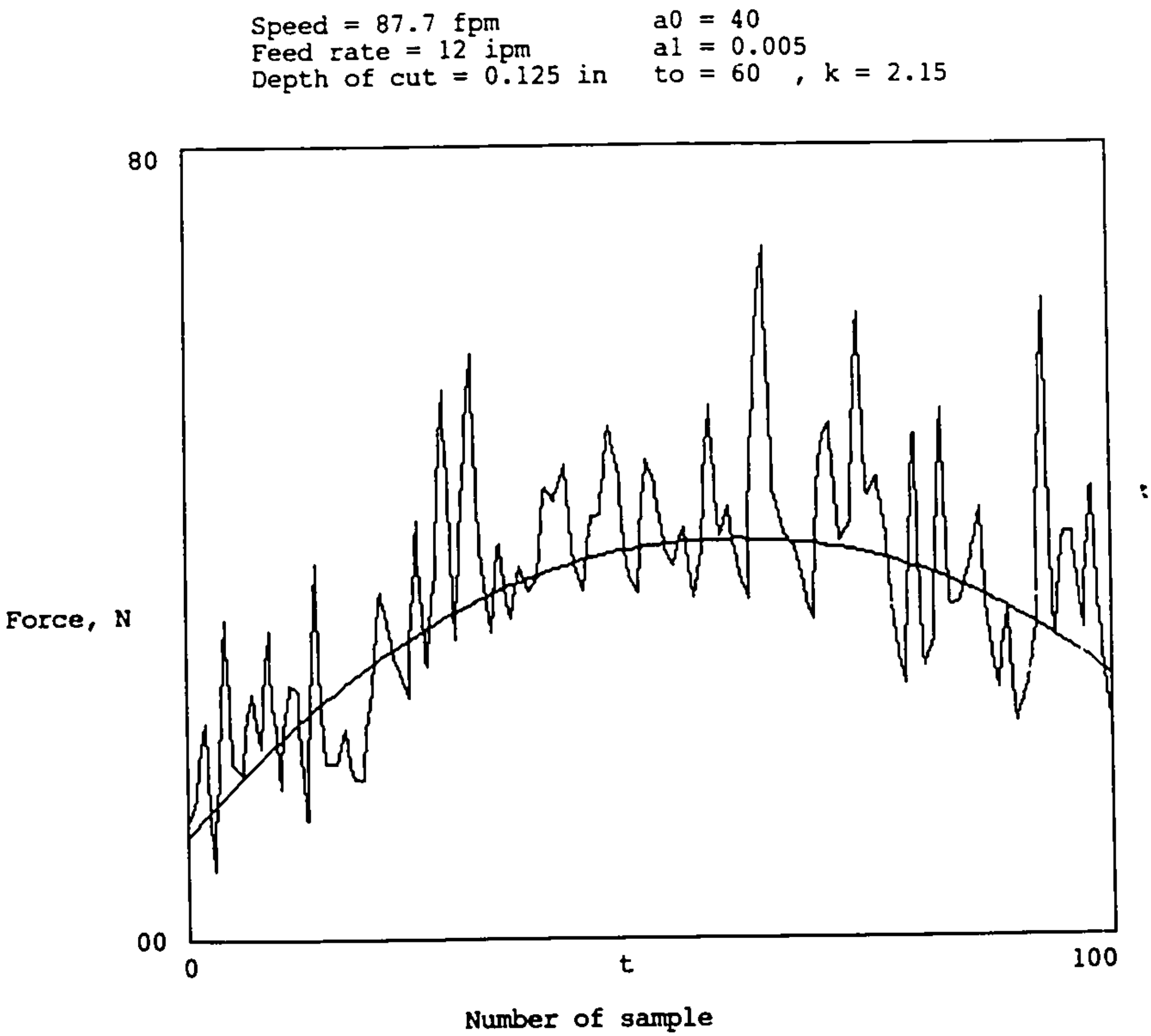

Non-linear Trend Smoothing

Speed = 87.7 fpm　　a0 = 38
Feed rate = 10 ipm　　a1 = 0.005
Depth of cut = 0.125 in　　to = 60 , k = 2.15

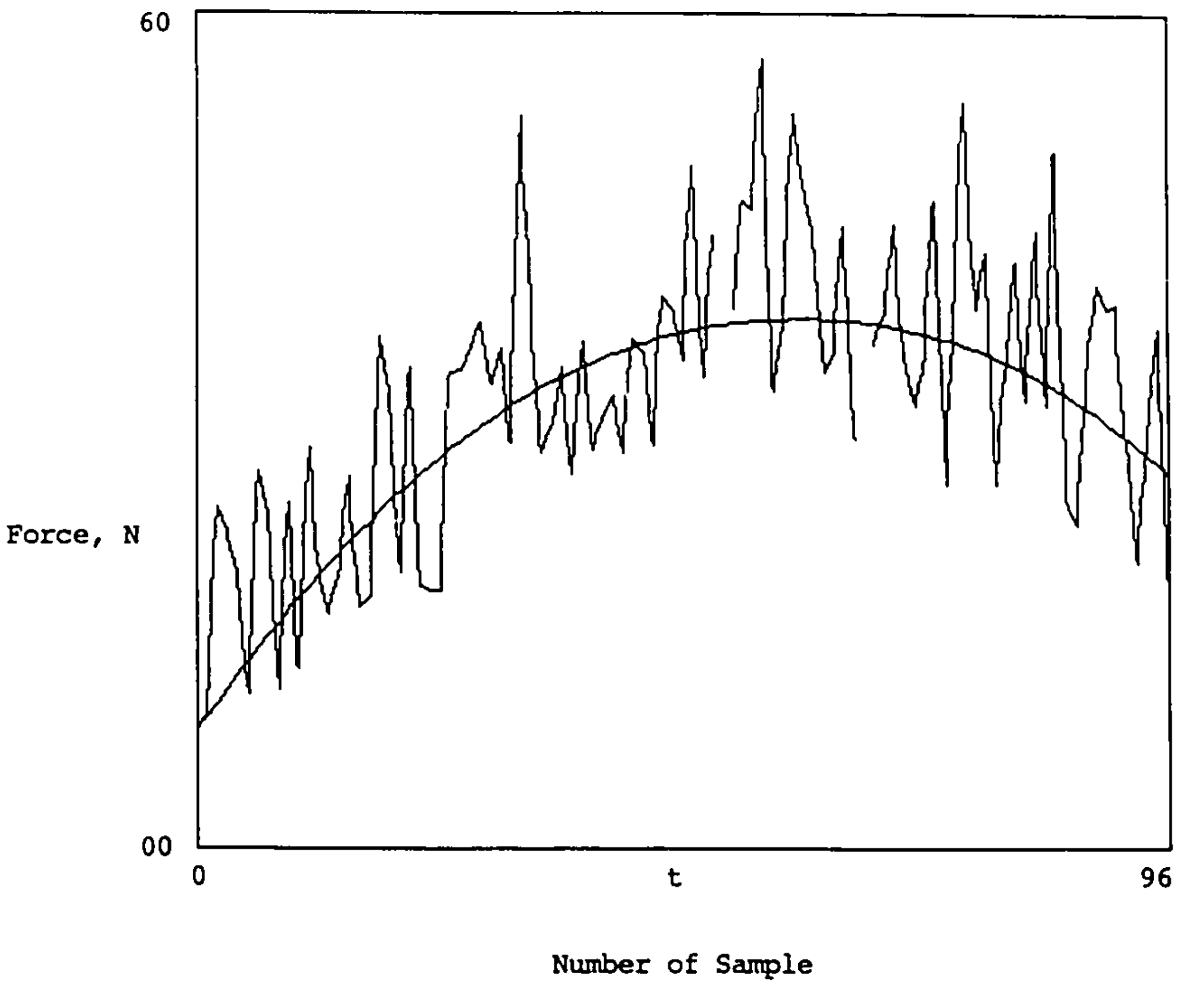

Non-linear Trend Smoothing

Speed = 87.7 fpm
Feed rate = 8 ipm
Depth of cut = 0.09375in.

a0 = 26
a1 = 0.002
to = 71 , k = 2.23

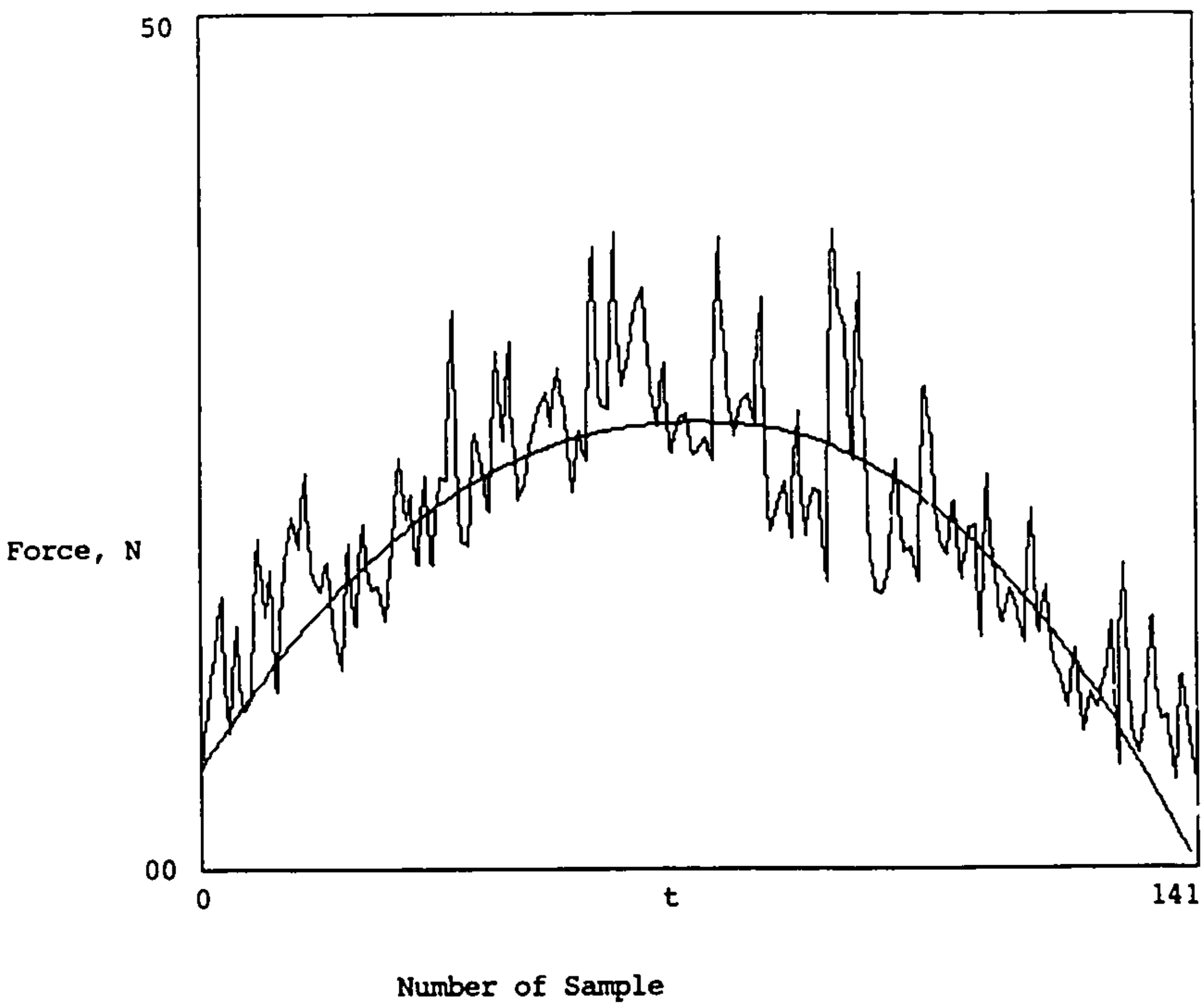

Non-linear Trend Smoothing

Speed = 185.9 fpm a0 = 38
Feed rate = 10 ipm a1 = 0.004
Depth of cut = 0.125 in. t0 = 57 , k = 2.25

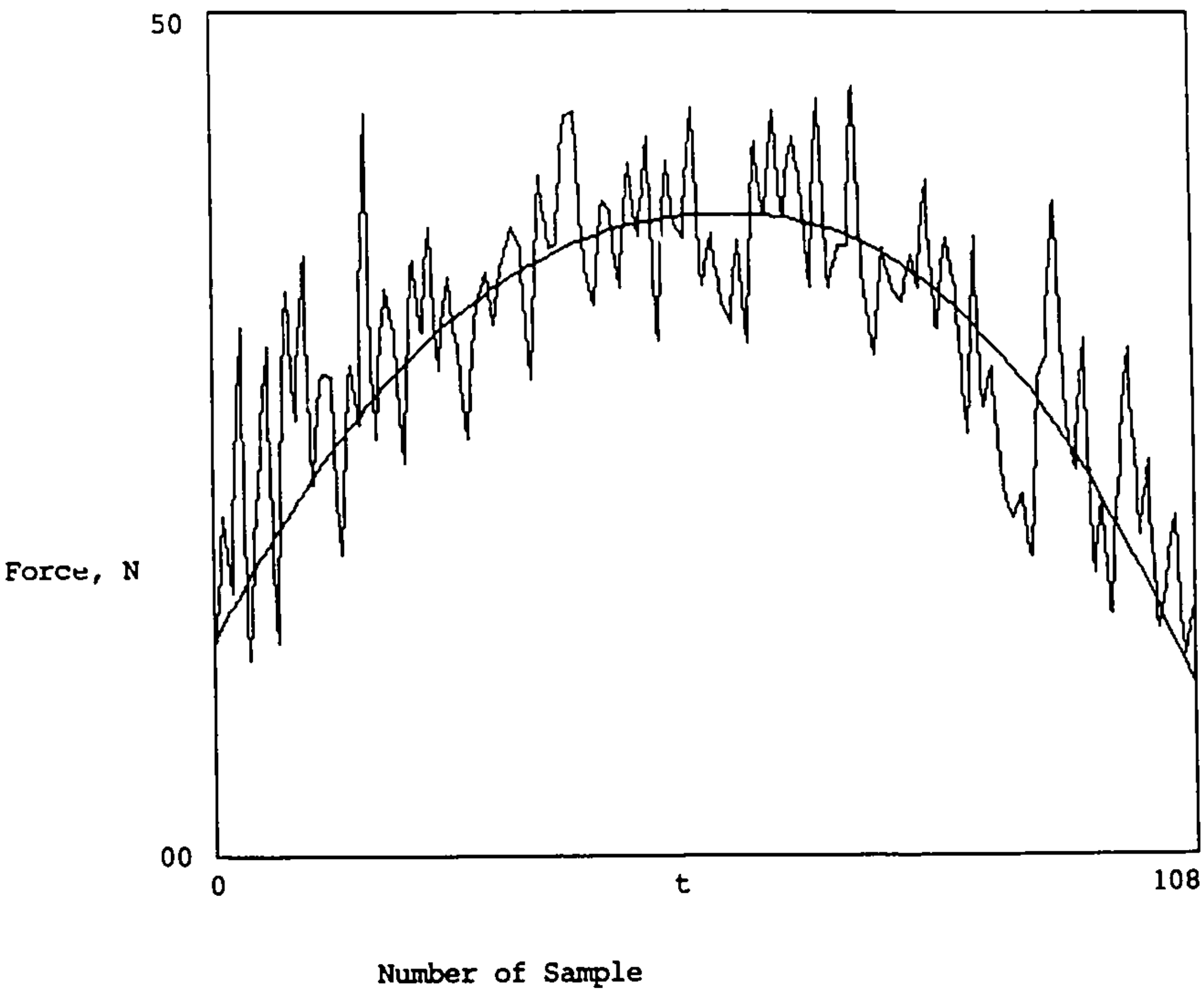

Non-linear Trend Smoothing

Speed = 185.9 fpm　　a0 = 63
Feed rate = 12 ipm　　a1 = 0.009
Depth of cut = 0.125 in.　　to = 50 , k = 2.26

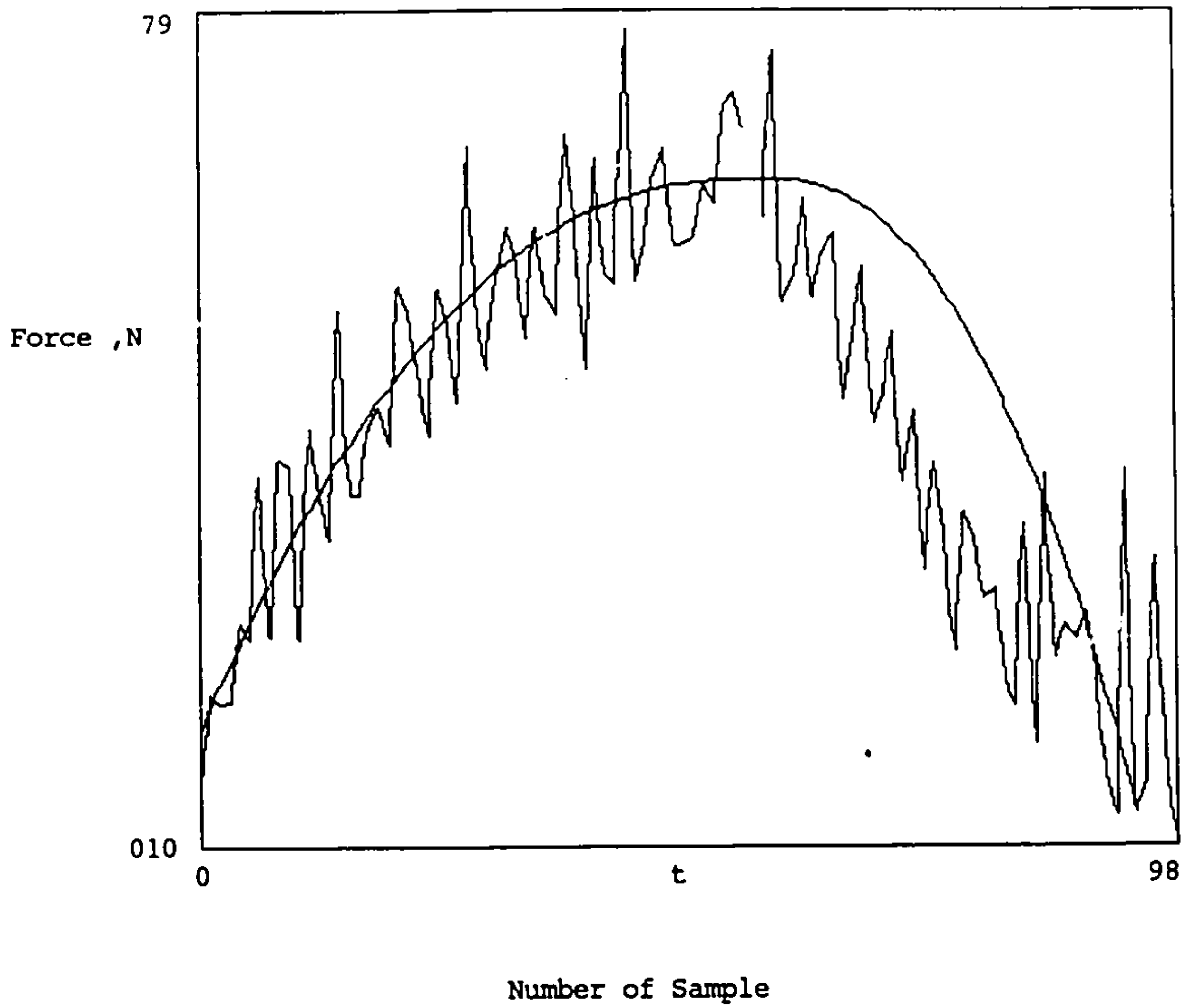

Non-linear Trend Smoothing

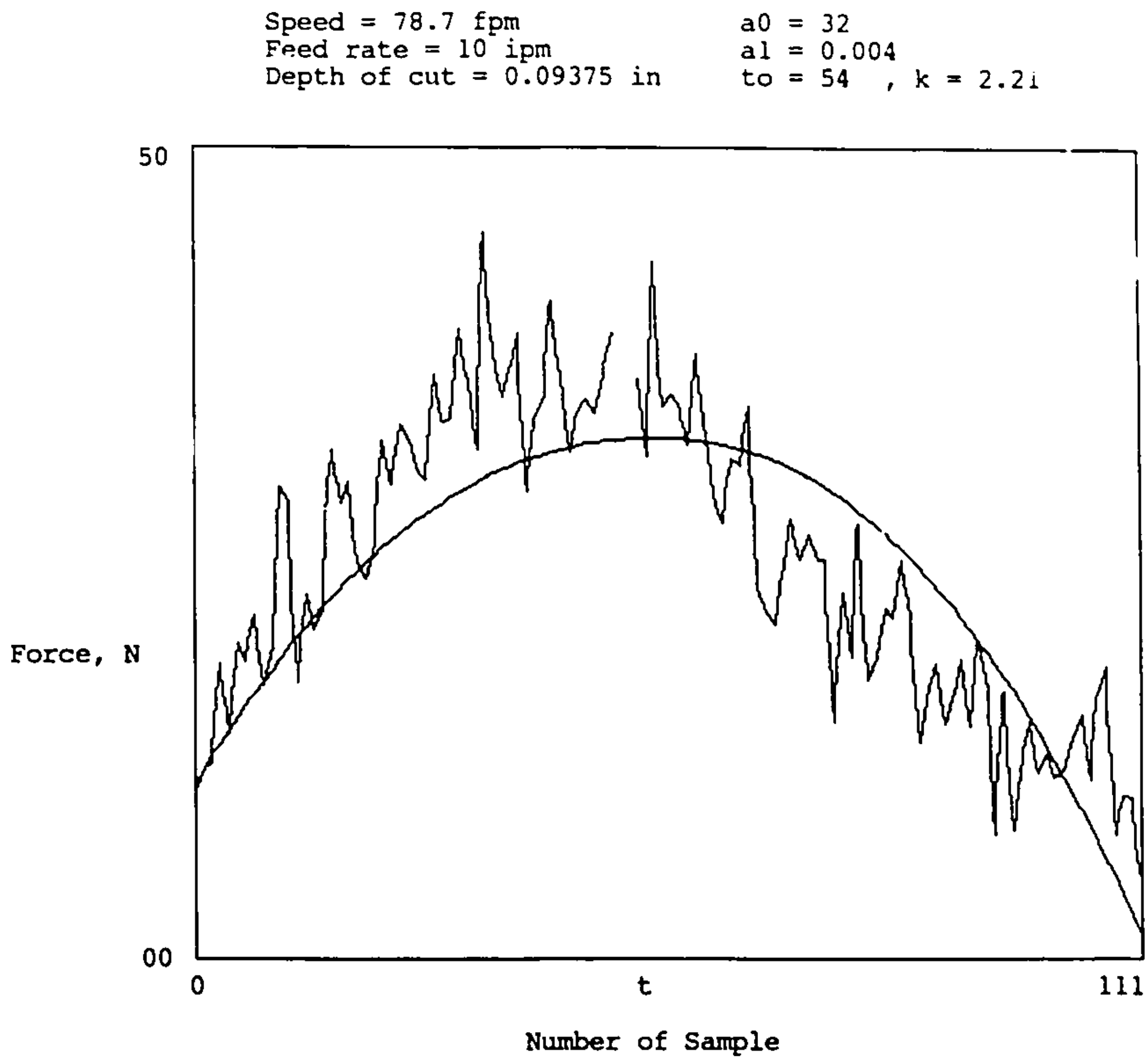

Non-linear Trend Smoothing

VITA AUCTORIS

1968	Born in Hong Kong on the 8^{th} of January.
1986	Complete high school education from Niagara Christian College, Fort Erie, Ontario, Canada.
1990	Graduate form University of Windsor, Windsor, Ontario, Canada, with a B.A.Sc. (Honors) Degree in Industrial Engineering.
1991	Currently a candidate for the M.A.Sc. Degree in Industrial Engineering at the University of Windsor, Windsor, Ontario, Canada.